ANL-91/36

Chemical Technology Division
Chemical Technology Division
Chemical Technology Division

Parametric Effects on Glass Reaction in the Unsaturated Test Method

by Alan B. Woodland, John K. Bates, and Thomas J. Gerding

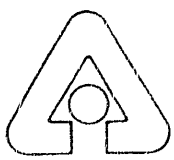

Argonne National Laboratory, Argonne, Illinois 60439
operated by The University of Chicago
for the United States Department of Energy under Contract W-31-109-Eng-38

Argonne National Laboratory, with facilities in the states of Illinois and Idaho, is owned by the United States government, and operated by The University of Chicago under the provisions of a contract with the Department of Energy.

Reproduced from the best available copy.

Available to DOE and DOE contractors from the
Office of Scientific and Technical Information
P.O. Box 62
Oak Ridge, TN 37831
Prices available from (615) 576-8401, FTS 626-8401

Available to the public from the
National Technical Information Service
U.S. Department of Commerce
5285 Port Royal Road
Springfield, VA 22161

Distribution Category:
High-Level Radioactive Waste
Disposal in Tuff
(UC-814)

ANL-91/36

ANL--91/36

DE92 007578

ARGONNE NATIONAL LABORATORY
9700 South Cass Avenue
Argonne, IL 60439

PARAMETRIC EFFECTS ON GLASS REACTION IN THE UNSATURATED TEST METHOD

by

Alan B. Woodland, John K. Bates, and Thomas J. Gerding

Chemical Technology Division

December 1991

TABLE OF CONTENTS

TABLE OF CONTENTS - Cont'd

LIST OF TABLES

LIST OF FIGURES

LIST OF FIGURES - Cont'd

LIST OF FIGURES - Cont'd

LIST OF FIGURES - Cont'd

PARAMETRIC EFFECTS ON GLASS REACTION IN THE UNSATURATED TEST METHOD

by

Alan B. Woodland, John K. Bates, and Thomas J. Gerding

ABSTRACT

The Unsaturated Test Method has been applied to study glass reaction under conditions that may be present at the potential Yucca Mountain site, currently under evaluation for storage of reprocessed high-level nuclear waste. The results from five separate sets of parametric experiments are presented wherein test parameters ranging from water contact volume to sensitization of metal in contact with the glass were examined. The most significant effect was observed when the volume of water, as controlled by the water inject volume and interval period, was such to allow exfoliation of reacted glass to occur. The extent of reaction was also influenced to a lesser extent by the degree of sensitization of the 304L stainless steel. For each experiment, the release of cations from the glass and alteration of the glass were examined. The major alteration product is a smectite clay that forms both from precipitation from solution and from in-situ alteration of the glass itself. It is this clay that undergoes exfoliation as water drips from the glass. A comparison is made between the results of the parametric experiments with those of static leach tests. In the static tests the rates of release become progressively reduced through 39 weeks while, in contrast, they remain relatively constant in the parametric experiments for at least 300 weeks. This differing behavior may be attributable to the dripping water environment where fresh water is periodically added and where evaporation can occur.

PARAMETRIC EFFECTS ON GLASS REACTION IN THE UNSATURATED TEST METHOD

I INTRODUCTION

The Unsaturated Test method has been developed[1,2] as a procedure to monitor the reaction of glass with water under conditions that are relevant to the potential repository at Yucca Mountain, Nevada. The Yucca Mountain site is located in the unsaturated zone and the repository horizon is composed of beds of welded and devitrified tuff. During the waste containment period (300/1000 years), heat generated by the radioactive waste is expected to maintain the temperature of the near-field environment above 100°C.[3] In addition, the metal containers which surround the waste are anticipated to retain their integrity during this period. Thus, for the initial 300/1000-year period, the glass waste form is unlikely to contact liquid water. However, once the temperature has cooled to below 96°C, the local boiling point of groundwater at the Yucca Mountain Site, and the container is breached, liquid water will have access to the waste form.

Water contact is likely to occur in several modes: (1) continuous contact between the waste form and water vapor, (2) slow ingress and accumulation of water in the container, and (3) intermittent contact between water and glass as water periodically flows into and passes through the container. The Unsaturated Test method was developed to study glass-water reaction where a number of glass/water contact modes exist so that site-relevant data can be generated to assess the importance of interactive effects between waste package components. The data provide a release rate or glass reaction progress for a specific set of conditions and, if the physical parameters incorporated into the test are chosen judiciously, may be able to provide information to bound releases expected to occur in the repository. The release data can also be used in the validation of geochemical modeling methods that are being developed to project glass reaction.[4,5]

To facilitate performance of the Unsaturated Test, a rigorous procedure and set of test parameters have been employed. The test is designed to study the three types of interactions that affect the reaction of the glass and that are anticipated to occur under unsaturated conditions. These include (1) contact between the glass and moist air, followed by periodic rinsing of the glass surface with flowing water; (2) contact between the glass and standing water; and (3) contact between the glass and standing water in close contact with partially sensitized 304L stainless steel. The Unsaturated Test provides for the possibility that these interactions will occur and specifies analyses to be performed that are designed to judge the importance of each one.

The apparatus used in the Unsaturated Test has been described previously[1,2] and a schematic diagram of the system is shown in Fig. 1. The components of the test apparatus are the test vessel, which provides for collection and containment of liquid and support of the waste package; the waste package assemblage (WPA), which consists of the waste form and presensitized metallic components representing the canister (Fig. 1b); and a solution feed system to inject water.

(a)

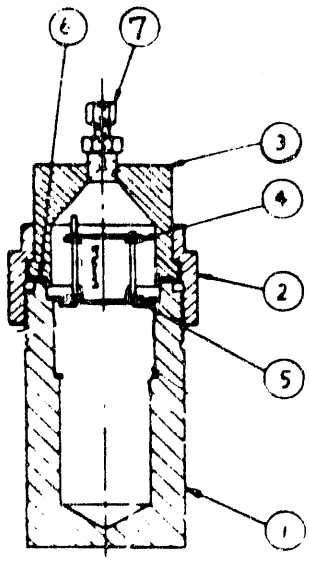

1. Body
2. Nut
3. Cap
4. Retainer Top
5. Retainer Bottom
6. Ethylene Propylene Gasket
7. Swagelok Fitting

(b)

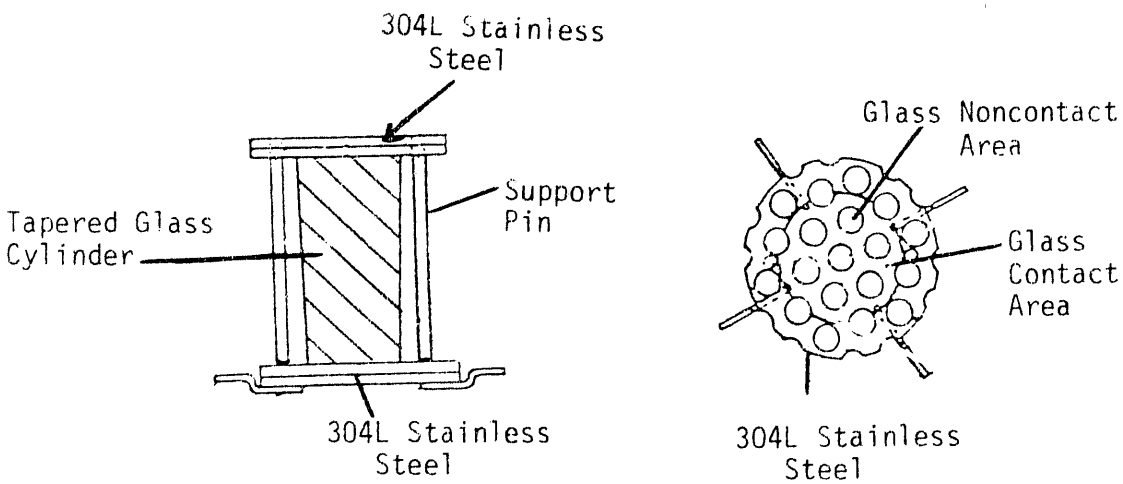

Fig. 1. (a) Schematic Drawing of Unsaturated Test Apparatus. (b) Schematic Drawing of the Side and Top Views of the Waste Package Assemblage

The WPA is contacted every 3.5 days by 0.075 mL (drops) of water from the J-13 well that was preequilibrated with Topopah Spring tuff at 90°C. The tests are conducted at 90°C and the fluid injection system is configured so that the water attains a temperature of ~90°C before contacting the glass. Elemental release is determined by chemical analysis of the water that contacted the WPA and by surface analysis of the assemblage components. Solution samples are collected immediately upon termination of the experiment and after the vessel has been acid stripped to remove any material that may have precipitated or adsorbed onto the vessel walls. Although the solution is sampled at ambient temperature, it dripped from the WPA and collected in the vessel bottom at 90°C. Material interactions are noted and secondary phases, which may influence elemental release, are identified.

The test procedure incorporates batch and continuous tests (Table 1). In the batch mode, tests are terminated at 13-week intervals through 52 weeks. In the batch mode, the apparatus is disassembled, and analyses of both the solution and components are performed. In the continuous mode, the WPA (including liquid associated with the WPA) is transferred to a new vessel, and the test is continued. For the first 52 weeks the continuous tests are sampled at 6.5-week intervals. After 52 weeks, 13- or 26-week intervals are used. Analyses are done on the solution in the old vessel. In addition, visual investigation of the components is possible at the termination points, and yet the test can continue for an unspecified period or until information most useful to repository evaluation is obtained.

One key to the applicability of the data generated by the Unsaturated Test is the relationship between the set conditions used in the test, e.g., temperature, water contact interval, water composition, drop volume, condition of the stainless steel in contact with the glass, and surface area of the glass, and the eventual conditions encountered in the repository. Since it is likely that many of the conditions listed above may vary between individual waste packages, and will certainly vary with time, the conditions were set using reasonable values at the time the test procedure was developed (1984). At that time, it was recognized that the set conditions chosen may not have been the best possible, based on refinement of the description of the waste package environment and on parametric effects not yet identified. Thus, a series of parametric experiments were initiated to determine to what degree each parameter affected the glass reaction.

The parameters chosen to study were:

(1) exclusion of stainless steel contact with the glass;

(2) the surface area of the glass;

(3) the volume of water contacting the glass;

(4) the interval of water injection; and

(5) the effect of stainless steel composition and extent of sensitization.

Table 1. Test Matrix for Unsaturated Tests

Test No.	Components	Test Duration, weeks: 0	6.5	13	19.5	26	32.5	39	45.5	52	65[a]
#1 Batch	glass, 304L ss holder	—		|						
#2 Batch	glass, 304L ss holder	—		|						
#3 Batch	glass, 304L ss holder	—				|				
#4 Batch	glass, 304L ss holder	—				|				
#5 Batch	glass, 304L ss holder	—						|		
#6 Batch	glass, 304L ss holder	—						|		
#7 Batch	glass, 304L ss holder	—								|	
#8 Batch	glass, 304L ss holder	—								|	
#9,10,12 Continuous	glass, 304L ss holder	—	v	v	v	v	v	v	v	v	v
#11 Continuous	blank	—	v	v	v	v	v	v	v	v	v

v = periodic change

| = termination

ANALYSES REQUIRED[b]

Total radionuclide (solution and metal)	√√	√√√√	√√	√√√√	√√	√√√√	√√	√√√√	√√
Total matrix element (solution Li, B)	√√	√√√√	√√	√√√√	√√	√√√√	√√	√√√√	√√
Wt loss and surface analyses		√√		√√		√√		√√	
Interaction of stainless steel		√√		√√		√√		√√	

[a]The continuous tests are sampled every 13 weeks after the 52-week interval.

[b]A check means this analysis is required; the number of checks indicate replicate analyses possible. The wt loss and surface analyses for the continuous test will be done when the tests are terminated.

These parametric experiments have now been in progress for up to four years. In this report the details of each experiment are described, the results are presented, and a comparison is made between the results from the various parametric experiments and the N2 Unsaturated Test series[6] to determine the relative importance of each parameter in affecting glass reaction.

II. EXPERIMENTAL PROCEDURE

A. Overview

The apparatus used in the parametric experiments is the same as used in the Unsaturated Test except for the containment vessel and gasket (items 1, 2, 3, and 6 in Fig. 1). In the parametric experiments a 22 mL Parr vessel #4703 modified by reducing the wall thickness 1/32" to a depth 1" from the top of the vessel is used as the vessel body (item 1). This modification creates a ledge on which the retainer bottom (item 5, Fig. 1) is positioned. The cap for the vessel (item 3) was machined to provide the umbrella effect shown in Fig. 1 which directs condensation on the vessel lid to the walls of the vessel body instead of to the glass. All the material used in construction of the vessel is 304L stainless steel. The gasket material used in the parametric experiments is Teflon^{TM}. The above changes were made to reduce the cost of the apparatus and to aid in ease of performing the experiments. None of the changes should appreciably affect the extent of glass reaction except that the vessel used in the parametric experiments is ten times less massive than the one used in the Unsaturated Tests. This reduced mass may increase the effect of the small temperature fluctuations caused by the ovens. As temperature gradients between the vessel and WPA will cause vapor transport, this is an important process that must be considered when comparing results from different experiments.

The conditions used in each parametric experiment plus the rationale for performing the experiment are given in Table 2. The experimental matrix used for each series is detailed in Section III, but in most cases both batch and continuous experiments were run. All of the batch experiments have been terminated, while the continuous experiments are still in progress.

The solutions from the vessel bottom are analyzed for Al, B, Ca, Fe, K, Li, Mg, Mn, Na, Ni, Si, and S using Inductively Coupled Plasma/Atomic Emission Spectroscopy (ICP/AES). The analytical uncertainty is 3-10% depending on the element and its concentration. Uranium is determined by the Sintrex method which is based on laser-induced fluorescence (±10% uncertainty). When enough solution is available, the pH (glass electrode, Orion model 501 Digital Ionanalyzer), total and organic carbon (Dohrmann Total Organic Carbon Analyzer Model DC-80), and the anions F^-, Cl^-, NO_2^-, NO_3^-, $SO_4^{=}$, $HPO_4^{=}$, CHO_2^-, and $C_2O_4^{=}$ (ion chromatography) are measured with uncertainties all in the range of 5-10%.

Table 2. Description, Purpose, and Status of Parametric Experiments and N2 Unsaturated Test

Experiment #	Description	Purpose	Status
P-II	Regular-sized glass waste form, no ss holder, 0.075 mL J-13/ 3.5 days, continuous and batch experiments	To study the release from glass only	Initiated 2/20/84. Batch experiments completed 2/18/85. Continuous experiments in progress.
P-III	Half-sized glass waste form, ss holder, 0.075 mL and EJ-13/ 3.5 days, continuous and batch experiments	To study the effect of changing the waste form surface area by reducing the as-cast surface area by half	Initiated 12/6/84. Batch experiments completed 12/5/85. Continuous experiments in progress.
P-IV	Half-sized glass waste form, ss holder, 0.0375 mL and EJ-13/ 3.5 days, continuous and batch experiments	To study the effect of drop volume by reducing the amount of water added and the as-cast surface area by half	Initiated 2/18/85. Batch experiments completed through one year. Continuous experiments in progress.
P-V	Regular-sized glass waste form ss holder, 0.075 mL and EJ-13/ 14 days, continuous and batch experiments	To study the effect of lengthening the time interval between water additions	Initiated 6/10/85. Batch experiments completed through one year. Continuous experiments in progress.
P-VIII	Regular-sized glass waste forms in presensitized ss holders (heat #22841), 0.075 mL EJ-13/ 3.5 days, continuous and batch experiments	To study the effect of presensitized the ss waste form holder	Initiated 2/27/86. Batch experiments completed through six months. Continuous experiments in progress.
Test #			
N2	Regular-sized glass waste forms in presensitized ss holders (heat #699960), 0.075 mL and EJ-13/3.5 days, continuous and batch experiments	QA I execution of Unsaturated Test on glass doped with Np, Pu, and Am	Initiated 2/3/86. Batch tests completed. Continuous tests in progress.

Raw and "corrected" solution analyses are presented in the appendices. The "corrected" data account for the elemental contribution from the injected water. This is done by subtracting from the total solution analysis the amount of each element contained in the water that was injected during the experiment period and added at the beginning of an experiment period. Such a correction assumes that all the water injected actually goes into the vessel. This concern exists because after several years, the injection lines may become partially plugged which makes complete water injection uncertain. The correction also assumes that any leakage from the vessel is only water (presumably as vapor) and that all cations are retained in the vessel. It should be noted that, when analyzed concentrations were reported to be below the detection limit, the detection limit value was used. Thus, the results for elements frequently at very low concentration represent maximum values. These elements include Al, Mg, Ni, and Sr.

Interpretation of the solution data requires consideration of processes that may occur intermittently during the experiment. For example, if during a certain period there has been considerable evaporation from the WPA surface, it is possible that none of the water that contacts the top surface actually drips off of the glass to be collected in the test solution. If this happens, then all elements will show a negative deviation. However, if during the next period effective water transfer from the glass to the test vessel occurs, then a sharp positive deviation in elemental release may be observed. Consequently, elemental release should be viewed as a trend over the entire experiment duration with little weight given to individual deviations from this trend.

In the batch experiments analysis is also performed on the metal and glass components of the systems. The components are observed first using a low-power optical microscope where color photographs are taken and the surfaces mapped for scanning electron microscopy (SEM) and secondary ion mass spectroscopy (SIMS) analysis. If appropriate, samples are taken for x-ray diffraction (XRD) analysis. The samples are then examined by SEM with associated energy dispersive spectroscopy (EDS) and wavelength dispersive spectroscopy (WDS) to characterize the alteration products that formed during the reaction.

B. Starting Components

The procedures used in setting up, performing, and analyzing the experiments are essentially the same as used in the Unsaturated Test.[1,2,6] Throughout the entire series of experiments a consistency in methods was maintained.

1. Glass Composition and Homogeneity

The basis for the glass composition is SRL 165 black frit doped with Cs, Sr, and U.[7] In this report this glass is referred to as SRL U glass. This composition was chosen because of the data available as part of the SRL testing program[7] and because at the time the experiments were initiated, 165 type black frit was the reference glass composition for processing in the

Defense Waste Processing Facility (DWPF). Subsequently, the glass processing procedure has been altered and glasses based on frit 200 with both sludge and precipitate hydrolysis components added have been designated as DWPF candidate glasses.[8] Based on hydration theory,[9] SRL 165 black frit type glasses should have the best durability of glasses that fit into the potential range of glasses to be produced by the DWPF.

A single quantity of SRL black frit has formed the basis of all the parametric experimentation described in this report. The glass composition is given in Table 3 together with analyses of the starting material as obtained by different laboratories. EDS spectra of the glass at 10 and 20 keV are presented in Figs. 2a and 2b for reference.

2. Water

A 5-gal batch of J-13 water from the J-13 well located near the potential repository horizon was used as the source of water for these experiments. In some experiments the water was used as received and in other experiments the J-13 water was equilibrated with tuff at 90°C following established procedures[1] to produce EJ-13 water, which is taken to be more representative of water that will be present in the waste package environment. Several equilibrations have been done over the course of these experiments and the water compositions used in the parametric experiments are given in Table 4.

3. 304L Stainless Steel Waste Form Holders

The waste form holders that enclose the glass during the experiments consist of perforated pieces of 304L stainless steel. The perforations are present to permit direct contact between the dripping water and the glass. Steel from two different heats was used during the course of the experiments (Table 5). In addition, different heat treatments were imposed on the steel to simulate heating that may occur during glass processing and long-term storage in the repository at elevated temperatures. Such heat treatment may cause the steel to lose its resistance to corrosion and become sensitized. In some of the experiments the starting metal was purposely sensitized to measure its influence on glass reaction. Details of the sensitization treatments are presented in the sections describing each individual series of experiments. For reference, an EDS spectrum of 304L stainless steel is presented in Fig. 2c.

III. RESULTS AND DISCUSSION

The results from each series of parametric experiments are presented below as individual subsections. Thereafter a comparison is made between the different series to assess the importance of each physical parameter on glass reaction.

Table 3. Composition of Glasses Used in the Parametric Experiments

Formula	SRL U Glass		Black Frit Oxide wt %	
	Oxide wt %	Element wt %	Ferro[a]	MCC[b]
Al_2O_3	4.08	2.16	4.1	4.3
B_2O_3	6.76	2.09	6.8	6.8
BaO	0.06	0.05		0.1
CaO	1.62	1.16	1.5	1.6
CeO_2	<0.05	<0.04		
Cr_2O_3	<0.01	<0.007		
Cs_2O	0.072	0.07		
Fe_2O_3	11.74	8.20	12.3	11.7
K	NA[c]			
La_2O_3	<0.05	<0.004		0.2
Li_2O	4.18	1.94	4.7	4.8
MgO	0.70	0.42	0.8	0.6
MnO_2	2.79	1.76	2.9	2.8
MoO_3	<0.01	<0.007		
Na_2O	10.85	8.05	10.3	10.8
Nd_2O_3	<0.05	<0.005		
NiO	0.85	0.67	0.9	0.8
P_2O_5	0.29	0.13		0.3
SiO_2	52.86	24.71	54.1	51.6
SrO_2	0.11	0.10		0.2
TiO_2	0.14	0.08		<0.1
UO_2	0.92	0.81		
ZnO	0.04	0.03		
ZrO_2	0.66	0.48	1.2	0.7
F			0.06	
Cl			0.05	
Pb			0.05	

[a]Black frit supplied to ANL by SRL, composition as determined by Ferro Corp.

[b]Black frit supplied by SRL to the Materials Characterization Center (MCC), composition as determined by MCC.

[c]NA = not analyzed.

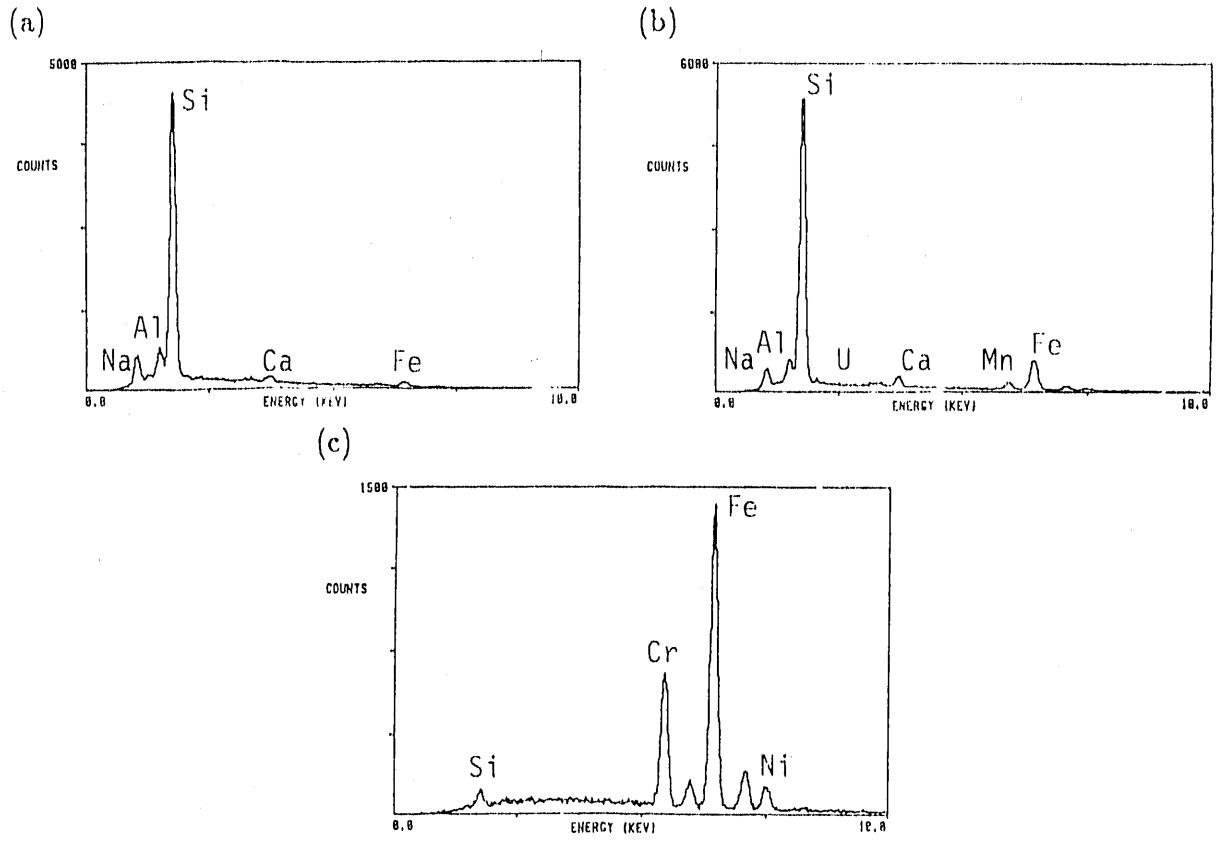

Fig. 2. EDS Spectra of (a) Unreacted Glass at 10 keV, (b) Unreacted Glass at 20 keV, and (c) 304L Stainless Steel at 20 keV

A. P-II Experiments

This set of experiments is being performed following the Unsaturated Test protocol,[2] except that there is no metal retainer and all vessel components are made of Teflon™. All measured release should be solely due to glass/water interaction. This provides a baseline for comparison with the results of other experiments where metal components are present. In addition, the results are directly applicable to those areas of the glass where there is no direct metal contact (i.e., the top portions of the glass in the pour canisters).

The detailed experimental matrix and weight change measurements are presented in Table 6.

The experiments were initiated 2/20/84 and have been completed through 301 weeks. For the first year, batch experiments were terminated at the 6.5-, 13-, 26-, 39-, and 52-week periods, while the continuous experiments were sampled every 6.5 weeks. For the second year, the continuous experiments were sampled every 6.5 weeks and thereafter at irregular intervals of approximately 13 weeks.

Table 4. Composition of J-13 and EJ-13 Water Used in the Parametric Experiments

Water Type	Water Composition (ppb)												
	Al	B	Ca	Fe	K	Li	Mg	Mn	Na	Ni	Si	Sr	U
J-13	<100	130	11,800	<10	4500	40	1940	<5	44,700	<20	29,100	37	<1
EJ-13	780	180	4500	18		64	390	<5	46,600	<20	36,300	30	4
4/30/84	720	200	4550	ND		75	415	ND	47,800	92	37,900	39	4.7
	680	190	4560	ND		70	420	ND	49,900	57	38,000	44	4.6
	660	170	4390	<10		79	400	<5	48,200	ND	37,800	47	4.3
	720	180	4370	<10		71	400	<5	46,500	ND	36,900	41	3.9
	750	180	4150	17		66	390	<5	47,800	ND	36,200	41	ND
	710	170	4100	<10		71	390	<5	46,800	ND	36,900	37	3.7
	700	180	4100	<10		79	400	<5	48,700	ND	36,200	37	2.8
EJ-13	250	150	7120	<10		54	270		48,400	<20	35,300	35	<1
5/28/86	240	163	7160	<10		49	260	<5	50,300	ND	33,600	35	<1
	230	170	7170	<10		ND	260	<5	49,000	<20	33,800	35	
	240	160	7570	<10	6930	45	270	<5	54,400	42	38,500	32	<1
	230	180	7230	15	660	42	260	<5	50,400	<49	33,100	28	<1

Table 5. Composition of 304L Stainless Steel Used in the Parametric Experiments and N2 Unsaturated Test

Composition	Heat #	Element %											
		C	Mn	P	S	Si	Cr	Ni	Cu	Co	N	Mo	V
Retainer N2 and P-IV, -V, and -XII	699960	0.022	1.49	0.025	0.003	0.40	18.22	10.02	0.12	NA	0.036	0.24	NA
Posts (all tests)	70815	0.027	1.61	0.028	0.021	0.26	18.50	10.62	NA	NA	NA	NA	NA
Retainer P-VIII	22841	0.016	1.33	0.029	0.003	0.51	18.15	9.22	0.36	0.11	0.082	0.28	NA

NA = not reported in certificate of analysis.

Table 6. Experimental Matrix and Weight Change Results from the P-II Series

Test #	Test Period (weeks)	Date Started	Date Stopped	Initial Glass Mass (gm)	Final Glass Mass (gm)	Δ Mass ($gm \times 10^{-5}$)	SA Ends (cm^2)	SA Sides (cm^2)	SA Total (cm^2)	J-13[a] Added Drops (gm)
P-II-1a	6.5/13	2/20/84	in progress	9.9678			3.82	9.70	13.52	0.98/6.5 weeks
P-II-2a	6.5/13	2/20/84		10.0990			3.82	9.56	13.38	0.98/6.5 weeks
P-II-3	6	2/20/84	4/02/84	9.9378	9.9379	10	3.82	9.56	13.38	0.98
P-II-4	13	2/20/84	5/21/84	10.0620	10.0627	70	3.82	9.65	13.47	1.95
P-II-5	26	2/20/84	8/20/84	9.6495	9.6507	80	3.73	9.39	13.12	3.9
P-II-6	39	2/20/84	11/19/84	9.5870	9.5885	150	3.66	9.34	13.00	5.85
P-II-7	52	2/20/84	2/25/85	9.6366	9.6368	20	3.71	9.36	13.07	7.80

[a]The J-13 water was not pretreated.

The experiments have been conducted using J-13 water of composition given in Table 4. The water was received from Lawrence Livermore National Laboratory (LLNL) and has been stored in its original shipping container. The source water has been analyzed periodically and its composition remains relatively stable (Table 4).

The results of these experiments will be discussed by describing the general appearance of the glass as observed throughout the test period, by examining the glass surfaces from the batch experiments, and by correlating the solution results with these observations.

1. General Observations

(a) The waste form steadily gained weight during successive sampling periods through 39 weeks. This is the result of precipitation on the glass surface. The precipitates were clearly visible after 6.5 weeks. They initially formed on the top surface and coverage began to extend onto the sides after 224.5 weeks in the continuous experiments. The accumulation of precipitates does not occur on the bottom surface. Based upon detailed investigation of the batch experiments, the precipitates are primarily aluminosilicates (see below).

(b) On the top surface, no accumulation of standing water appears to have occurred. Upon opening the vessels (after cooling), the top surface dries within 10-20 seconds and the surface changes from a dark gray to a dirty white color when drying.

(c) The bottom surface of the glass was usually in contact with standing water throughout the sampling interval and remained wet during sampling.

(d) There was some water loss during the sampling intervals due to vapor escaping from the vessels. However, some fluid was always present in the bottom of the vessels upon sampling or experiment termination, indicating that vapor-saturated conditions were maintained throughout the experiment. A new vessel design was introduced at the 210-week sampling in an attempt to reduce vapor loss and to provide a more secure positioning of the glass in the center of the vessel.

2. Component Analyses

Selected samples from the batch experiments were examined by SEM/EDS/WDS. To do this, the top and bottom faces were carefully cut from the waste form and mounted on aluminum stubs. The reaction products observed on all samples are generally similar with greater coverage evident on the longer duration samples. The following is a description of the 26- and 52-week samples.

a. P-II-5, 26-Week Sample

A Si-rich surface layer is well developed on the glass with two types of reacted areas present. In some areas, the surface is covered by a smooth deposit which is similar in composition to that of the unreacted glass, except that it is somewhat depleted in Na and enriched in Mg, S, and K (Figs. 3a and 3b/EDS, compare with Fig. 2a/EDS). This deposit covers ~25% of the surface and appears to have formed by precipitation. The remainder of the surface has a rougher textured appearance, which at high magnification reveals many small platelets (Fig. 3d). This material is similar in composition to the smooth regions (compare Figs. 3e/EDS and 3b/EDS). There are many small areas which are somewhat enriched in S and Ca relative to the typical surface layer suggesting the presence of gypsum or anhydrite.

Many small grains are distributed over the surface (Fig. 3f). The two most common have been identified by XRD as calcite and gypsum. Calcite takes the form of vertical protrusions from the surface. Gypsum grains are typically very irregular in form (Fig. 3a) and have easily distinguishable EDS spectra (Fig. 3c/EDS). Both phases occur up to 100 μm across. Since gypsum is not stable above 42°C, at 1 atm, it must have formed either by low-temperature hydration of preexisting anhydrite or by direct precipitation during cooling of the WPA when the experiment was terminated.[10] There are a number of other phases present; however, they were too fine grained to permit identification by XRD. These other grains are rich in Na, K, or Mg.

The bottom surface has far fewer grains on it compared to the top surface. The points of contact between the Teflon™ grid and the glass are evident to the eye and in the SEM (Fig. 4a). The contours of the as-cut surface are still visible but some places appear to be highly eroded. Some of the surface is covered by a smooth deposit; however, the majority has a rougher textured appearance (Fig. 4b). The roughness is more pronounced in the area of the Teflon™ contact. This reacted surface layer has a similar composition in the contact and noncontact areas (Fig. 4c/EDS). A reaction product, not observed on the top surface, occurs as dark splotches (Fig. 4d) and smooth rounded grains (Fig. 4e) on the SEM and is composed predominantly of Na (Fig. 4f/EDS). While it has not been possible to collect a sample for XRD analysis, the EDS spectra and the fact that the grains are beam sensitive suggests it is Na_2CO_3. The possibility of this being a borate may be excluded based upon WDS analysis of similar grains on the top surface which revealed no boron. The Si and Al in the EDS spectra probably result from excitation of the surface layer as the beam penetrated the grains.

b. P-II-7, 52-Week Sample

A reacted layer is well developed on the top surface. It has a rough textured appearance and is composed of staked irregular shaped platelets (Fig. 5a). There is heavier coverage of precipitated grains compared with P-II-5 (Fig. 5b). These grains are predominantly calcite and gypsum. However, there are also many very irregular shaped grains rich in Na and Cl and are presumably NaCl (Fig. 5c).

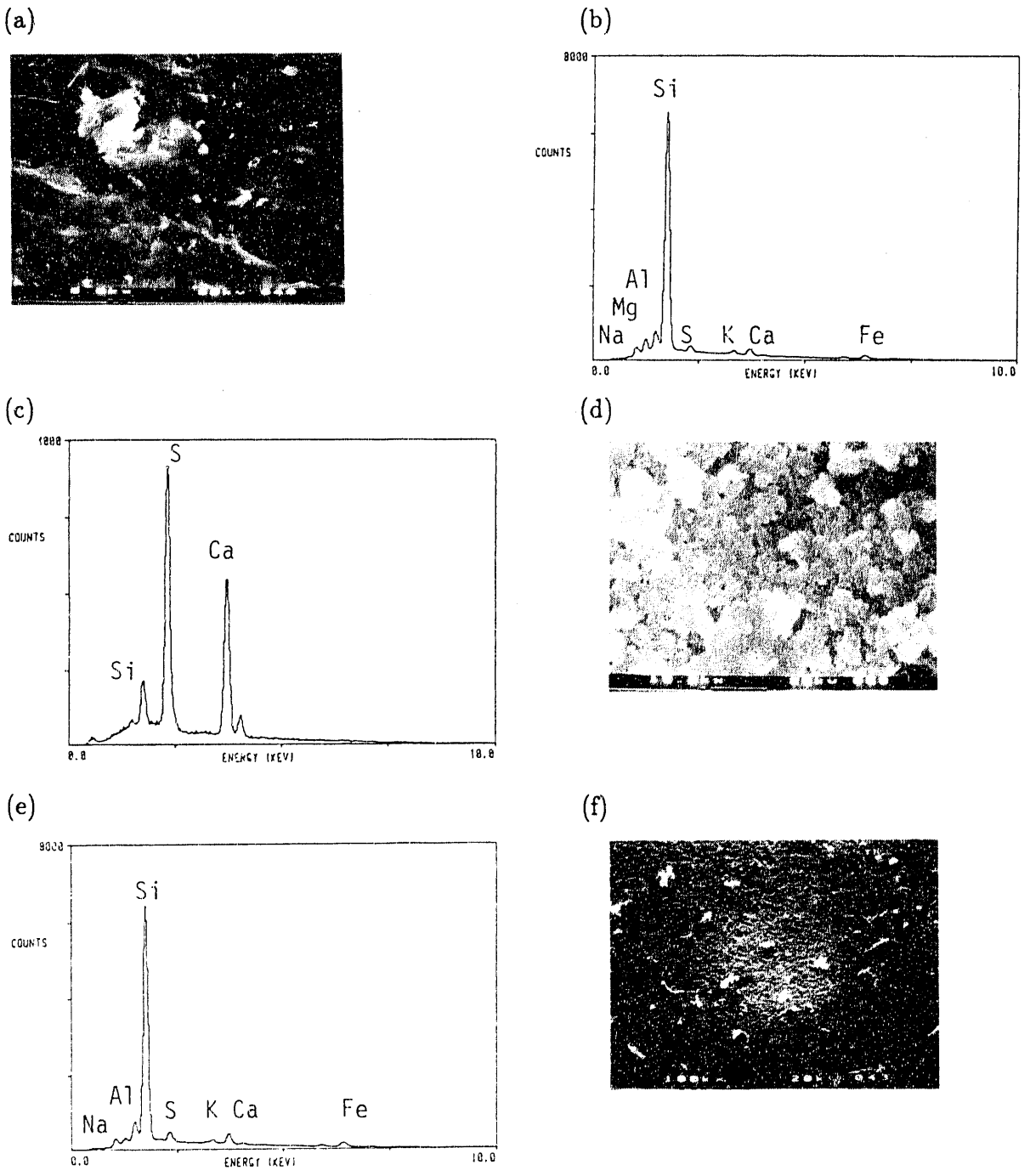

Fig. 3. SEM Micrographs and EDS Spectra of Reaction Products Formed on the Top Surface of Experiment P-II-5 (26-Week Sample) (a) 2000X, (d) 15,000X, and (f) 100X

(a)

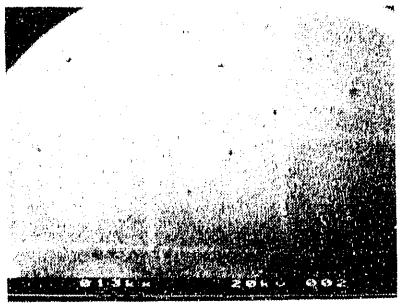

(b)

(c)

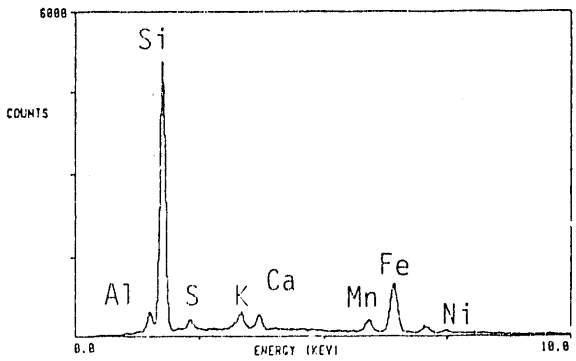

(d)

(e)

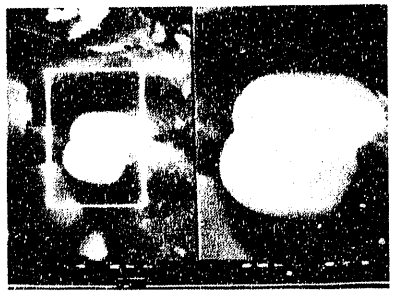

(f)

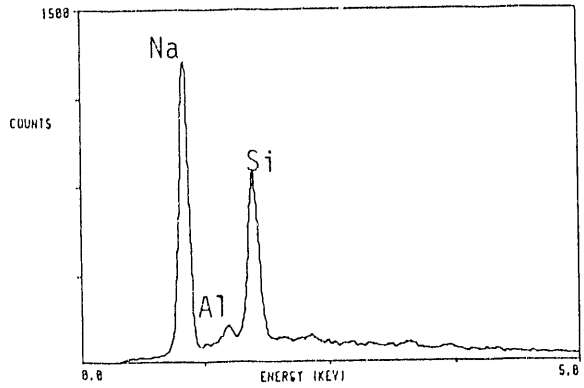

Fig. 4. SEM Micrographs and EDS Spectra of Reaction Products Formed on the Bottom Surface of Experiment P-II-5 (26-Week Sample) (a) 13X, (b) 2000X, (d) 1930X, and (e) 4200X/8400X

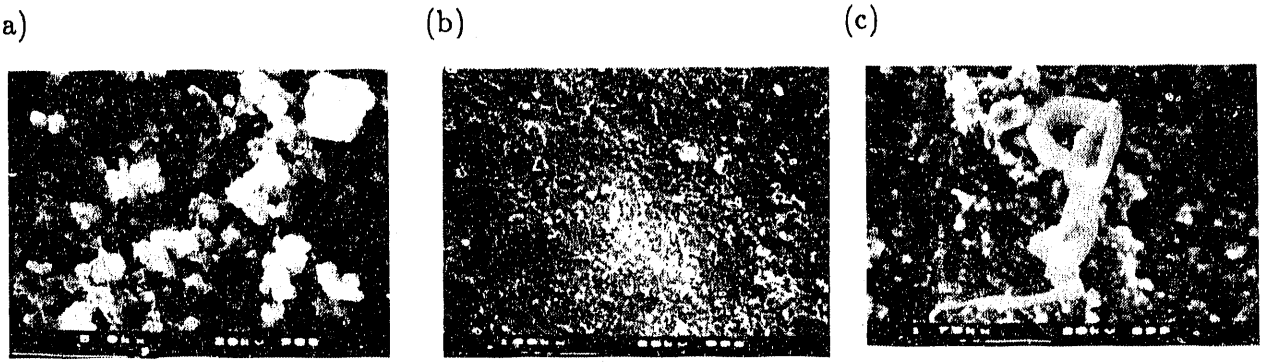

Fig. 5. SEM Micrographs of Reaction Products Formed on the Top Surface of Experiment P-II-7 (52-Week Sample) (a) 5000X, (b) 100X, and (c) 1750X

The bottom surface has a coarse texture similar to that observed on the top surface. A fine-grained precipitated deposit covers much of the coarse reacted layer (Figs. 6a and 6b/EDS). It is not a continuous deposit and it has a porous structure visible at high magnification. Its composition is essentially the same as the coarse reacted layer (compare Figs. 6b/EDS and 6c/EDS). In places, both the precipitated deposit and the reacted layer have exfoliated, exposing etched glass from below (Fig. 6d). The presence of precipitates on the exposed glass indicates that exfoliation occurred during the experiment rather than after termination. Many small grains of NaCl are present (Figs. 6e and 6f/EDS).

3. Solution Analyses

The elemental releases from the two continuous experiments are presented in Fig. 7. Selected element releases normalized for glass composition and sample surface area are given in Table 7. All raw and corrected solution data are presented in Appendix I for both the continuous and batch experiments.

The release of Li, B, and U can be used to monitor glass reaction because they occur in low concentration in the J-13 water. In addition, they are not generally observed to be incorporated in secondary phases.[11] However, some caution must be exercised since tincalconite (hydrated Na-borate) has been detected on the surface of steam-reacted West Valley glass.[11] The Li release in both continuous experiments is similar being released at a slowly declining rate over the course of the experiments, reaching a cumulative value of ~67 μg after 301 weeks. The release observed in the batch experiments, which includes a final rinse component not present in the continuous experiments, is only slightly greater than observed in the continuous experiments. The release of Li normalized to the total surface area of the sample and its concentration in the glass is ~2.5 g/m^2 after the 301-week sampling. Boron release is distinctly different from that of Li. Up through the 210-week period in the two

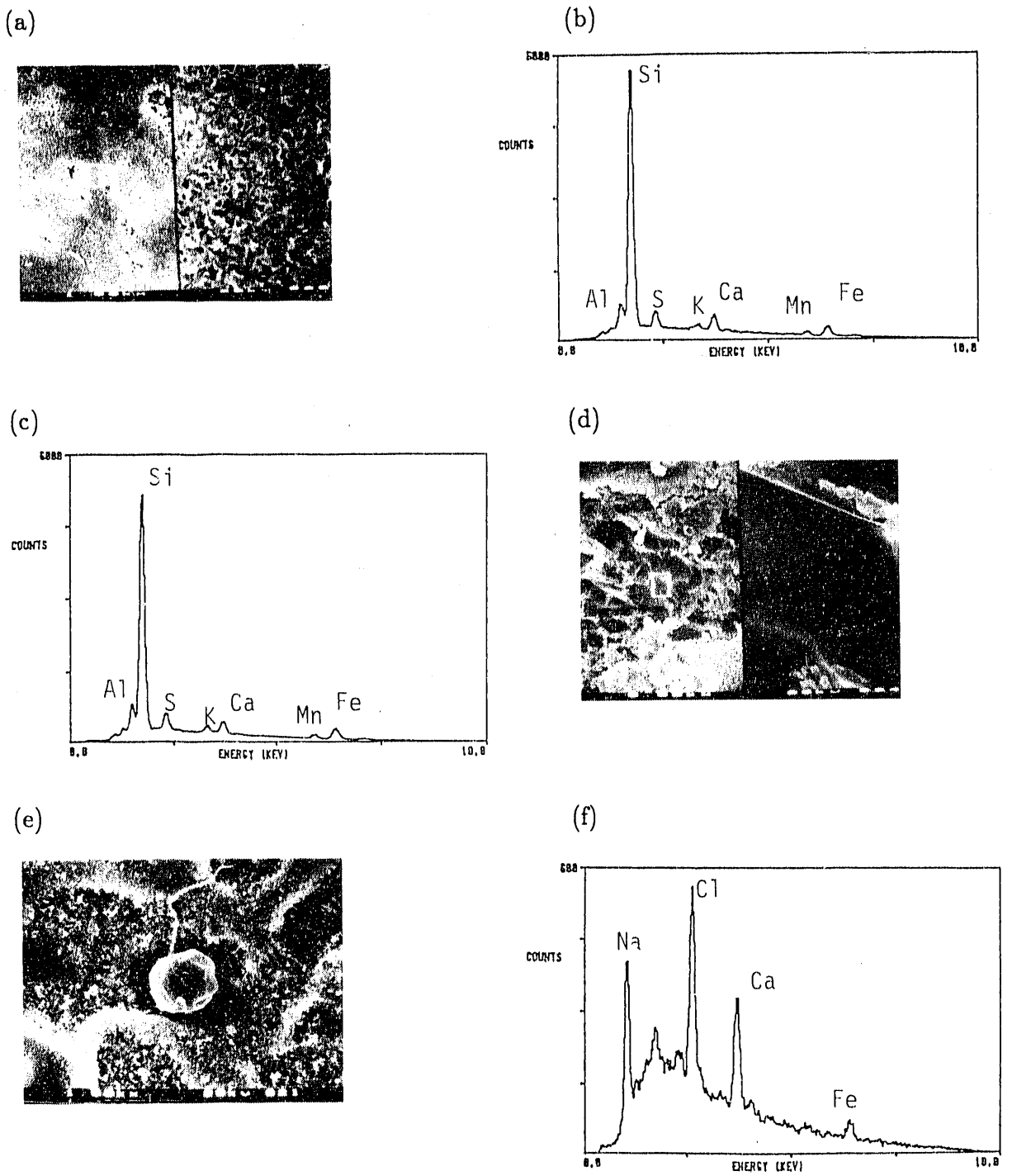

Fig. 6. SEM Micrographs and EDS Spectra of Reaction Products Formed on the Bottom Surface of Experiment P-II-7 (52-Week Sample) (a) 1000X/10,000X, (d) 500X/5000X, and (e) 1500X

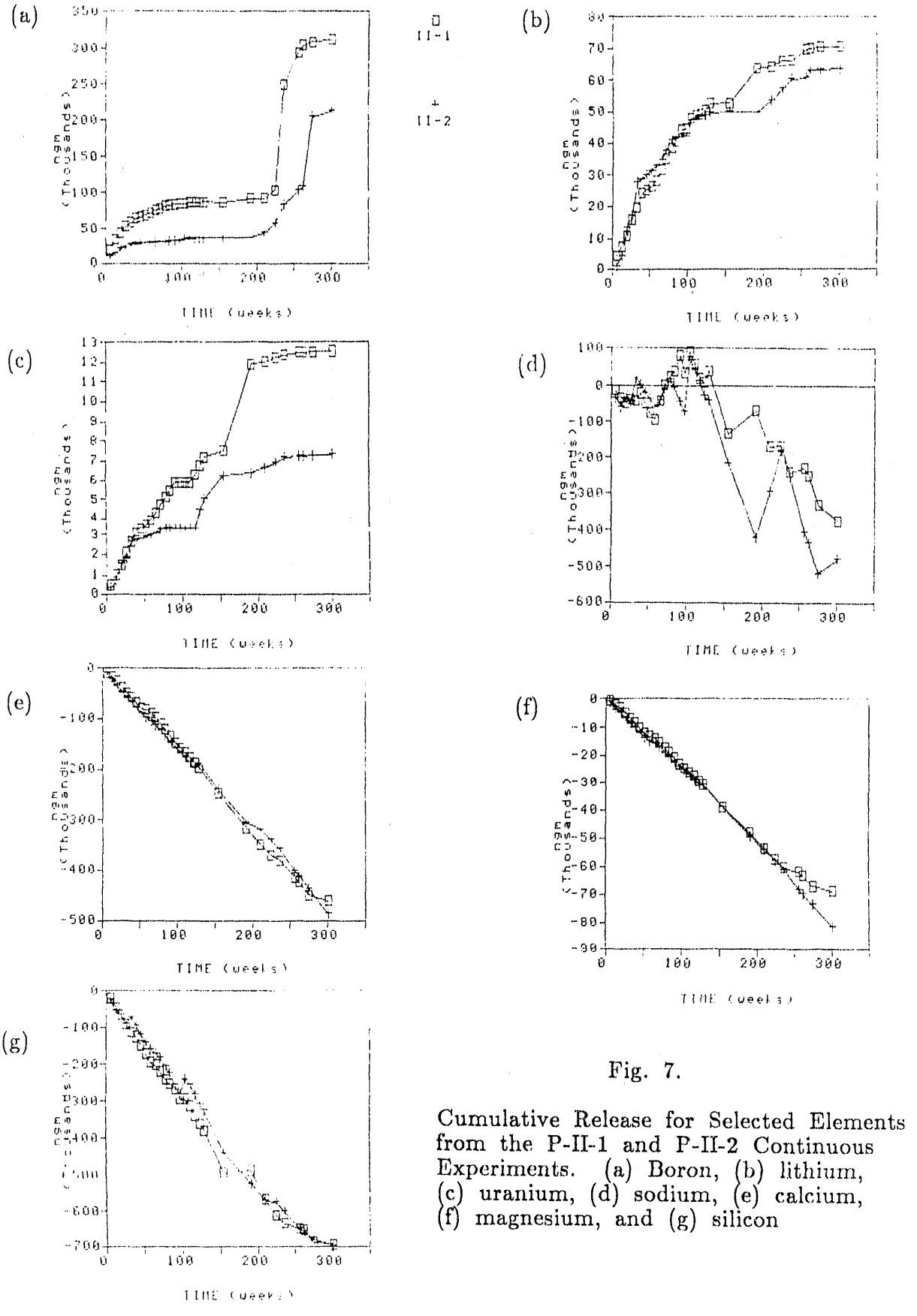

Fig. 7.

Cumulative Release for Selected Elements from the P-II-1 and P-II-2 Continuous Experiments. (a) Boron, (b) lithium, (c) uranium, (d) sodium, (e) calcium, (f) magnesium, and (g) silicon

Table 7. Normalized Release in the P-II Series

Test #	Period (weeks)	Normalized Release (g/m^2)		
		B	Li	U
P-II-3	6	0.3	0.4	0.07
P-II-4	13	0.9	0.9	0.16
P-II-5	26	0.4	0.8	0.14
P-II-6	39	0.8	1.1	0.27
P-II-7	52	0.9	1.6	0.77
P-II-1	52	2.4	1.0	0.32
	104	3.0	1.8	0.53
	155	3.0	2.0	0.68
	210	3.2	2.5	1.10
	262	10.8	2.7	1.14
	301	11.0	2.7	1.14
P-II-2	52	1.0	1.2	0.26
	104	1.2	1.8	0.31
	155	1.3	1.9	0.57
	210	1.5	2.1	0.61
	262	3.8	2.4	0.65
	301	7.6	2.4	0.66

continuous experiments, B release leveled off. This was followed by a sharp increase in release. This increase coincides with the time when the vessels were modified to reduce fluid loss. After 301 weeks, release in the P-II-1 experiment is about 50% greater than in P-II-2. There are two possible explanations for this behavior. The first is that little or no reaction took place between 80 and 200 weeks due to vapor loss. Reaction then resumed once the vessel design was modified to retain more water. This is unlikely since the release of Li indicates that reaction continued throughout the entire duration of experiments. An alternative is that a B-bearing phase precipitated and then dissolved once more water was retained. As the continuous experiments are still ongoing, it is not yet possible to verify this contention.

There is a slow, steady release of U throughout the 301-week duration of the experiments. Like B, the release of U is about 50% greater in the P-II-1 experiment. It is not clear why this difference exists, although it is probably attributable to differing degrees of water retention in the two experiments.

There is a distinct and regular net negative release of Ca, Mg, and Si. This indicates that these elements were removed from solution during the experiment. This is consistent with the observed occurrence of calcite and gypsum on a Si-rich surface layer on samples from the batch experiments. This behavior suggests that some of the surface layer has formed by precipitation rather than transformation of the glass. Sodium also has a net negative release but its behavior is erratic. This may be the result of periodic precipitation and subsequent redissolution of NaCl and Na_2CO_3. The behavior of these elements demonstrates that the J-13 water plays a role in the formation of the secondary phases.

B. P-III Experiments

The glass surface area is the modified parameter in these experiments. The surface area is reduced by ~50% by shortening the glass cylinders. The area ratio of the "as cut" top and bottom surfaces to the side is reduced from ~2.6 to 0.8. The stainless steel components are from heat #22841. The metal was not heat treated except for the two TIG welds that join the supporting pins to the bottom part of the holder.

This set of experiments was initiated on 12/6/84 and the continuous experiments are still in progress, having completed the 260-week sampling. The experiments were performed at 90°C with an injection volume of 0.075 mL of EJ-13 water every 3.5 days. The batch experiments were terminated in duplicate after 13, 26, 39, and 52 weeks. The continuous experiments were sampled every 6.5 weeks through the 78th week and then about every 13 weeks thereafter. Two different batches of EJ-13 water were used, the compositions of which are given in Table 4. The change in EJ-13 water was on 10/1/86. The experimental matrix, along with selected weight change data, are presented in Table 8.

1. General Observations

(a) The WPA generally lost weight during the experiments. In most cases, the metal components gained a small amount of weight, presumably from precipitating phases; however, this gain was much less than the amount lost from the glass (Table 8). The one exception to this behavior is P-III-9 which showed a small net increase in weight.

(b) The top glass was always damp during sampling of the continuous experiments and termination of the batch experiments. The amount of water varied from being only at the rims of the metal perforations in the metal to almost filling the noncontact areas.

(c) Standing water was present on the bottom surface of the WPA. In some cases, water bridged the gap between the metal support posts and the side of the glass.

(d) Both the top and bottom metal components showed no local discoloration after the experiments. This suggests that reaction of the metal was minimal.

Table 8. Experimental Matrix and Weight Change Results for the P-III Series

Test No.	Test Period (weeks)	Date Started	Date Stopped	Initial Glass Mass (gm)	Final Glass Mass (gm)	Δ Mass ($gmx10^{-5}$)	SA Glass (cm^2)	Initial Top Canister Mass (gm)	Final Top Canister Mass (gm)	Δ Mass ($gmx10^{-5}$)
P-III-1a	6.5	12/06/84	in progress	3.16816			6.95	2.34690		
P-III-2a	6.5	12/06/84	in progress	2.70018			6.64	2.35423		
P-III-3	13	12/06/84	3/07/85	3.10109	3.10105	(4)	6.95	2.34086	2.34081	(5)
P-III-4	13	12/06/84	3/07/85	3.02165	3.02153	(12)	7.04	2.34245	2.34249	4
P-III-5	28	12/06/84	6/20/85	3.02670	3.02625	(45)	6.93	2.34668	2.34680	8
P-III-6	28	12/06/84	6/20/85	3.09710	3.09528	(182)	7.04	2.33905	2.33922	17
P-III-7	39	12/06/84	9/05/85	3.15518	3.15361	(157)	7.06	2.34517	2.34517	0
P-III-8	39	12/06/84	9/05/85	3.09808	3.09707	(101)	6.87	2.48966	2.48971	5
P-III-9	52	12/06/84	12/05/85	3.13821	3.13785	(36)	6.85	2.36099	2.36133	34
P-III-10	52	12/06/84	12/05/85	3.00496	3.00395	(101)	6.99	2.35664	2.35685	21

Cont'd

Table 8 (Cont'd)

Initial Bottom Canister Mass (gm)	Final Bottom Canister Mass (gm)	Δ Mass ($gmx10^{-5}$)	Initial Total Vessel Mass (gm)	Final Total Vessel Mass (gm)	Δ Mass ($gmx10^{-5}$)	Water Added During Testing
3.34069			318.94	319.74	0.80	0.975
3.34735			312.07	312.99	0.92	0.975
3.34158	3.34152	(6)	316.93	318.64	1.71	1.95
3.34538	3.35432	(6)	313.36	314.96	1.60	1.95
3.32778	3.32782	4	318.62	322.23	3.61	4.20
3.33474	3.33526	52	318.12	321.46	3.34	4.20
3.35074	3.35113	39	318.48	323.32	4.84	6.15
3.32720	3.32739	19	318.49	323.29	4.80	6.15
3.33064	3.33098	34	319.14	325.31	6.17	7.80
3.34616	3.34637	21	321.49	327.07	5.58	7.80

2. Component Analyses

The glass and metal components were first examined optically up to a magnification of 140X. At this time, surface features were mapped and areas for further investigation were identified. Some samples were examined by SEM/EDS/WDS and/or SIMS. At least one sample from each experiment was examined.

a. P-III-3 and P-III-4, 13-Week Samples

The metal components of the P-III-3 and P-III-4 samples are very similar in appearance. The parts of the components not in direct contact with the glass have no evidence of accelerated reaction. In the areas where glass contact occurred, there is a thin Si-rich mat developed (Fig. 8a, 8b/EDS). Its texture is essentially the same as that observed on the glass (see below). In a few places this mat forms thicker clumps (Figs. 8c, 8d/EDS, 8e, and 8f/EDS). Overall, precipitate coverage is heavier on the bottom component. Aside from the Si-rich deposit, other precipitated phases include chloride (NaCl?) and sulfates ($CaSO_4$?) as shown in Figs. 8e, 8f/EDS, 8g, and 8h/EDS. Note the small Ca and S peaks in the EDS spectrum in Fig. 8f/EDS. This suggests the intermingling of phases at a very fine scale. There are also some small irregular-shaped masses rich in Na (Figs. 8i and 8j/EDS). These are electron beam sensitive and are similar to that observed on the P-II samples which were tentatively identified as Na_2CO_3 (compare Fig. 8i with Figs. 4d and 4e).

The bottom glass surface has partially defined regions of metal and nonmetal contact. This duality in appearance suggests that there was not close metal-glass contact over the entire surface. The contact and noncontact regions have the same appearance where the "as-cut" contours of the glass are still clearly defined but the surface appearance has been transformed from a smooth fractured surface to one covered with an interwoven phase with a "cardhouse" texture (Fig. 9a). Its texture and composition are consistent with a smectite clay (Figs. 9b/EDS and 9c/EDS). Small precipitates are present in crevices and fractures on the glass surface (Fig. 9d). From EDS analysis, these range in composition from only containing Si to having Si and Al to having Si, Al, Cr, and Mn (Figs. 9e/EDS, 9f/EDS, and 9g/EDS). This apparent compositional range may be attributable to the presence of multiple phases at a fine scale.

On the top glass surface, the noncontact areas are clearly defined as light gray to tan circular regions set on a dark brown-black background. The contact areas (with the metal component) have the same textured appearance as observed on the bottom glass (Fig. 9a), but the noncontact areas either retain an unreacted appearance or show incipient development of a textured layer (Fig. 9d). EDS spectra taken from all regions of the top surface are similar to unreacted glass.

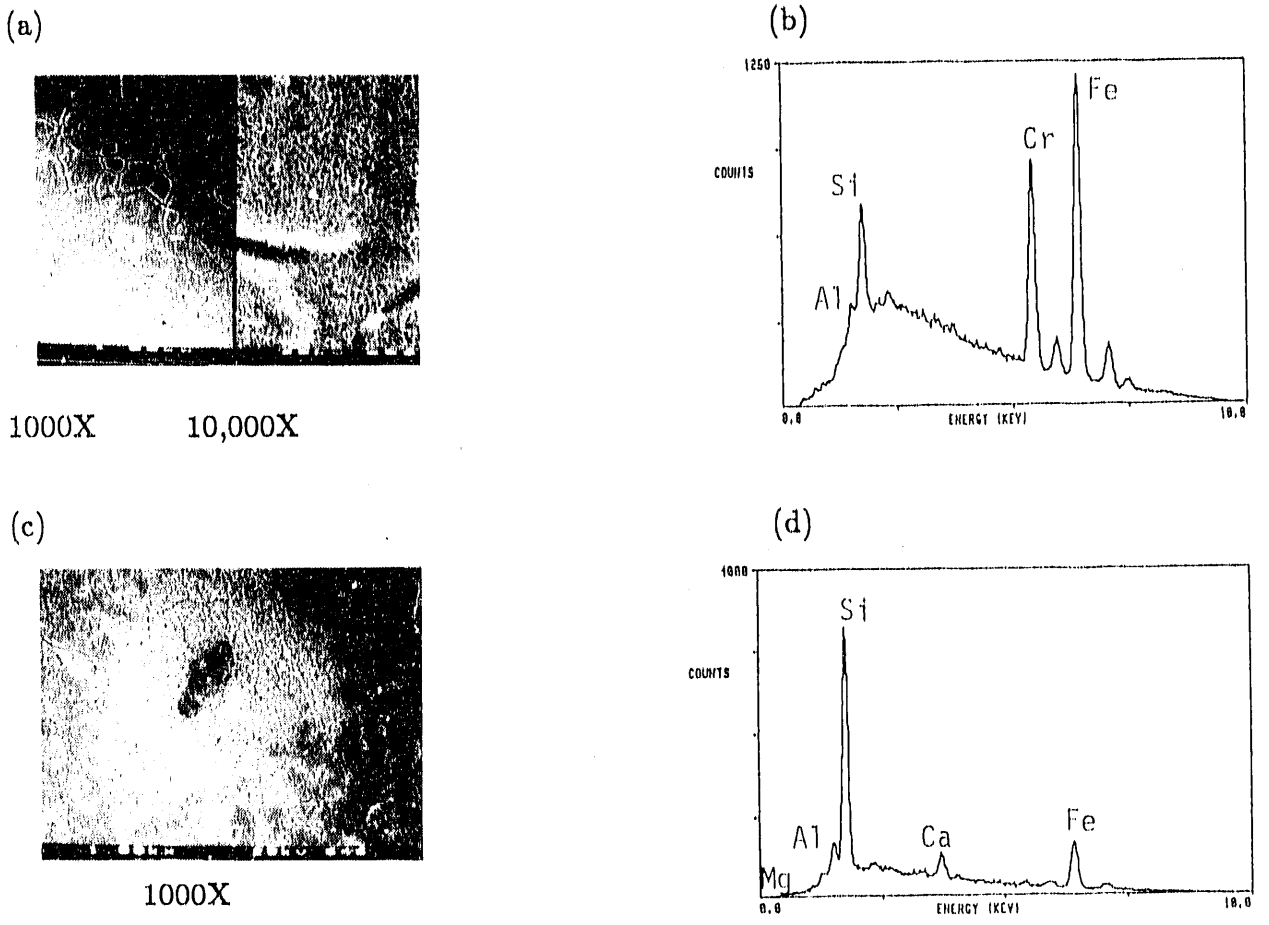

Fig. 8. SEM Micrograph and EDS Spectrum of (a and b) the Metal Surface in Contact with Glass from the Top Section of the Waste Form Holder in Experiment P-III-4; (c and d) Clumps of the Mat Materials that Formed on the Top and Bottom Metal Sections from Experiment P-III-4; (e-j) Reaction Products Observed on the Bottom Metal Section from Experiment P-III-4.

(e)

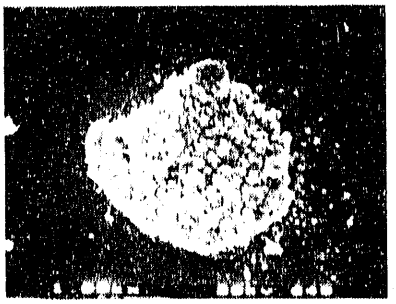

1000X

(f)

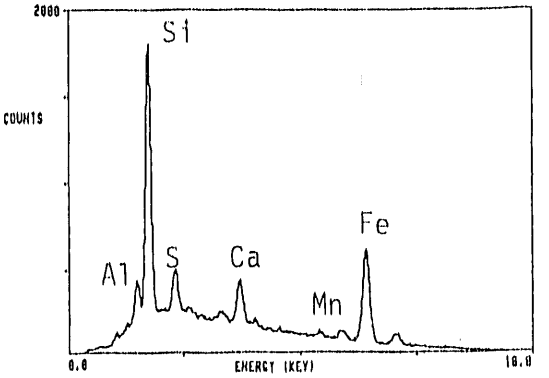

(g)

800X

(h)

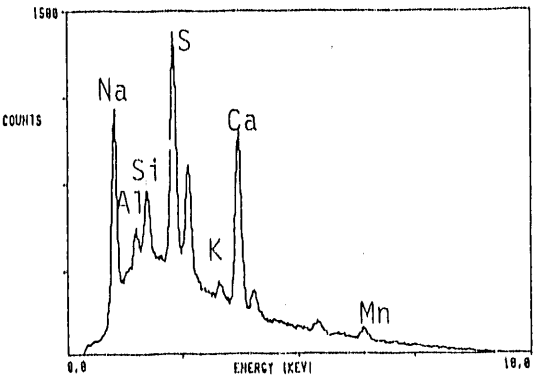

(i)

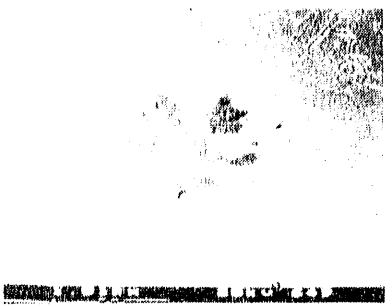

1010X

(j)

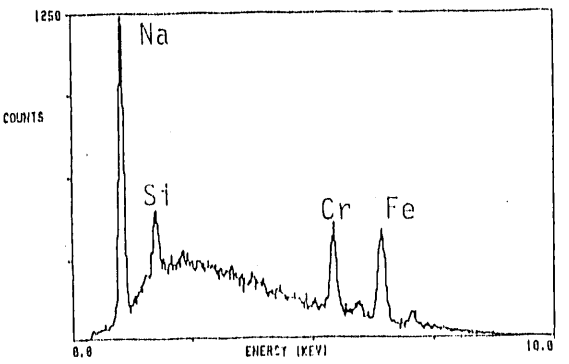

Fig. 8. Cont'd

(a)

(b)

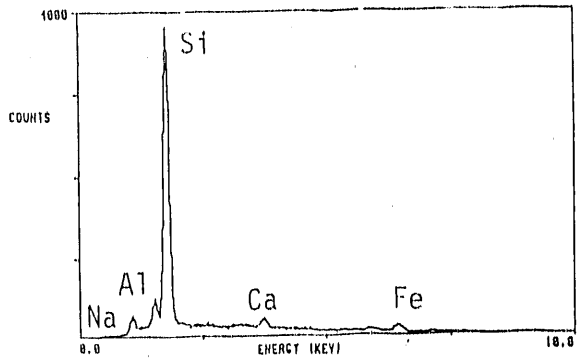

(c)

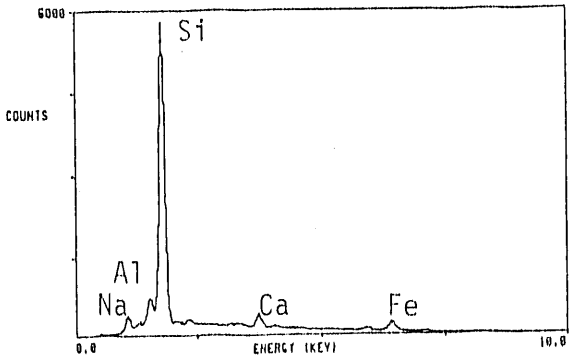

(d)

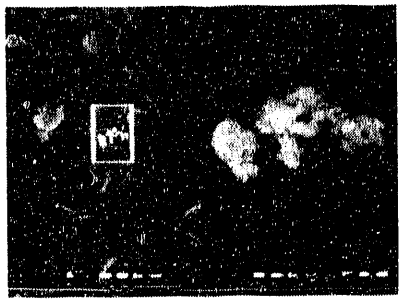

Fig. 9. SEM Micrographs and EDS Spectra of Reaction Products on the Bottom Surface of the Glass from Experiment P-III-4. This is typical of both metal contact and noncontact regions. (a) 1000X/10,000X. EDS spectra of the contact and noncontact regions are shown in (b) and (c), respectively, (d) 1000X/10,000X (see text)

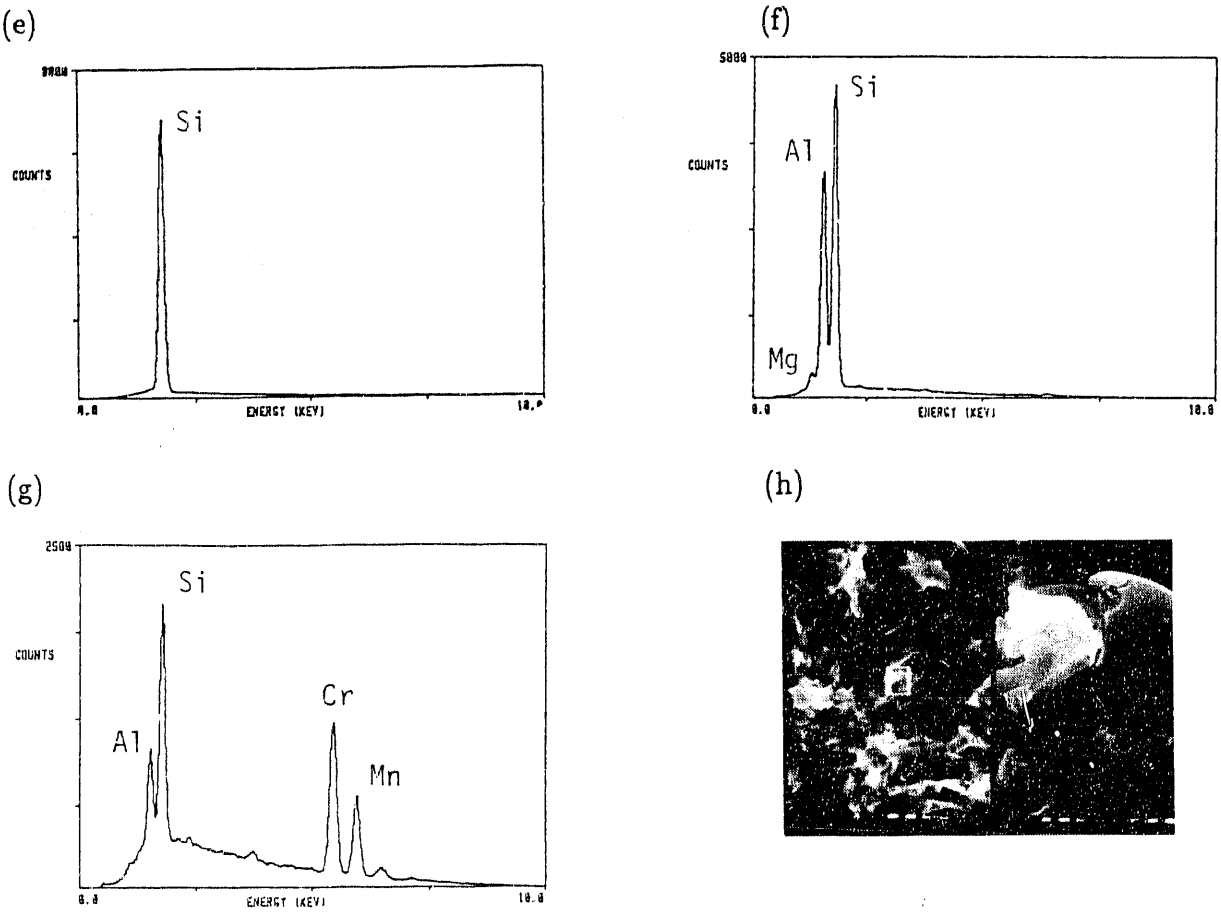

Fig. 9. Cont'd
SEM Micrograph and EDS Spectra of Reaction Products on the Bottom Surface of the Glass from Experiment P-III-4. (h) 1000X/10,000X view of noncontact area

SIMS depth profiling was performed on the P-III-3 glass. The profiles are normalized to ^{28}Si intensity. The normalization is a standard technique used to account for variations in the sputtering conditions. As a result, the profiles only show preferential depletion or enrichment relative to Si which is the most abundant component in the glass. Depth profiles of Li, B, and Mg from the contact and noncontact areas of the bottom glass and from the side glass are presented in Fig. 10. In all cases, Li is depleted to a depth of at least 1 μm. The depletion is not sharp, but instead is of a gradual nature. Boron is also depleted on the bottom surface but it appears to be restricted to the outer 0.3 μm (see mark on Fig. 3b profile). No B depletion is apparent on the side glass surface, however. Relative to Si, the distribution of Mg is constant.

In summary, the extent of reaction is greatest on the bottom surface and least on the sides. Depletion of Li appears to occur to a greater depth than B. Precipitation of Si-rich "clay" and other phases occurs on both the metal and glass components. This masks the original concoidally fractured appearance of the glass surfaces.

b. P-III-5 and P-III-6, 26-Week Samples

The metal components have the same general appearance as that described for sample P-III-4. The noncontact-contact boundaries are well defined. A Si-rich deposit covers the metal especially where it was in contact with the glass and is much thicker on the P-III-6 components. Development of this deposit is greatest on the bottom component in the contact areas and in the noncontact areas where standing water was present during the experiment (Fig. 11a). This Si-rich material also occurs in clumps. Some of these clumps contain a mixture of phases which may be rich in Ti, Cl, and/or S (Figs. 11b, 11c/EDS, 11d, and 11e/EDS). The presence of anhydrite or gypsum is suggested by the Ca and S peaks in the EDS spectrum shown in Fig. 11e/EDS. A U-bearing phase occurs on the noncontact area (Figs. 11f and 11g/EDS). It contains Si and Ca and has an acicular form, suggestive of uranophane. There was not enough material available for XRD analysis.

The top glass surface has no clearly marked circular noncontact regions and the original surface contours are still apparent. The surface is covered by a Si-rich layer similar in composition to that observed on other samples. Clumps of this same material are also present.

The bottom glass surface is megascopically different in appearance from the outer samples. It has a uniform gold-colored haze and the contact and noncontact areas are only partially visible. At higher magnification, the surface has a thick textured surface layer which is somewhat coarser than observed elsewhere (Fig. 12a). Its composition is consistent with a Ca-smectite (Fig. 12b/EDS). The original surface contours are only barely visible and are considerably rounded. In one region, the surface layer is discontinuous, exposing the glass from below (Fig. 12c). Here, it appears that the thick surface layer exfoliated during the experiment and the glass is now partially overgrown by precipitation of Si-rich "clay." A small cluster of yellow grains is also present on the exfoliated surface (Figs. 12d and 12e/EDS). These grains contain Na, Ca, S, and Cl but have not been positively identified.

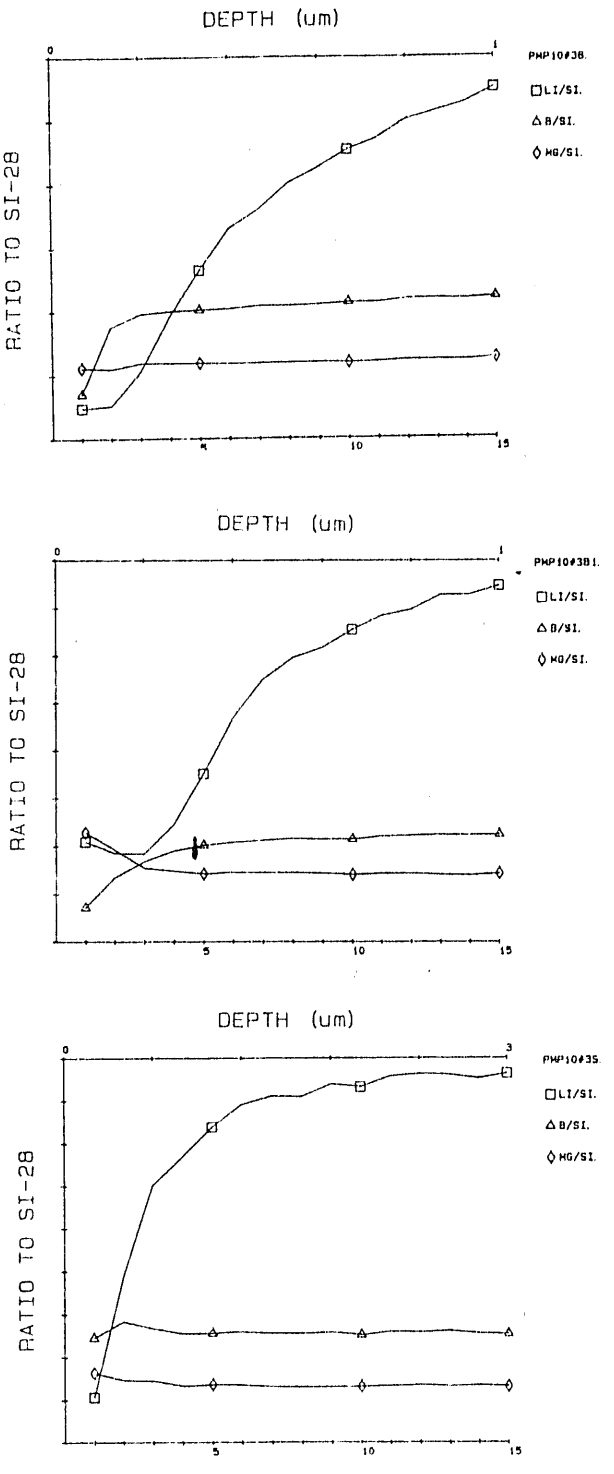

Fig. 10. SIMS Spectra Showing the Profiles of Li, Mg, and B Relative to Si for Sample P-III-3 (a) Bottom Section Non-Metal Contact, (b) Bottom Section Metal Contact, and (c) Side Surface. Note the different depth scale in (c)

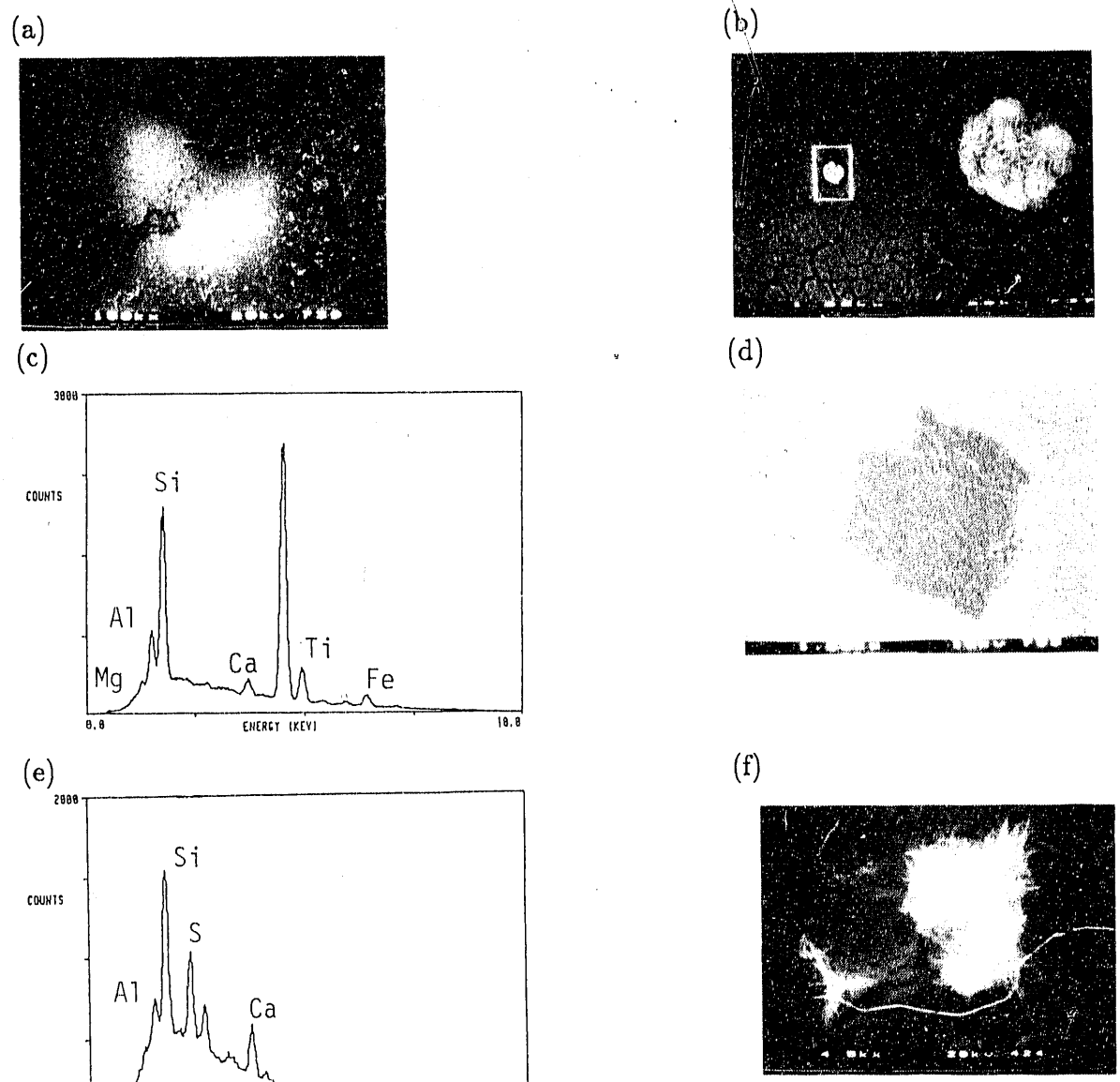

Fig. 11.
SEM Micrographs and EDS Spectra of Reaction Products on the Metal Components of P-III-6. (a) 150X, contact area, (b and c) SEM micrograph (3500X) and EDS spectrum of a Ti-rich alteration product. Note the thick matted appearance of the metal surface. (d) SEM micrograph 1250X of Si-rich alteration product. (e) EDS spectrum of Deposit shown in (d), (f) SEM micrograph of U-rich phase at 4500X, and (g) EDS spectrum of phase shown in (f).

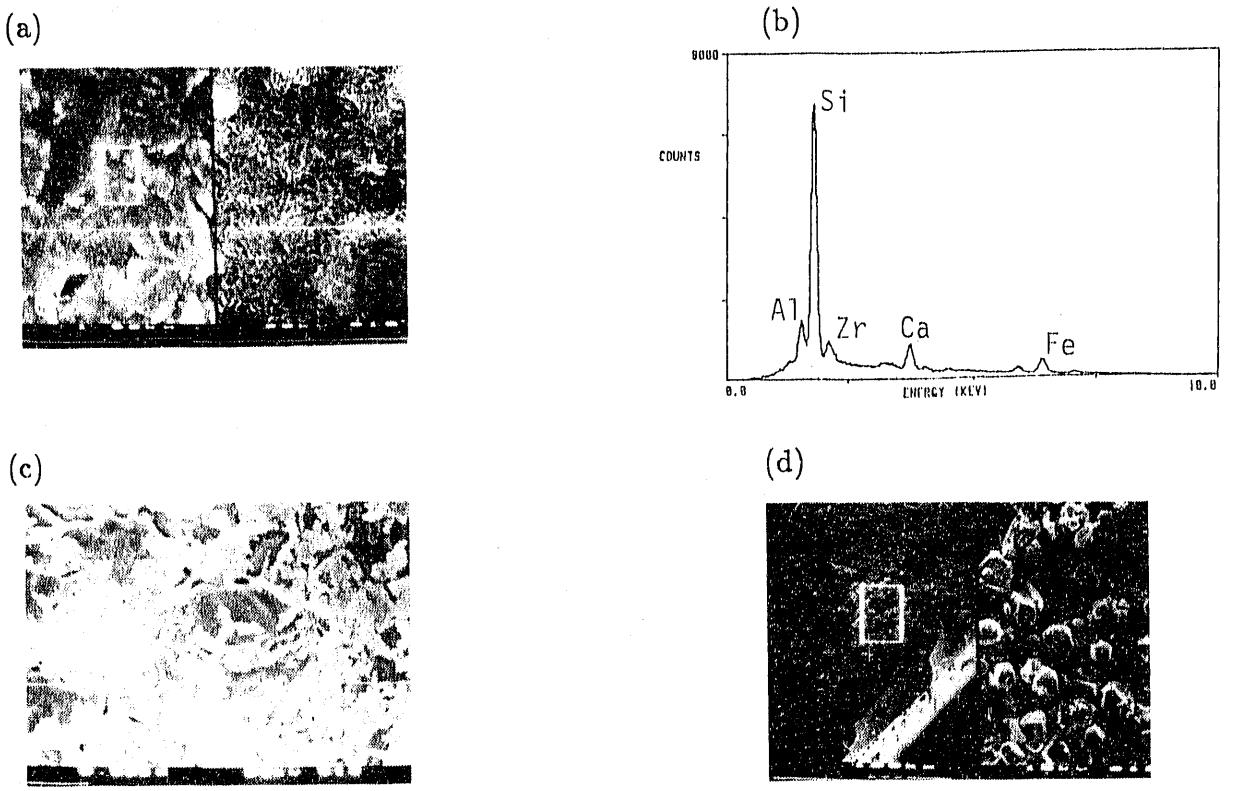

Fig. 12.
SEM Micrographs and Associated EDS Spectra from the Bottom Glass Section from Experiment P-III-6. (a) Reacted contact area (1000X/10,000X); (b) EDS spectrum of surface in (a); (c) exfoliated, precipitated area (990X); (d) yellow crystals (100X/1000X) from near the exfoliated region; and (e) EDS spectrum of yellow crystals. Note the high Na and Cl content

c. P-III-7 and P-III-8, 39-Week Samples

Sample P-III-8 visually appears to be somewhat more altered so it was investigated further by SEM/EDS. A Si-rich deposit, probably smectite, occurs on both the contact and noncontact regions of the top metal component. The noncontact-contact boundary is well marked (Fig. 13a). The Si-rich deposit also occurs in clumps, some of which contain Mn, Cr, or Fe (Figs. 13b and 13c/EDS). Based upon numerous EDS spectra, the Al content appears to be somewhat variable. A Ti-rich phase occurs rarely and seems to be intimately associated with clumps of Si-rich "clay" (Fig. 13d/EDS). It may be anatase (TiO_2), but XRD analysis was not possible to confirm this.

The bottom metal component is discolored in areas around the support pin welds, but there is no indication of glass-metal reaction. The noncontact-contact boundary is well defined. Like the top component, a Si-rich deposit also covers the bottom metal piece. Clumps of precipitates are extensively developed, many of which have the same composition as the deposit (Fig. 13e). Some thin disc-shaped masses are present which are rich in Ca and S suggesting they are either gypsum or anhydrite (Figs. 13f and 13g/EDS). Other, thicker disc-shaped grains occur which appear to be pieces of the surface layer that stuck to the metal when the sample was disassembled after termination of the experiment (Fig. 13h).

The circular noncontact areas are well marked on the top glass surface. However, there is no significant difference in composition between the noncontact and contact areas. The "as-cut" contours are partially obscured by growth of the reacted layer. Exfoliation of this layer has occurred in places, exposing the glass from below. In these areas, precipitates now partially cover the glass surface. These precipitates, like numerous clumps elsewhere, have a similar composition and appearance to that of the surface layer.

The bottom glass surface also appears highly reacted with the identity of the "as-cut" contours being almost obscured by the presence of a surface layer. The layer, as well as many clumps on the surface, have the same texture and composition as found on the top glass. However, in one area, a smooth overgrowth is present that is somewhat enriched in Ca. The surface layer has exfoliated in some places and a discontinuous cover of precipitates is present on the newly exposed surface.

The side glass near the bottom surface was also investigated by SEM/EDS. The surface has a textured appearance with a "cardhouse" type structure and composition consistent with smectite. There are two layers closest to the bottom surface with a precipitation front visible several millimeters up the side (Fig. 14a). Many chloride-bearing grains are present at this front (Fig. 14c/EDS). Some mottled regions of the upper layer are rich in Fe and Mn suggesting the presence of Fe-Mn oxides or hydroxides intermingled with smectite (Figs. 14d and 14b/EDS). The lower layer has a similar morphology and composition to the upper layer. In places where the lower layer has broken away during sample preparation, a view in the third dimension is possible (Fig. 14d). The layer appears to only be a coating on an otherwise smooth glass surface which suggests the layer developed solely by precipitation rather than by direct glass reaction. This is supported by the presence of small regions

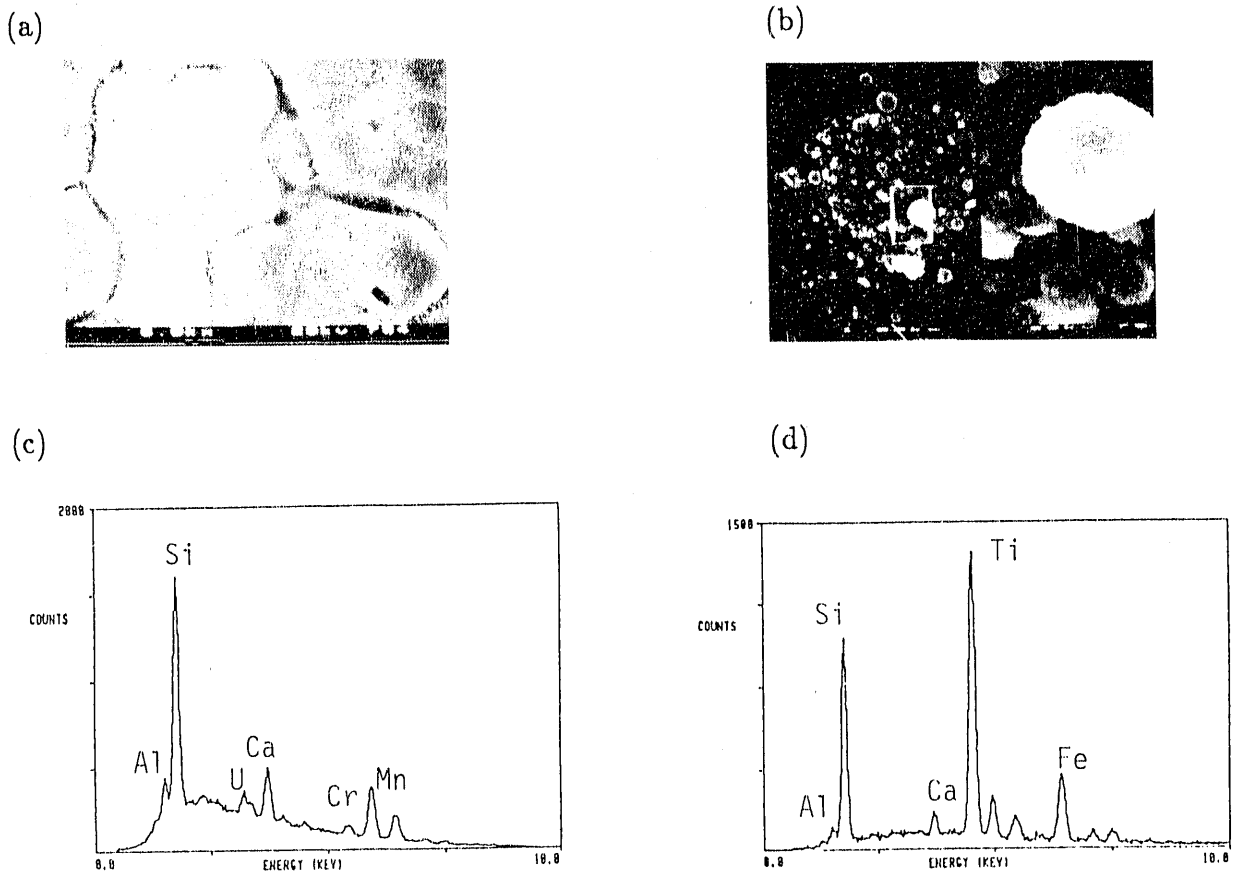

Fig. 13. SEM Micrographs and EDS Spectra of Features from the Top Metal Component of Experiment P-III-8. (a) Glass contact/noncontact interface (6000X); (b) Mn-enriched cluster of alteration products (1000X/10,000X); (c) EDS spectrum of material shown in (b); (d) EDS spectrum of Ti-rich grain

(e)

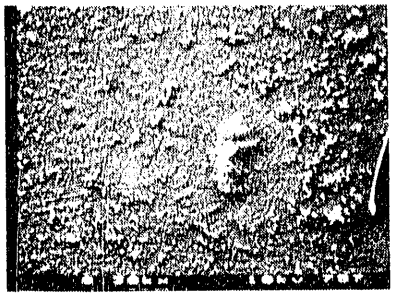

(f)

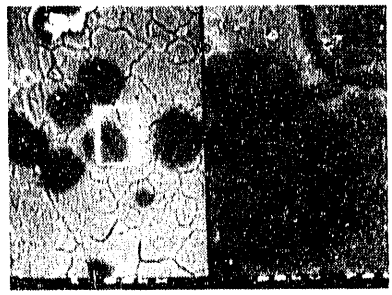

(g)

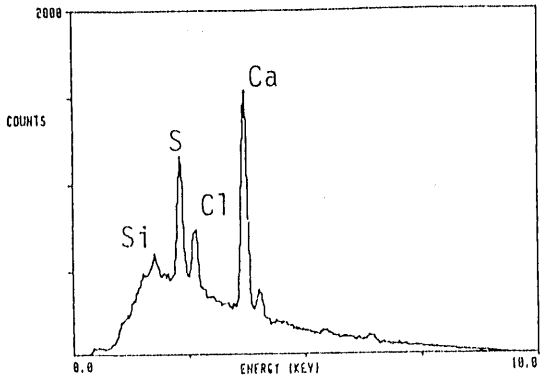

(h)

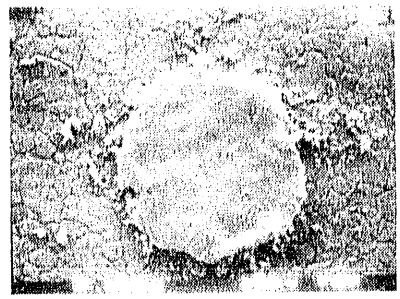

Fig. 13. Cont'd
SEM Micrographs and EDS Spectra of Features from the Top Metal Component of Experiment P-III-8. (e) micrograph (300X) showing general view of precipitate coverage; (f) micrograph (1000X/5000X) of dark splotches. (g) EDS spectrum of splotches shown in (f); and (h) micrograph (600X) of a piece of the altered layer from the glass that stuck to the metal component on separation

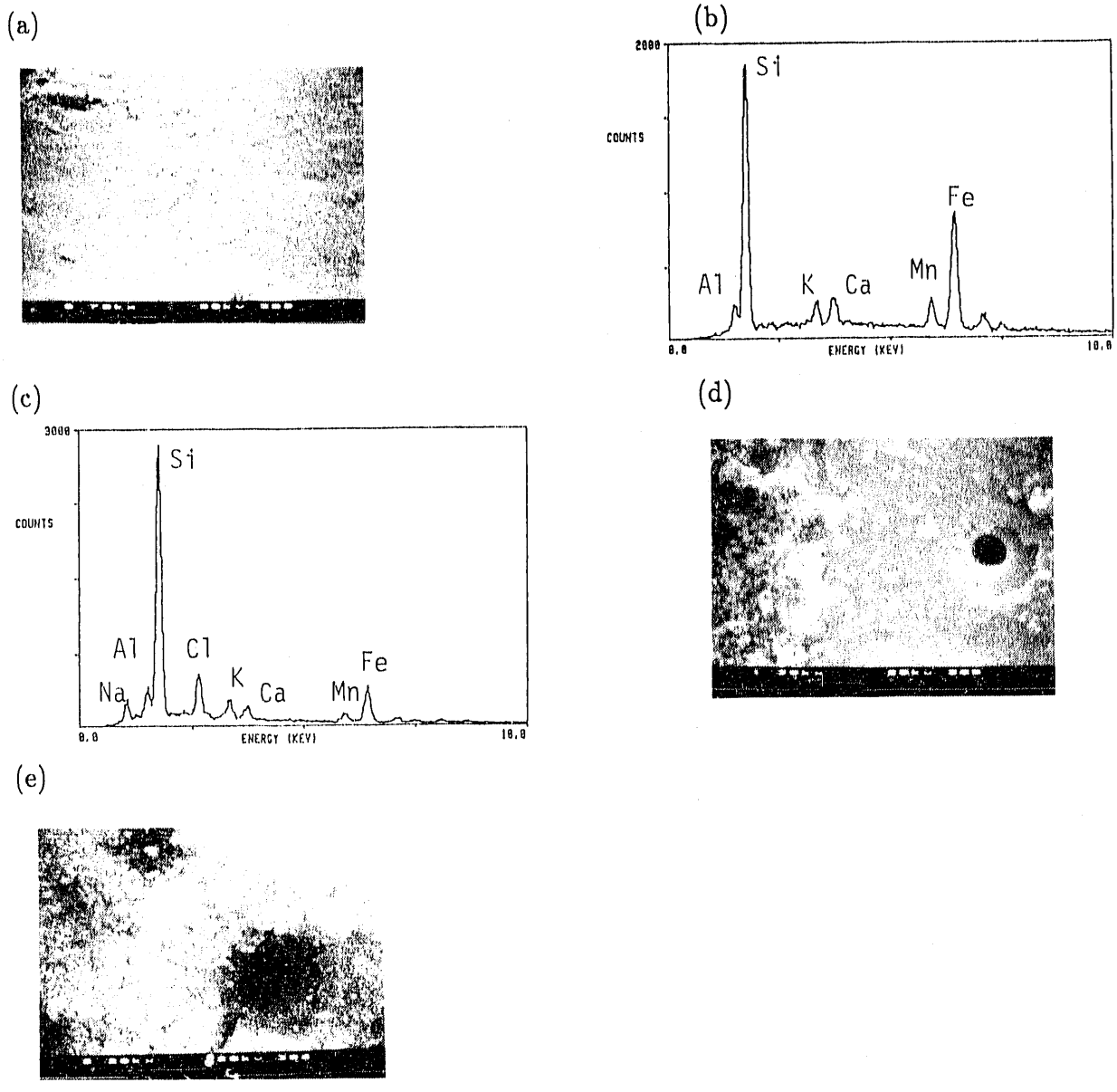

Fig. 14. SEM Micrographs and EDS Spectra of the Side Glass of P-III-8. (a) View (700X) of the precipitation front (see text); (b) EDS spectrum of precipitated surface layer; (c) EDS spectrum from the precipitation front where chlorides are intergrown with the Si-rich "clay"

where the lower layer is incomplete. Here, loosely connected precipitates encroach on small open areas where apparently etched glass is exposed (Fig. 14f). However, investigation of the layer formed on the side surface using analytical electron microscopy provides a more detailed description of the structure of the reacted glass, and should help identify the process by which the glass reacts (see addendum).

d. P-III-9 and P-III-10, 52-Week Samples

The glass surfaces of both samples were analyzed by SEM/EDS and SIMS, but the metal components were not examined.

(1) P-III-9

This sample appears to be more reacted than P-III-10. The top glass surface looks highly reacted and cracked and is covered with precipitates (Fig. 15a). However, the noncontact areas are not distinct from the contact areas. The light-colored streaks in Fig. 15a are due to charging along cracks in the surface layer. The layer is Si-rich and is essentially the same composition as observed for other samples (Fig. 15b/EDS). Exfoliation of portions of the surface layer is common (Fig. 15a). Other areas are in the processes of exfoliating as shown in Fig. 15c. The newly exposed glass has the appearance of having been etched (Figs. 15a and 15c). There are numerous precipitates on the surface, often associated with the exfoliated areas. Many are Ca- and S-rich and are probably gypsum or anhydrite (Figs. 15d and 15e/EDS). Round grains and thin threads of NaCl occur over the entire surface (Fig. 15f). Other chlorides, possibly $CaCl_2$, are also indicated from the EDS spectrum shown in Fig. 15g/EDS. Small grains of Fe-Mn oxide or hydroxide are often intimately associated with the Si-rich "clay" surface layer.

The bottom glass surface has distinctly lighter color noncontact areas (Fig. 16a). Like the top surface, a thick surface layer has developed which is extensively cracked and is exfoliating, especially in the noncontact areas (Figs. 16a, 16b, and 16c). The "as-cut" appearance is completely masked and there are numerous precipitates on the surface. Most of the precipitates, like those in Fig. 16c, are probably either gypsum or anhydrite.

SIMS profiles were obtained from the top and bottom surfaces. Silicon normalized profiles for several elements from the bottom surface are presented in Fig. 17. Lithium is depleted relative to Si to a depth of 2.5 μm, while Mg, Mn, and K (not shown) are relatively enriched close to the surface. Boron shows some depletion in the near-surface region.

(2) P-III-10

Only the bottom surface of P-III-10 was investigated. The noncontact areas are partially visible and the "as cut" contours are obscured by the growth of a Si-rich surface layer. This layer is generally coarser grained than observed on P-III-9 (Fig. 18a). Exfoliation of the surface layer has occurred in places, although to a lesser extent than on P-III-9. The newly exposed glass is etched and appears to be somewhat altered (Fig. 18b). Small round precipitates dot the surface which contain Ca and S and are probably either gypsum or anhydrite.

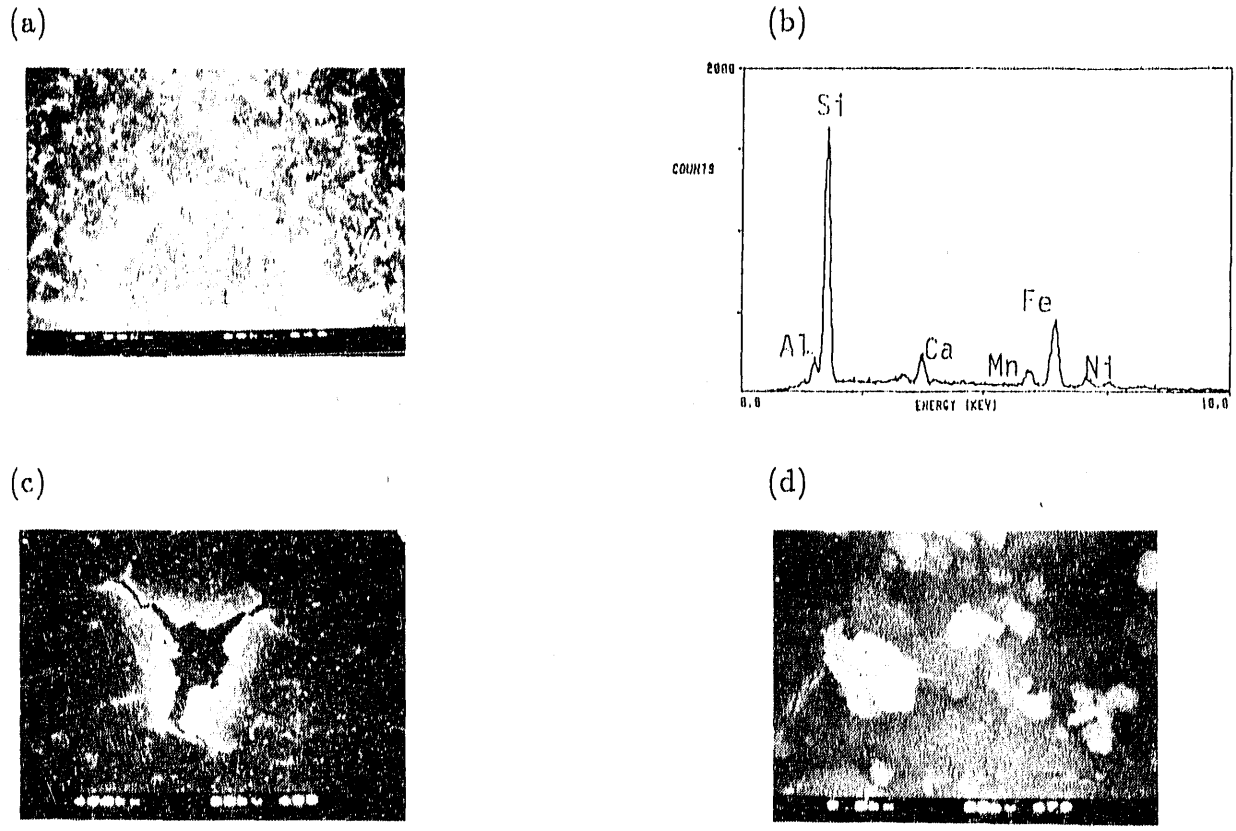

Fig. 15. SEM Micrographs and EDS Spectrum from the Top Glass Surface of P-III-9. (a) General surface with Ca/S-rich precipitates and exfoliated region (500X), (b) EDS spectrum of surface layer, (c) initial phase of exfoliation (400X), and (d) Ca-S precipitates on surface (5000X)

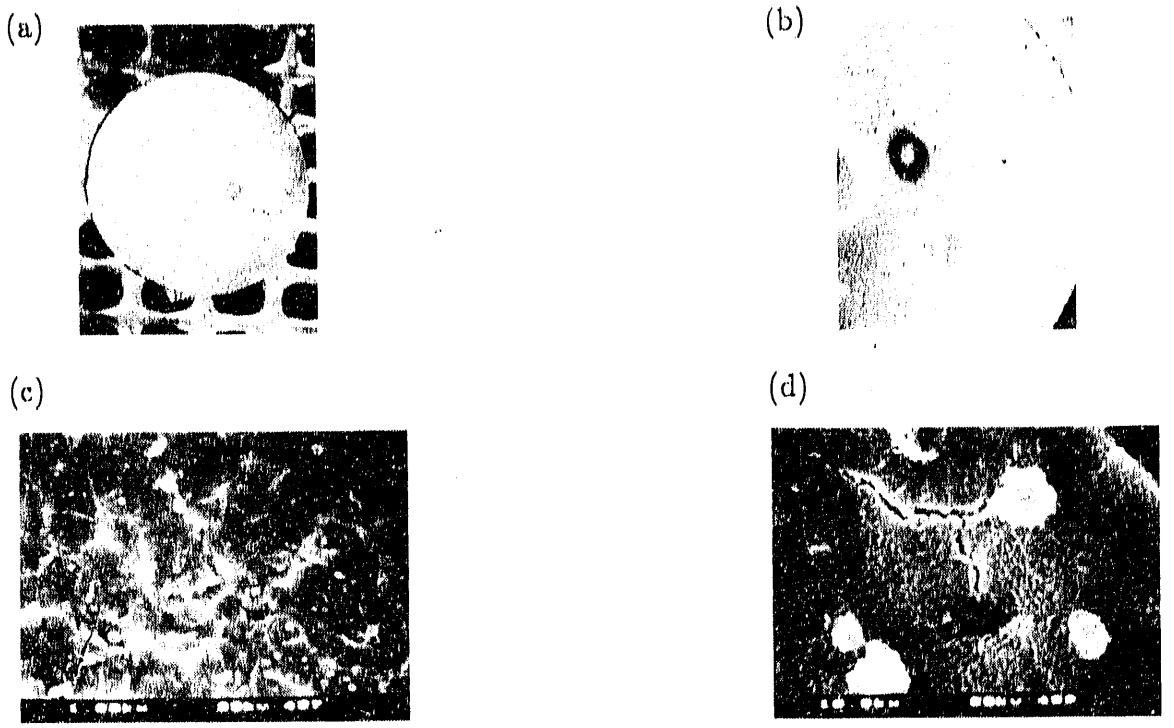

Fig. 16. Optical Photographs of the Bottom Glass Surface of P-III-9. (a) 6X; (b) ~12X, the spot with the dark halo is the result of a SIMS analysis. SEM micrographs of features from the bottom glass surface of P-III-9. (c) General surface appearance (1000X) and (d) higher magnification of surface (10,000X) showing a cracked region plus small Ca/S-rich grains

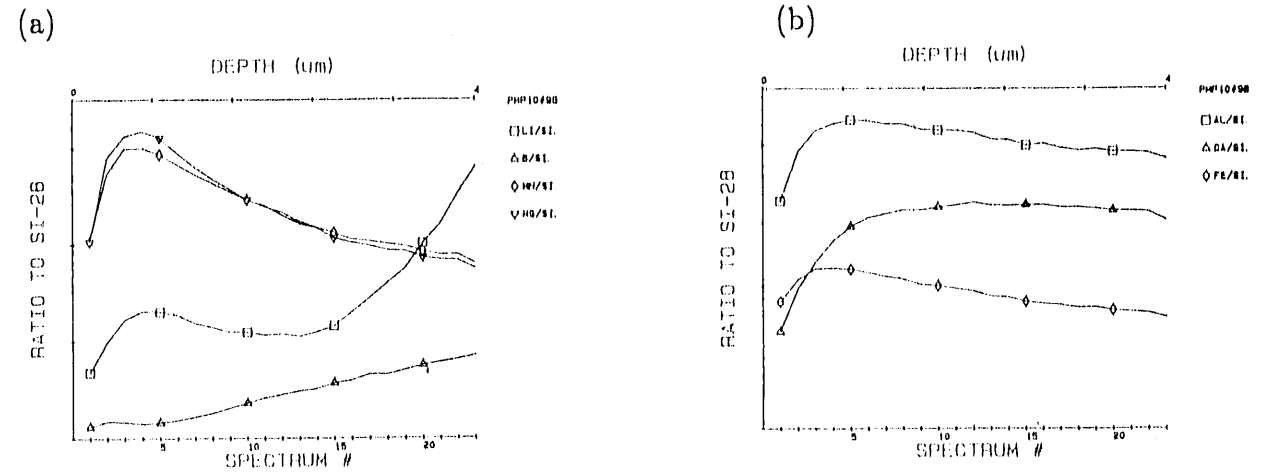

Fig. 17. SIMS Profiles of the Bottom Glass Section from Experiment P-III-9 in a Region of Glass-Metal Contact

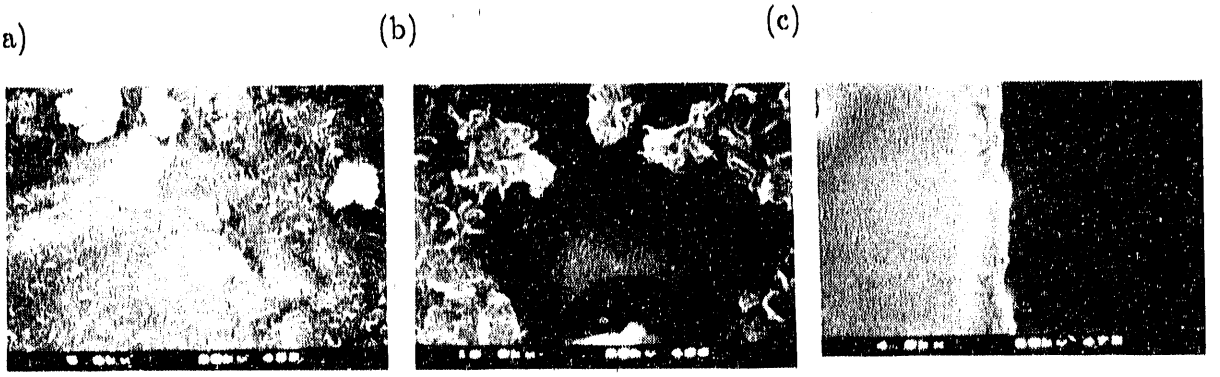

Fig. 18. (a) SEM Micrograph (5000X) Showing the Coarse-Grained Appearance of the Surface Layer; (b) Micrograph (10,000X) Showing Exposed Etched Glass; and (c) SEM Micrograph of a Cross Section of the Bottom Glass Surface from P-III-10

A polished cross section of the bottom glass was also prepared and studied by SEM (Fig. 18c). A band ~1.5 μm thick is visible at the edge of the glass. The band is comprised of regions of varying electron density contrast with the bright streaks due to charging at the sample-epoxy interface. A survey of the unreacted glass was performed to check for inhomogeneities in the glass. Overall, the composition is quite uniform except that traces of S and Cl are intermittently detectable.

SIMS profiles were obtained from the bottom surface and the side of the glass (Figs. 19a and 19b). The profiles, normalized to Si, are broadly similar to those from P-III-9. Lithium is depleted to a depth of ~1.5 μm on the bottom surface, which is consistent with the thickness of the altered layer observed by the SEM (Fig. 18c). Boron is also depleted in the near surface. The depletion is more gradual on the bottom than it is on the side.

3. Solution Analyses

Elemental releases from the continuous experiments are shown in Fig. 20, and normalized releases for selected elements are given in Table 9. The raw data and the background subtracted cumulative releases are included in Appendix I for both the continuous and batch experiments.

Partial blockage of the inlet lines occurred in P-III-2 after the second year of the experiment and has continued intermittently to date despite efforts to clear the line without disassembly of the system. However, at no time was the line completely blocked. As a result, less water was injected during these periods than was required.

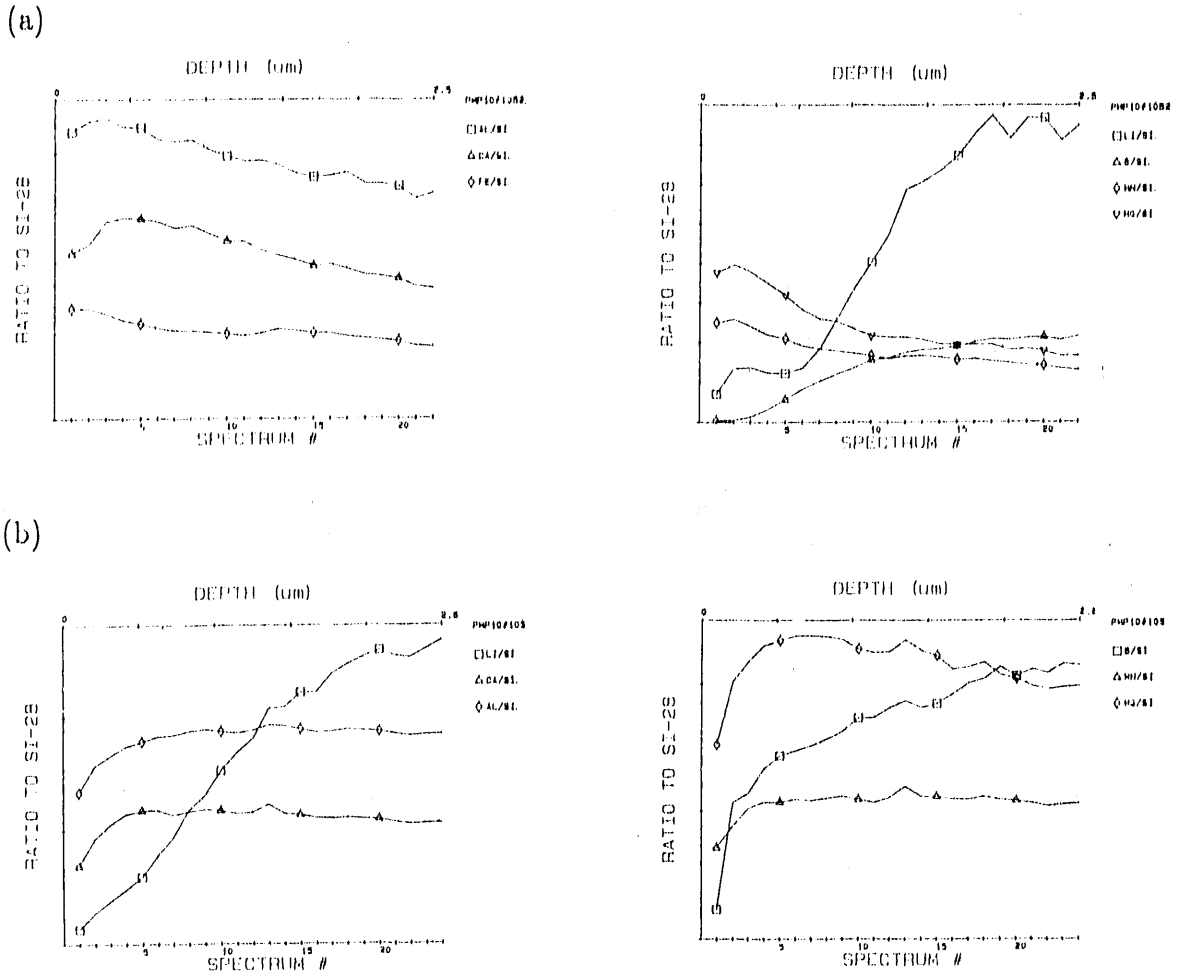

Fig. 19. SIMS Profiles of the Reacted Bottom and Side Surfaces of the Glass from Experiment P-III-10. (a) Bottom surface metal contact and (b) side surface

There is good agreement in the element release trends between the P-III-1 and P-III-2 experiments. There is some divergence apparent in the most recent analysis, which correlates with the smaller amount of fluid recovered from the P-III-2 vessel. Normalized release of Li is the greatest of all elements, reaching a value of ~6.5 g/m^2 after 260 weeks. The rate of Li release in both experiments decreased steadily for the first two years after which the rate became relatively constant. However, since about 170 weeks, the rate has increased fairly sharply, especially in the P-III-1 experiment (Fig. 20). The normalized release of B at 260 weeks is ~3.1 g/m^2 or about half that of Li. The trend of release closely follows that of Li over the entire duration of the experiments. The rate of U release has been fairly constant, although a slight increase seems to have occurred after about 170 weeks. The normalized release reached ~3.3 g/m^2 after 260 weeks which is about the same as for B.

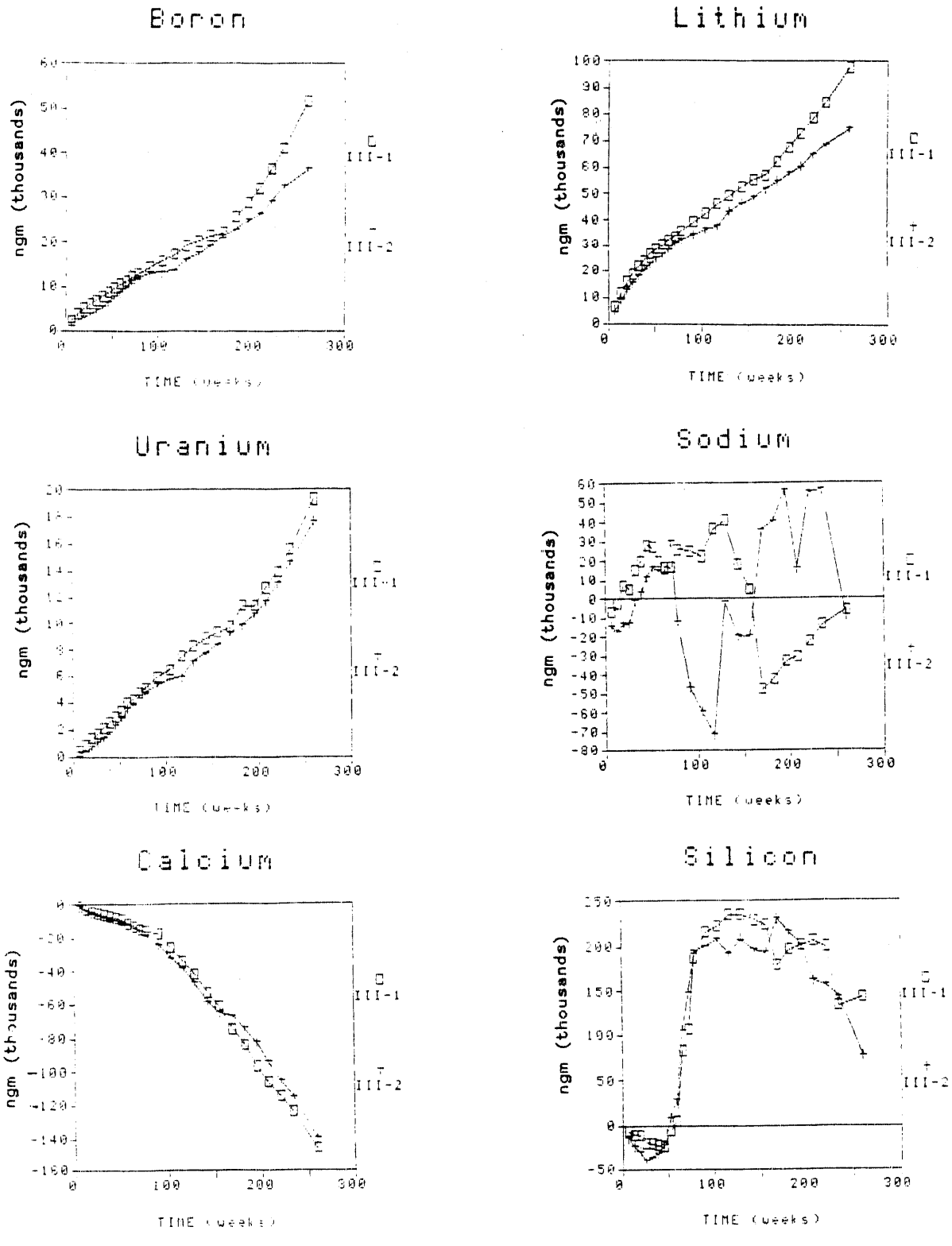

Fig. 20. Cumulative Release of Selected Elements from the P-III-1 and P-III-2 Continuous Experiments

Table 9. Normalized Release in P-III Series

Test #	Period (weeks)	Normalized Release (g/m^2) B	Li	U
P-III-3	13	0.2	1.0	0.1
-4	13	0.3	1.1	0.2
-5	28	0.7	1.8	0.6
-6	28	3.2	4.3	2.3
-7	39	3.1	4.2	2.1
-8	39	2.0	3.3	1.5
-9	52	3.7	5.6	2.6
-10	52	2.3	4.0	1.7
P-III-1	52	0.7	2.1	0.6
	104	1.1	3.2	0.8
	156	1.5	4.1	1.2
	208	2.2	5.4	2.3
	234	2.8	6.3	2.8
	260	3.6	7.3	3.4
P-III-2	52	0.5	1.9	0.4
	104	0.9	2.8	0.8
	156	1.4	3.8	1.1
	208	1.9	4.7	2.2
	234	2.3	5.3	2.7
	260	2.6	5.8	3.3

There is a consistent net negative release of Ca and Mg, indicating that these elements have been removed from the injected EJ-13 water and incorporated into the secondary phases. This is consistent with the ubiquitous occurrence of gypsum or anhydrite on the batch samples. The Mg may be accommodated in the Si-rich "clay" layer.

Both Na and Si have erratic release patterns which are similar in the P-III-1 and P-III-2 experiments. This variable behavior may be attributable to periodic precipitation and redissolution of NaCl (or Na_2CO_3?) which is observable on the batch samples. There was a net negative release of Si through the first year followed by a sharp positive release. Then, at the 104-week period for P-III-1 and the 91-week period for P-III-2, the Si release rate diminished. The reason for this behavior is unclear; however, it may be caused by secondary phase formation such as smectite. The sharp increase in release may indicate the initiation of surface layer exfoliation. Since the surface layer is composed predominantly of Si, if pieces of the layer were to fall into the solution, the subsequent acidification of the solution during sampling would preferentially enhance the Si concentration relative to the other elements.

Except for the 13-week samples, elemental release is usually much greater in the batch experiments compared to the continuous experiments (Table 9). At the 13-week period, releases are about the same in both types of experiments. While the WPA wash that is incorporated into the termination procedure of the batch experiments adds about 10% to the total release, this cannot account for the up to five-fold difference that is observed for some elements (Appendix I). The extent of element release is markedly different between the duplicate batch experiments terminated after 28 and 52 weeks. The reason for this discrepancy is unknown, although there is a correlation between larger release and a greater volume of solution recovered from the vessel upon termination of the experiments.

4. Discussion

The observation that normalized release of Li is twice that of B suggests these elements behave differently during glass reaction and that nonstoichiometric dissolution has occurred. SIMS profiles are consistent with the solution release trends in that B is retained to greater degree than Li in the residual altered layer (Figs. 10, 17, and 19). Another possibility is that B is incorporated in secondary phases. No B-bearing phases have been detected using the WDS system. While both Li and B are removed from the glass during reaction, Li is depleted to a greater depth than B (Figs. 10, 17, and 19). This suggests that Li is more mobile than B and, therefore, a greater volume of glass is leached of Li per unit time. Correlation of the SIMS data with AEM data will hopefully more clearly define the leaching process.

Depletion of Ca, Mg, and Na in solution is associated with the formation of secondary phases on the WPA. The erratic nature of Na release may be due to periodic precipitation of NaCl or Na_2CO_3? followed by dissolution.

The most abundant secondary phase is the Si-rich layer that is present on both the glass and metal components. Its composition and "cardhouse" type texture suggests it is composed of smectite (e.g., Figs. 12a and 12b/EDS). The deposit on the metal and at least some of the layer on the glass formed by precipitation. Other parts of the layer on the glass may have transformed in situ from the altered glass, although this has not been demonstrated definitively. Release of Si into solution does not follow a systematic trend (Figs. 20a and 20b). This may in part be due to exfoliation of the surface layer.

Exfoliation of the surface layer is observed in all samples that reacted for at least 26 weeks (i.e., P-III-6, P-III-8, P-III-9, P-III-10). Precipitation of Si-rich "clay" on the newly exposed glass indicates that exfoliation must have occurred during the experiment. This process has important implications for the rate of glass reaction and for interpretation of solution chemistry data.

C. P-IV Experiments

The purpose of these experiments is to examine the effect of reducing the water volume during each injection period. While maintaining the normal injection interval of 3.5 days, the drop volume is reduced by 50% to 0.038 mL. The surface area of the glass is also reduced by ~50%, which is the same as for the P-III experiments.

The experiments were initiated on 2/18/85 and have been completed through 247 weeks. The batch experiments were terminated in duplicate at 25.5 and 52 weeks. The continuous experiments are ongoing and have been sampled every 13 weeks up to 221 weeks and for longer intervals since. Two batches of EJ-13 water have been used (Table 4). The switch in batches occurred after 91 weeks. The experimental matrix is given in Table 10.

1. General Observations

The appearance of the WPA during the sampling periods and at termination was very similar to that noted for the P-III experiments. The top surface of glass was damp in the areas not in contact with the stainless steel and there was standing water around the circumference of each hole in the metal. There were small droplets of water present on the top surface of the stainless steel. However, there was no evidence of localized reaction between the metal and glass. The bottom surface had standing water around the circumference of the glass and between the glass and the metal rim. The regions of nonmetal contact were also wet. In some experiments water bridged the gap between the glass and the metal support pin(s).

The weight change measurements (Table 10) indicate that the glass lost weight during all experiments. There is good reproducibility between duplicate samples, and the 52-week samples show slightly more than twice the weight loss of the 25.5-week samples. The metal sections gained weight in most cases with the weight gain being greater for the shorter tests than the longer.

2. Component Analyses

The glass from all the terminated batch experiments was examined optically, and the top and bottom surfaces of P-IV-3 and P-IV-5 were investigated by SEM/EDS.

a. P-IV-3 and P-IV-4, 25.5-Week Samples

The general appearance of the two samples is similar. The noncontact areas on the bottom surfaces are clearly visible, appearing as light gray circles on a dark background. There is no such demarkation on the top surface of P-IV-3. However, small irregular whitish patches occur in the central portions of the noncontact areas. Dark circular regions are discernible on the top surface of P-IV-4. The side surfaces are generally shiny brown-black with irregular-shaped areas that correspond to regions of standing water during the experiments. This includes the lower third of the sides where a cracked and peeled bronze-colored scale is present. Near the top surface is an irregularly distributed whitish deposit.

Table 10. Experimental Matrix and Weight Change Results for the P-IV Series

Test No.	Test Period (weeks)	Date Started	Date Stopped	Initial Glass Mass (gm)	Final Glass Mass (gm)	Δ Mass ($gmx10^{-5}$)	SA Glass (cm^2)	Initial Top Canister Mass (gm)	Final Top Canister Mass (gm)	Δ Mass ($gmx10^{-5}$)
P-IV-1a	13	2/18/85	in progress	3.06736			6.90	2.35246		
P-IV-2a	13	2/18/85	in progress	2.92639			6.81	2.36709		
P-IV-3	25.5	2/18/85	8/19/85	3.17915	3.17880	(350)	6.84	2.35355	2.35306	310
P-IV-4	25.5	2/18/85	8/19/85	3.01384	3.01334	(500)	6.81	2.35334	2.35334	100
P-IV-5	52	2/18/85	2/17/86	3.03562	3.03438	(1240)	6.85	2.36914	2.36924	100
P-IV-6	52	2/18/85	2/17/86	2.74079	2.73976	(1030)	6.55	2.36495	2.36500	50

Cont'd

Table 10 (Cont'd)

Initial Bottom Canister Mass (gm)	Final Bottom Canister Mass (gm)	Δ Mass ($gmx10^{-5}$)	Initial Total Vessel Mass (gm)	Final Total Vessel Mass (gm)	Δ Mass ($gmx10^{-5}$)	Water Added During Testing
3.34578			319.14	319.65	0.51	0.975
3.33530			317.33	317.99	0.66	0.975
3.37079	3.37114	350	319.39	310.48	1.09	1.988
3.34849	3.34877	280	320.08	321.09	1.01	1.988
3.34193	3.34216	230	313.67	315.89	2.22	3.90
3.34688	3.34685	(030)	318.49	320.84	2.35	3.90

Examination of the bottom glass surface of P-IV-3 by SEM reveals a surface layer has developed similar to that observed on the P-III samples (compare Figs. 21a and Fig. 12a). The layer is Si-rich and is depleted in Na and enriched in Fe and Mn relative to the glass. The development of this layer in the noncontact areas is incomplete (Fig. 21b). Here, glass is still exposed over approximately 10% of the area. It appears that most of the surface layer has formed by precipitation (Figs. 21b and 21c). The glass is quite smooth, even at 10,000X magnification, although there is some fine-scale structure indicating reaction has occurred (Fig. 21c).

The top glass surface has retained most of its original "as cut" appearance; however, clear evidence of reaction is revealed at higher magnification (Figs. 22a, 22b, and 22c). A Si-rich layer has developed across the entire surface.

The contact and noncontact areas are texturally indistinguishable at the scale of the SEM. There are numerous isolated precipitates present which are too small for XRD analysis, but EDS spectra indicate several different compositions. Some have essentially the same composition as the surface layer, while others are composed only of silica and are possibly quartz or opal. Some calcite is present. There are also clusters of precipitates rich in Cr, Fe, and Mn and are probably an oxide or hydroxide phase.

b. P-IV-5 and P-IV-6, 52-Week Samples

The bottom surfaces of these two samples have clearly marked noncontact areas that are light gray in color. These areas are intact on P-IV-6, but on P-IV-5, a surface layer is observable which is cracked and has separated from the glass in many places. This is similar to the appearance of several samples from the P-III experiments.

The top surfaces are very different in appearance. The noncontact areas on P-IV-5 are fairly well marked, being darker than the light blue-green to brown contact areas. Small whitish patches of precipitates are present in the center of a few of the noncontact areas. The noncontact areas on P-IV-6 are barely discernible. An extensive array of saw marks is the most prominent feature which form whitish streaks on a relatively uniform dark background.

The bottom surface of P-IV-5 has a similar appearance to that of P-IV-3 under the SEM, except that there are many small Ca- and S-bearing grains which are probably gypsum or anhydrite (Fig. 23a). A Si-rich layer is present but it is incomplete, exposing glass from below. In some places, the layer is cracked and pieces have exfoliated (Fig. 23a). The process of cracking and exfoliation has begun even before the surface layer has completely developed. The exposed glass surface shows only slight evidence of etching but, otherwise, it looks unreacted (Figs. 23a and 23b). However, the early stages of alteration, where a gel layer forms, may not be readily discernible by SEM.[12] Precipitation of a Si-rich layer appears to be quite rapid in the freshly exposed areas.

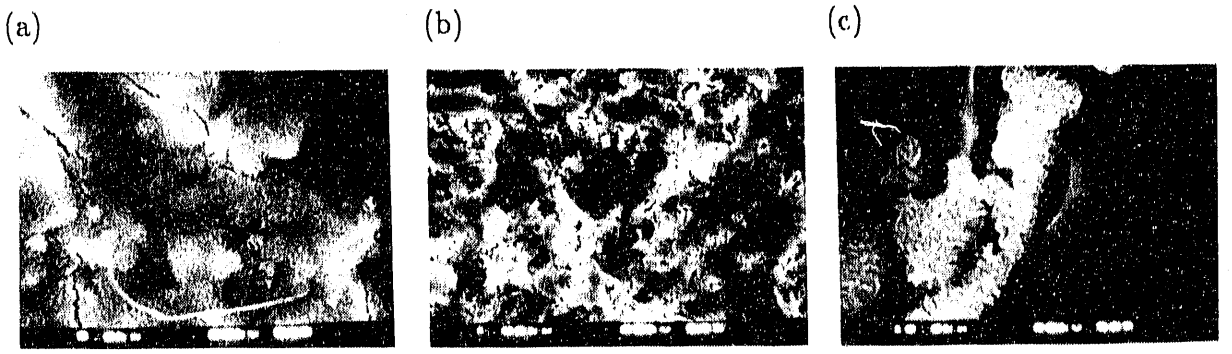

Fig. 21. SEM Photomicrographs of the Bottom Glass Surface from Experiment P-IV-3. (a) General surface, ss contact (5000X); (b) general surface, noncontact (1000X); and (c) localized precipitation in the noncontact area (10,000X)

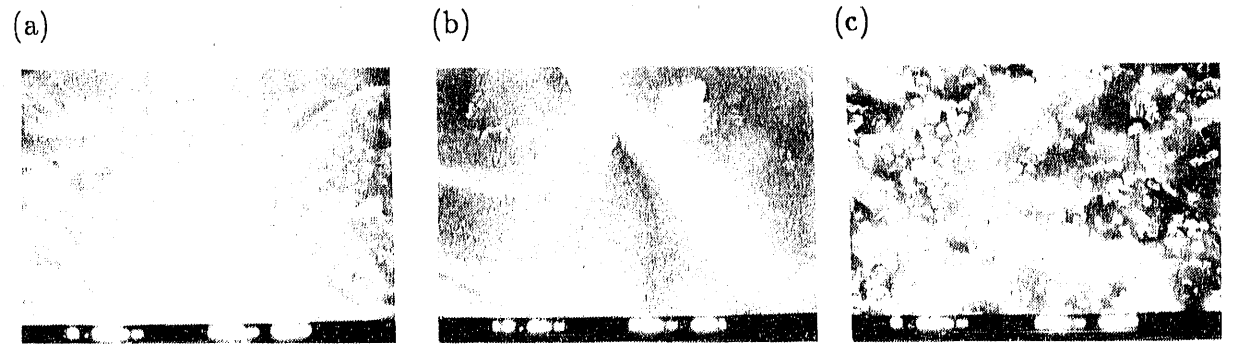

Fig. 22. SEM Photomicrographs of the Top Glass Surface from Experiment P-IV-3. (a) General surface (2000X); (b) general surface texture (10,000X); and (c) general surface (5000X)

Fig. 23. SEM Micrographs of the Bottom Glass Surface from Experiment P-IV-5. (a) Exfoliation of surface layer and numerous Cs-S grains (600X) and (b) glass surface with only partial coverage of precipitates (300X)

The top surface of P-IV-5 is also similar to the top of P-IV-3. Although the "as cut" contours are still readily visible, a uniform continuous fine-grained surface layer has developed (Fig. 24a). Its Si-rich composition is typical of the layers developed on other samples. No exfoliated areas are present. However, there are numerous places where the layer is cracked and small pieces are raised up from the glass (Fig. 24a). This suggests an incipient stage in the exfoliation process. The surface is dusted with small (≤ 2 μm) round grains of gypsum or anhydrite (i.e., Ca + S bearing). Other precipitates include clusters of Cr-, Mn-, Fe-, and Ni-bearing grains (Fig. 24b) which are probably oxide or hydroxide phases. Their composition is variable from containing mostly Fe and Ni, to containing Ni only, to containing predominantly Cr and Mn (Figs. 24c/EDS, 24d/EDS, and 24e/EDS). Others have compositions similar to stainless steel (compare Fig. 24f/EDS with Fig. 2c/EDS).

3. Solution Analyses

Elemental releases from the continuous experiments are presented in Fig. 25 and normalized release of Li, B, U, Na, and Si are given in Table 11. The raw data and the background subtracted cumulative releases are included in Appendix I for the batch and continuous experiments.

The trends in element release are similar between experiments P-IV-1 and P-IV-2 (Fig. 25). However, the magnitude of release from P-IV-2 is on the order of two times that of P-IV-1. It is not clear why these two experiments, which show the same release pattern, should have such different overall release. In both experiments Li, B, Na, Si, and U all have positive releases. After 182 weeks, however, a sharp reduction in the rate of release is apparent for all these elements suggesting a slowing of glass reaction and/or release from the WPA.

Lithium has the greatest normalized release, although it is not much greater than B or Na (Table 11). Release of U is only slightly less than B and Na. Silicon release is much less than these elements. This is attributable to the formation of the Si-rich surface layer on the glass and metal which acts as a sink for Si. The only element with a negative release is Ca. This indicates significant precipitation of a Ca-bearing phase or phases which depletes Ca in the EJ-13 water. This correlates with the observation of tiny grains of gypsum or anhydrite distributed over the surfaces of the batch samples.

4. Discussion

The top and bottom surfaces in the P-IV batch experiments have a different appearance visually as well as under the SEM. The surface layer on the bottom surfaces has a textured appearance and coverage is incomplete. In some places, it is evident that pieces of the surface layer have exfoliated, exposing patches of glass from below. Elsewhere, it appears that the surface layer never developed completely across the glass. Based upon the generally unreacted appearance of the exposed glass, and the distribution of new deposits in the partially covered areas, it seems that the surface layer has formed mostly by precipitation. Other precipitated phases are conspicuous by their absence.

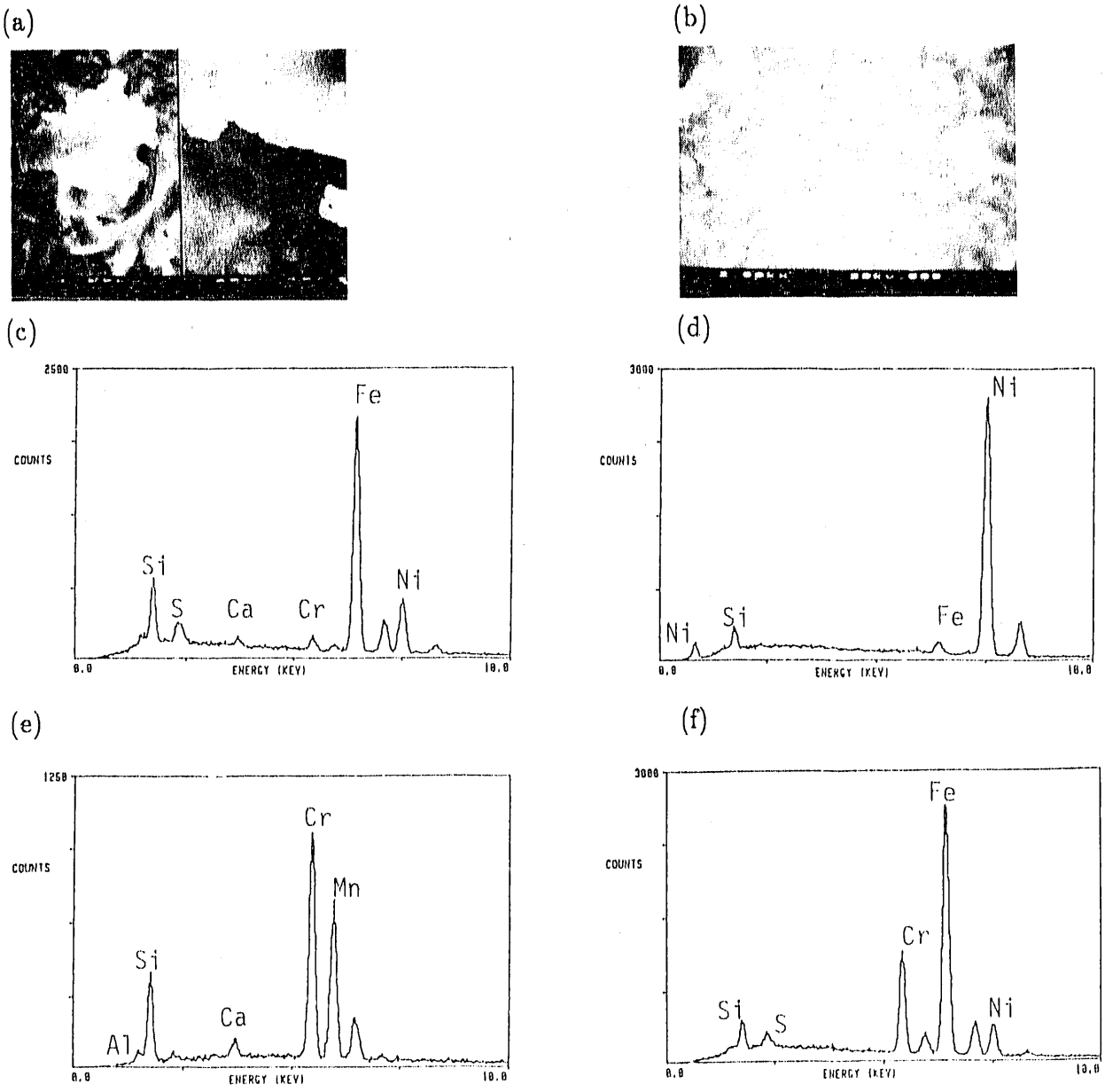

Fig. 24. SEM Micrographs and EDS Spectra of Reaction Products on the Top Surface of P-IV-5. (a) Micrograph (2000X/10,000X) of surface layer); (b) micrograph (2000X) of surface layer and Cr-, Mn-, Fe-, and Ni-bearing grains; (c-f) EDS spectra of grains shown in (b)

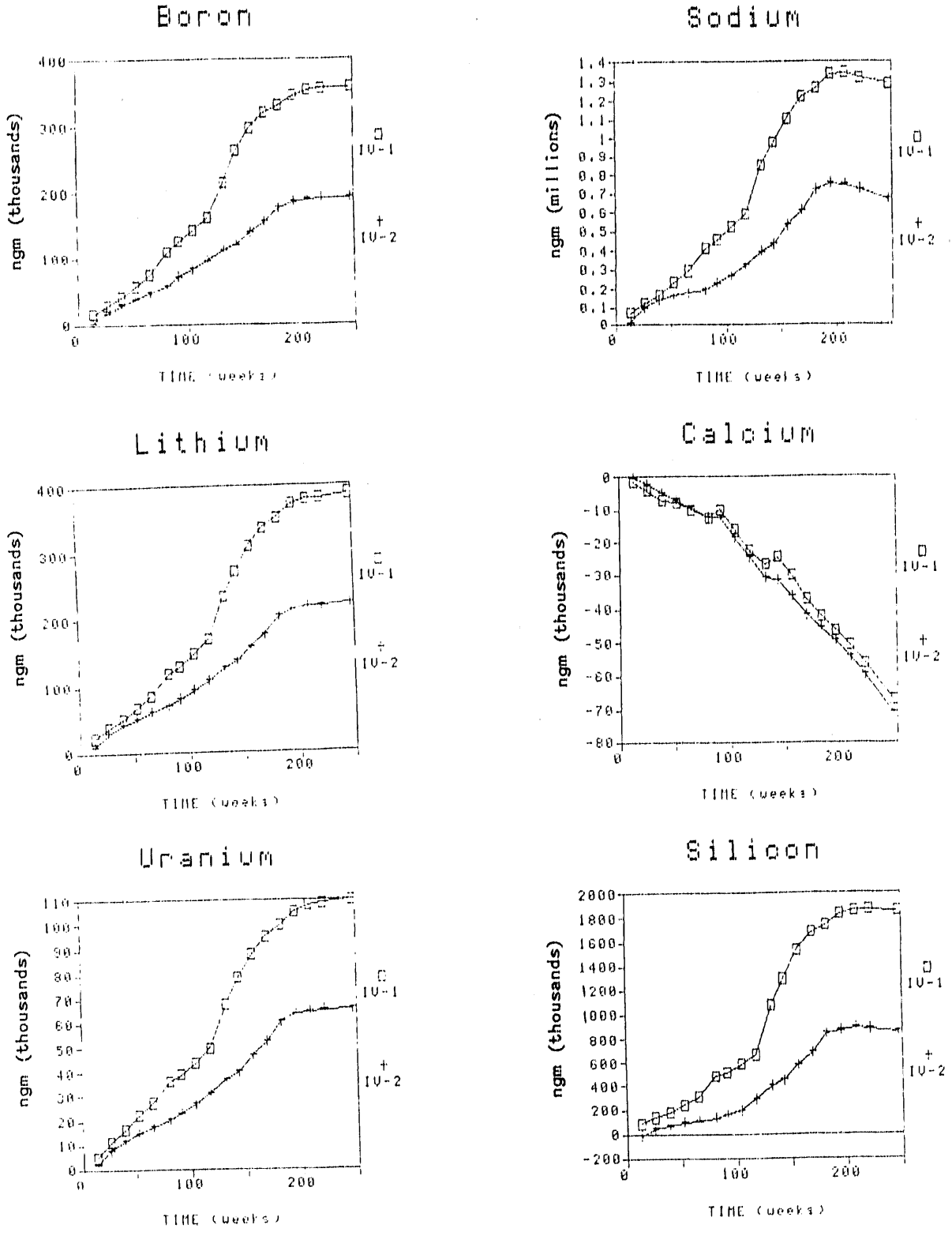

Fig. 25. Cumulative Release of Selected Elements from the P-IV-1 and P-IV-2 Continous Experiments

Table 11. Normalized Elemental Release for the P-IV Series

Test #	Period (weeks)	Normalized Release (g/m^2)				
		Na	Si	B	Li	U
P-IV-3	25.5	2.4	0.6	1.4	2.3	1.0
P-IV-4	25.5	2.1	0.6	1.2	2.0	1.0
P-IV-5	52	4.4	1.5	2.9	3.8	2.0
P-IV-6	52	4.5	1.0	1.7	3.1	1.0
P-IV-1	52	4.1	1.4	3.9	5.0	3.9
	104	9.3	3.4	9.8	11.0	7.8
	156	19.8	9.0	20.6	23.2	15.8
	208	24.2	10.9	24.6	28.4	18.8
	247	23.2	10.9	24.9	29.0	19.7
P-IV-2	52	2.9	0.6	2.7	3.8	2.7
	104	4.8	1.2	5.8	7.1	4.8
	156	9.7	3.4	9.7	11.9	8.5
	208	13.5	5.3	13.2	16.4	11.7
	247	12.2	5.1	13.4	16.7	12.0

In contrast, the top surfaces are completely covered with a rather uniform fine-grained material whose morphology is only apparent at very high magnification. The "as-cut" contours of the original glass surface are still easily discernible. Cracking and puckering of the layer are visible but this has not progressed to the point of exfoliation. The uniformity of this deposit, and the preservation of the original surface topography, suggest this layer formed mostly through alteration of the glass rather than by precipitation. A precipitated layer tends to have irregular coverage and masks surface features. However, numerous small precipitated grains rich in Ca and S or Cr, Mn, Fe, and Ni occur on the surface.

The P-IV experiments have the greatest normalized elemental release of any of the parametric experiments. This is a curious result considering that the volume of injected water is less than for the other experiments. It is possible that the smaller fluid volume saturates more rapidly, thereby causing precipitation of secondary phases. This could in turn enhance glass reaction by maintaining solute concentrations significantly below the apparent saturation level for the glass. However, the amount of precipitates on the P-IV samples is certainly no more and probably less than that observed on samples from other experiments. Furthermore, observation of the WPA's during sampling of the continuous experiments indicates that the surfaces were always wet or damp which is not the case for most other experiments. This suggestes greater

water-glass contact despite the fact that less water is injected. An explanation for the high release in the P-IV experiments may be that glass reaction is continuous due to the perpetual availability of water. In other experiments, where WPA surfaces are occasionally observed to be damp or dry, glass reaction would only be periodic in nature.

D. P-V Experiments

In this set of experiments, the injection rate is reduced from one drop every 3.5 days to one drop every 14 days. All other parameters follow the standard configuration and procedure. The experimental matrix is given in Table 12. The P-V series was initiated on 6/10/85 and the batch experiments were terminated after 26, 52, 110, and 254 weeks. One continuous experiment has been in progress for 234 weeks while the other was terminated after 39.5 weeks because of problems that arose with the WPA during sampling. At the onset, the experiments were conducted using silicone gaskets in an attempt to minimize water loss. This sort of gasket has been used in MCC-1 type leaching experiments with no observed loss of solution.[13] However, in the P-V experiments, the silicone rubber extruded inside the vessel during closure, providing the opportunity for Si contamination of the solution that collected at the bottom of the vessel. The gasket material in the continuous experiments was changed to Teflon^{TM} after the 26-week sampling.

1. General Observations

Upon termination of the batch experiments, the bottom of the WPA was always wet with some standing water present. The top of the WPA ranged from wet with standing water rimming the inside of the circular holes in the metal, to damp with no standing water, to completely dry in the exposed surface areas. For the continuous experiment, the bottom was usually wet with standing water, however, sometimes it was damp or dry. The top ranged from wet to dry, with dry being the most common state.

All the metal components have a shiny appearance with no local discoloration occurring in any of the experiments. No particulates were ever observed in the solutions during sampling. The glass gained a small amount of weight in all the experiments (Table 12). Some of the metal components gained a very small amount of weight while others showed a slight weight loss.

2. Component Analyses

The glass from all the terminated batch experiments was examined optically. The top and bottom surfaces of P-V-3, P-V-4, and P-V-7 were studied by SEM/EDS, but only the top of P-V-6 was investigated. None of the metal components were examined in detail.

Table 12. Experimental Matrix and Weight Change Results for the P-V Series

Test No.	Test Period (weeks)	Date Started	Date Stopped	Initial Glass Mass (gm)	Final Glass Mass (gm)	Δ Mass ($gmx10^{-5}$)	SA Glass (cm^2)	Initial Top Canister Mass (gm)	Final Top Canister Mass (gm)	Δ Mass ($gmx10^{-5}$)
P-V-1a		6/10/85	in progress	10.06318			13.6	2.63885		
P-V-2a	39.5	6/10/85	3/13/86	9.98827			13.4	2.61856	2.61860	4
P-V-3	26	6/10/85	12/09/85	10.13239	10.13270	310	13.6	2.62487	2.62490	30
P-V-4	52	6/10/85	6/09/86	9.99708	9.99739	310	13.5	2.62150	2.62150	0
P-V-5	52	6/10/85	6/09/86	10.09275	10.09309	340	13.5	2.62564	2.62552	(120)
P-V-6	110	6/10/85	7/20/87	9.89224	9.89259	350	13.2	2.61303	2.61300	(30)
P-V-7	254	6/10/85	4/23/90	9.91531	9.91535	4	13.4	2.61129	2.61133	4

Cont'd

Table 12 (Cont'd)

Initial Bottom Canister Mass (gm)	Final Bottom Canister Mass (gm)	Δ Mass ($gmx10^{-5}$)	Initial Total Vessel Mass (gm)	Final Total Vessel Mass (gm)	Δ Mass ($gmx10^{-5}$)	Water Added During Testing
3.41033			320.60			
3.40645	3.40668	23	325.98			
3.41020	3.41022	20	320.39	320.95	0.36	0.975
3.51410	3.51414	40	323.78	325.29	1.51	1.95
3.39282	3.39268	(140)	319.30	320.44	1.14	1.95
3.40535	3.40534	(10)	318.49	321.13	2.64	4.05
3.39052	3.39062	10	317.91	322.49	4.58	9.73

a. P-V-3, 26-Week Sample

The top surface has clearly marked circular regions corresponding to the noncontact areas. Five of the circular regions are a light gray in contrast to the brown/black background of the glass. The remaining two circular regions have a splotchy light blue-gray appearance, as though the reaction has not progressed to the extent observed in the other noncontact areas. The general appearance of the top surface is not much different than the bottom surfaces from the P-III and P-IV experiments. Several string-like deposits occur at the noncontact-contact boundary. Approximately one half of the contact area has a bluish cast. Superimposed upon this color scheme is a coarser area caused by saw marks. There is a mottled appearance in this region. This appears to be the result of puckering of the surface layer away from the glass. Within some of the saw marks there is a deep blue iridescent appearance, possibly from exposed glass.

For the most part, the top surface preserves the original "as-cut" appearance. A surface layer is developing, although it is not complete and glass is still exposed (Fig. 26a). The distinction between the original glass and the surface layer is not always clear. In general, the sharp edges and ridges become more rounded and stress and chattermarks begin to disappear (Fig. 26a). In some areas, a textured surface is beginning to develop, visible only at high magnification. A Si-rich deposit, essentially the same composition as the surface layer has locally precipitated (Fig. 26b). This is the origin of the string-like marks observed optically at the noncontact-contact boundary. In the rougher regions (caused by saw marks), the surface layer is beginning to pucker and pull away from the glass (Fig. 26c). No complete exfoliation has occurred.

There are a number of phases that have precipitated on the top glass surface. In addition to the Si-rich deposit, small isolated clumps of Si-rich "clay" are present on the surface. These often have $CaSO_4$ intermingled with the "clay". Small "flowers" of $CaSO_4$ (whether this is gypsum or anhydrite has not been determined) occur randomly on the surface (see Figs. 26a and 26c). The next most abundant phase is Cr-Mn rich and occurs mostly in small (<5 μm) spheres, although some grains are tabular. Some grains have Mn > Cr and contain Fe, but the dominant composition is Cr and Mn only with Cr > Mn (Fig. 26d/EDS). These are probably oxides or hydroxides. One portion of the surface has colonies of small Cr-Mn grains (Fig. 26e). The abundance of Cr is unusual and this phase has only rarely been observed on the stainless steel components of other experiments (e.g., on P-VIII-7). Several other precipitated phases include silica, Al-rich grains, NaCl, KCl, calcite, and a Ca-P phase, possibly apatite.

The noncontact areas on the bottom surface are poorly defined, being only a little lighter in color than the brown-black contact areas. Like the top, there is a rougher region which has a coarse speckled appearance.

The surface layer is less well developed than the top. The criteria described for the top glass were used to distinguish altered and unaltered surfaces. The layer consists of dispersed altered areas which have an irregular distribution and appear to be a function of the original surface roughness. No puckering of the altered surface was observed. Unlike most other experiments, the top surface appears to be more reacted than the bottom surface.

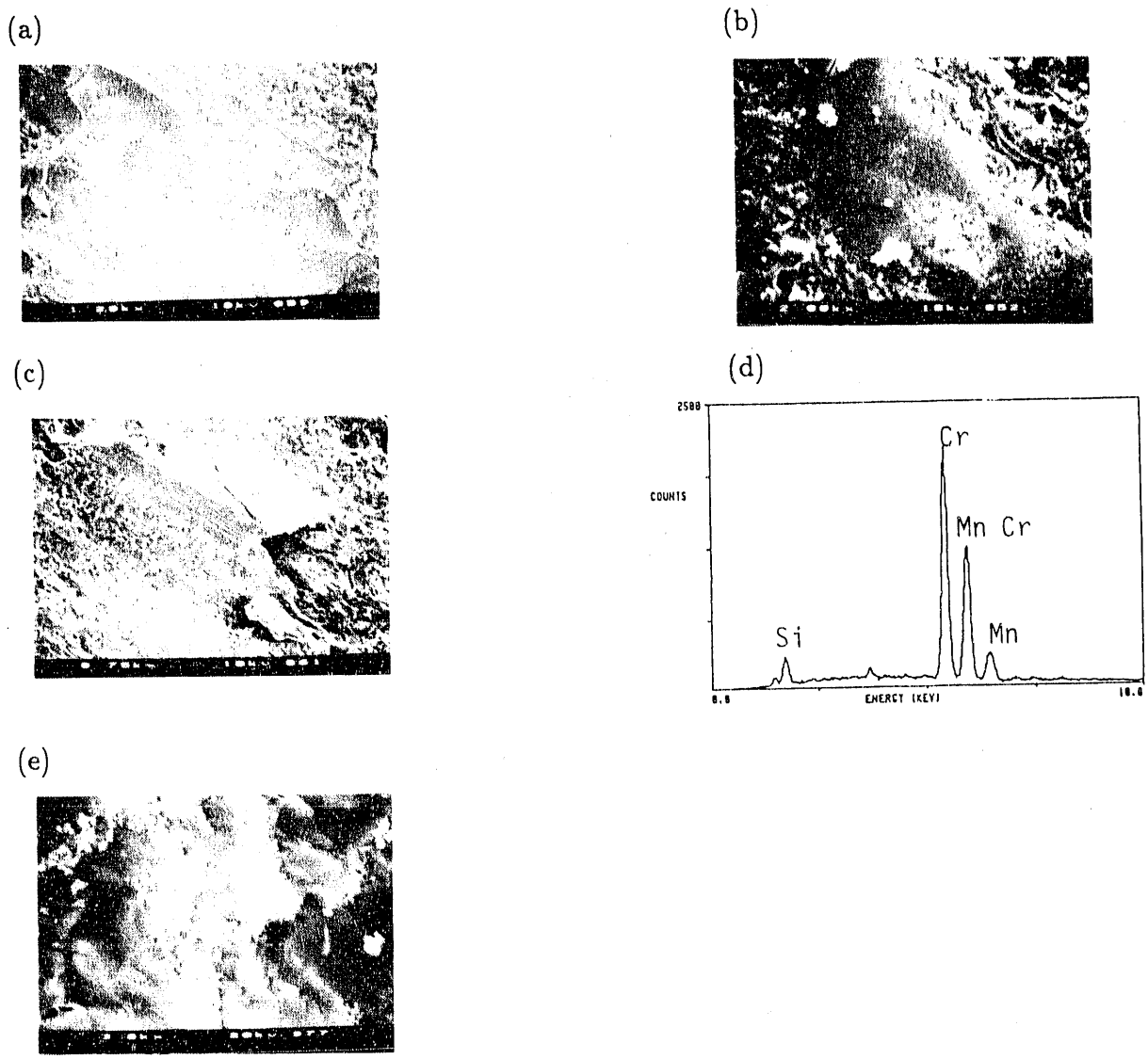

Fig. 26. SEM Micrographs of the Surface Layer and Reaction Products on the Top Surface of P-V-3. (a) 1200X, (b) 2000X, (c) 750X, and (e) 3000X (see text).

Small patches of precipitates occur on both the altered and unaltered surfaces. The amount of precipitates is small compared to the top glass. The most common phases are Si-rich "clay" and $CaSO_4$ (gypsum or anhydrite). In addition to occurring as small "flowers," there is a large round mat (~130 mm) of $CaSO_4$ near the edge of the glass There are a number of beam sensitive grains distributed on the surface that appear to only contain Na like those observed on the P-II experiments. These may very will be Na_2CO_3. Other phases include calcite, dolomite, Al-rich grains, mixed grains with Na, K, Ca, Cl, and S, and a Ti-bearing mixed grain.

b. P-V-2, 39.5-Week Sample

Although this sample was intended as a continuous experiment, it was abruptly terminated during the 39.5-week sampling due to problems with the WPA. The top surface has a similar appearance to the top of P-V-3. Most of the surface has a brown-black color. Several areas in the contact and noncontact areas have a light blue cast. The noncontact areas are partially covered by light-colored precipitates. String-shaped deposits occur at the noncontact-contact area boundaries. There is also a small coarse-grained area that has a speckled appearance.

The bottom is generally coarser grained with speckles like that of P-V-3. The noncontact areas are gray with bluish haloes extending into the contact areas. Very few precipitates are observable.

c. P-V-4 and P-V-5, 52-Week Samples

Sample P-V-4 was investigated optically and by SEM/EDS, but P-V-5 was only examined optically. The top glass surfaces are somewhat different in appearance. The contact areas on P-V-4 are either brown-black or have a milky blue hue, similar to the tops of P-V-3 and P-V-2. The majority of the P-V-5 contact area has a shiny honey-brown color. On both samples the noncontact areas have a deposit of precipitates in the middle, surrounded by a grayish region. Discontinuous string-shaped deposits are developed at several of the noncontact area boundaries.

From SEM/EDS observation, the top glass of P-V-4 has reacted much more than the top of the P-V-3 experiment. The surface has a fuzzy appearance at low magnification indicating that an altered layer has developed. At high magnification, the surface has a variable texture. In some places it is quite smooth with only a hint of fine scale structure. Elsewhere, a coarser texture is developed, reminiscent of the "cardhouse" texture observed on the P-VIII samples (Fig. 27a). There is a range in the coarseness which may correspond to progressive recrystallization of an initially amorphous hydrated layer, although this is only a hypothesis. Alternatively, the coarser areas may have formed by precipitation.

In a number of places the surface layer is cracked and exfoliation has begun. This is best developed in the noncontact areas although it also occurs in the contact areas, especially where the "as-cut" surface is rough. A more complex layer structure is revealed in these areas. The altered layer is actually composed of three or four discrete layers (Fig. 27b). The bottom layer has a coarse texture. Above this are one or two smoother layers. The outermost layer is coarse, having an appearance similar to the bottom layer. The outermost layer is discontinuous, suggesting it formed by precipitation. This patchy distribution results in the observed variation in surface texture described above. The compositions of all the layers are similar and are consistent with the coarse layers being Fe-rich smectite. Small clumps of precipitates are present on all exposed surfaces and have the same composition as the altered layer (see Figs. 27a and 27b). In some places the smooth layer has a mottled appearance (Fig. 27c). EDS analysis indicates that this is due to the incorporation of Cr-Mn±Fe oxide or hydroxide grains within this layer (Fig. 27d/EDS).

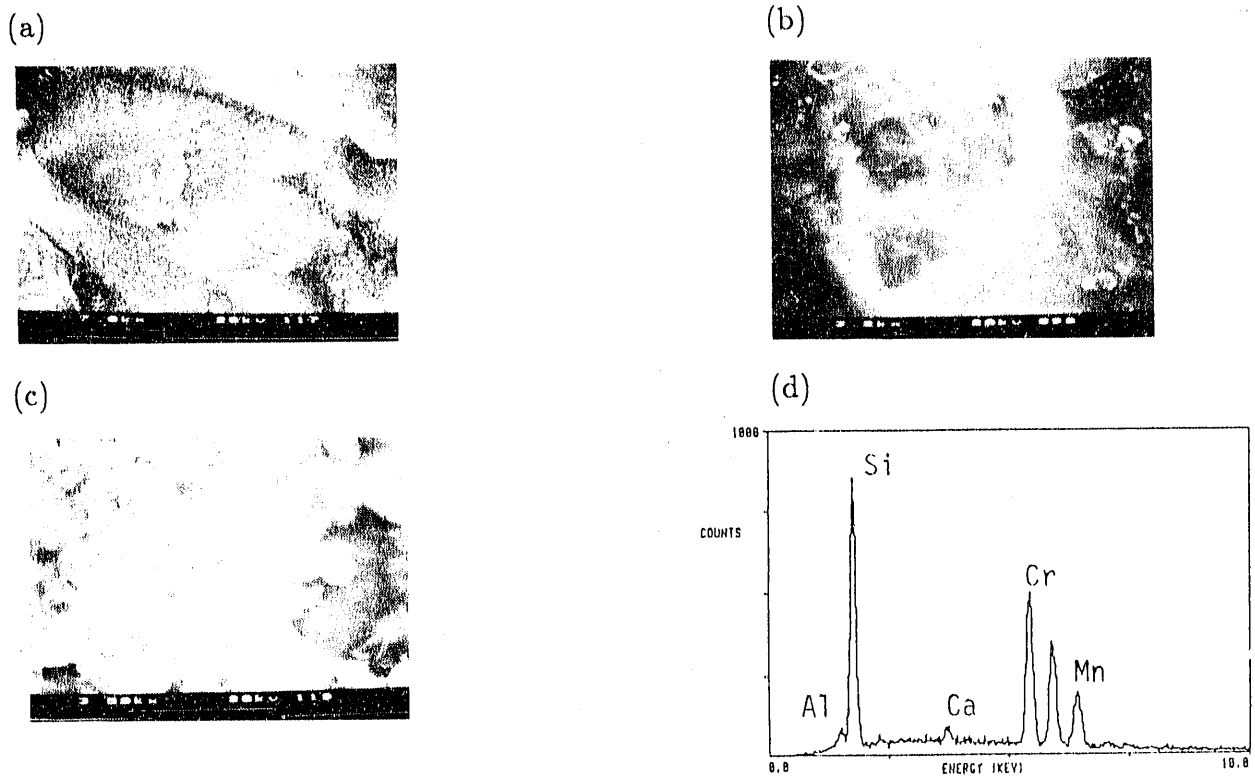

Fig. 27. SEM Micrographs and SEM Spectrum of Reaction Products on the Top Glass Surface of P-V-4. (a) 7000X, (b) 3200X, (c) 3500X (see text).

Aside from the Si-rich "clay" (smectite?) and the Cr-Mn±Fe oxide/hydroxide grains, $CaSO_4$ (gypsum or anhydrite) is the predominant secondary mineral. There are also some Al-rich grains present that may be gibbsite.

The bottom surfaces of P-V-4 and P-V-5 are coarser than the tops and are similar to P-V-3. The contact area of P-V-5 is generally brown-black while that of P-V-4 is a lighter shiny tan color. The noncontact areas are grayish on both samples and the circular marks extend into the contact area. There are very few precipitates optically visible.

The bottom surface of P-V-4 has a general fuzzy appearance but this is not as well developed as on the top surface. The altered surface is fairly smooth with only a little fine scale texture. In places the texture is somewhat coarser although this material may have formed by precipitation. This is suggested by the areas where the coarser material is restricted to high points and ridges and appears to spread into surface depressions (Fig. 28a). Etching of the surface is suggested by the presence of cuspate depressions on the surface. Preferential etching of stress marks is also apparent and, in some cases, these etched marks provide nucleation sites for Si-rich "clay" precipitates (Fig. 28b). In the rougher areas cracking and exfoliation have begun, but this is much less advanced compared to the top surface. The only other precipitated phase besides the Si-rich "clay" is $CaSO_4$ (either gypsum or anhydrite).

(a) (b)

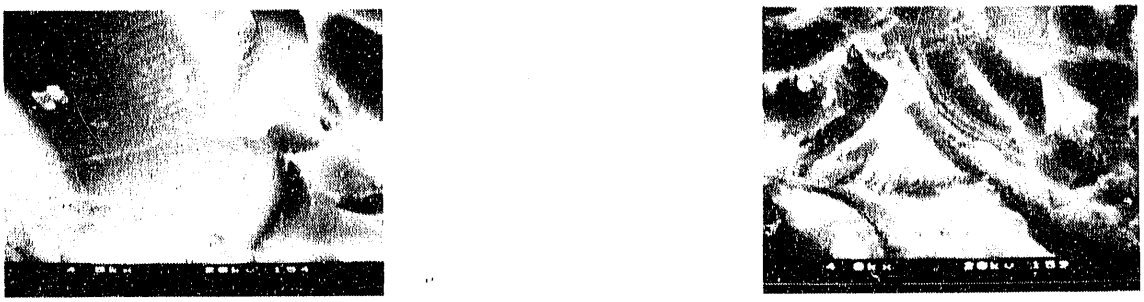

Fig. 28. SEM Micrographs of the Bottom Surface of P-V-4. (a) 4500X and (b) 4000X (see text)

d. P-V-6, 110-Week Sample

The top and bottom surfaces were examined optically but only the top surface was investigated by SEM/EDS. The bottom surface has an appearance like the other P-V samples (see above). The noncontact areas have complex variations in color, creating bull's eye type features. The central portions are gray and are surrounded by successive rings which are brown-black, then blue, followed by gray at the outer margins.

The top surface of P-V-6 is megascopically smoother than any other sample surface (Fig. 29a). It appears that the "as-cut" surface was ground down somewhat prior to the experiment. There are, however, numerous shallow striations with different orientations distributed across the surface, which occur as white streaks on a brown-black background. The noncontact areas have a variably developed milky white hue. Some light-colored precipitates occur in the noncontact areas.

From observation using the SEM/EDS, there is a fine-scale texture which varies from smooth to coarse, although it is never as coarse as observed on the top of P-V-4. The surface has more of a flaky texture rather than a "cardhouse" texture (Fig. 29b, compare with Fig. 27a). In some areas, mostly in proximity to the contact-noncontact boundaries there is a thicker buildup of the surface layer. This may be due to a thickening of the surface layer or from precipitation. There is no evidence for the presence of a complex layer structure. Some minor cracking and puckering of the surface layer is observable (Fig. 29c). The location of the puckered areas seems to be controlled by the shallow striations and the few remaining saw marks on the surface. Overall, the surface layer appears to be less well developed compared to P-V-4, even though the duration of P-V-6 was twice as long. This suggests that initial surface roughness may play a role in accelerating surface layer development and the initiation of exfoliation.

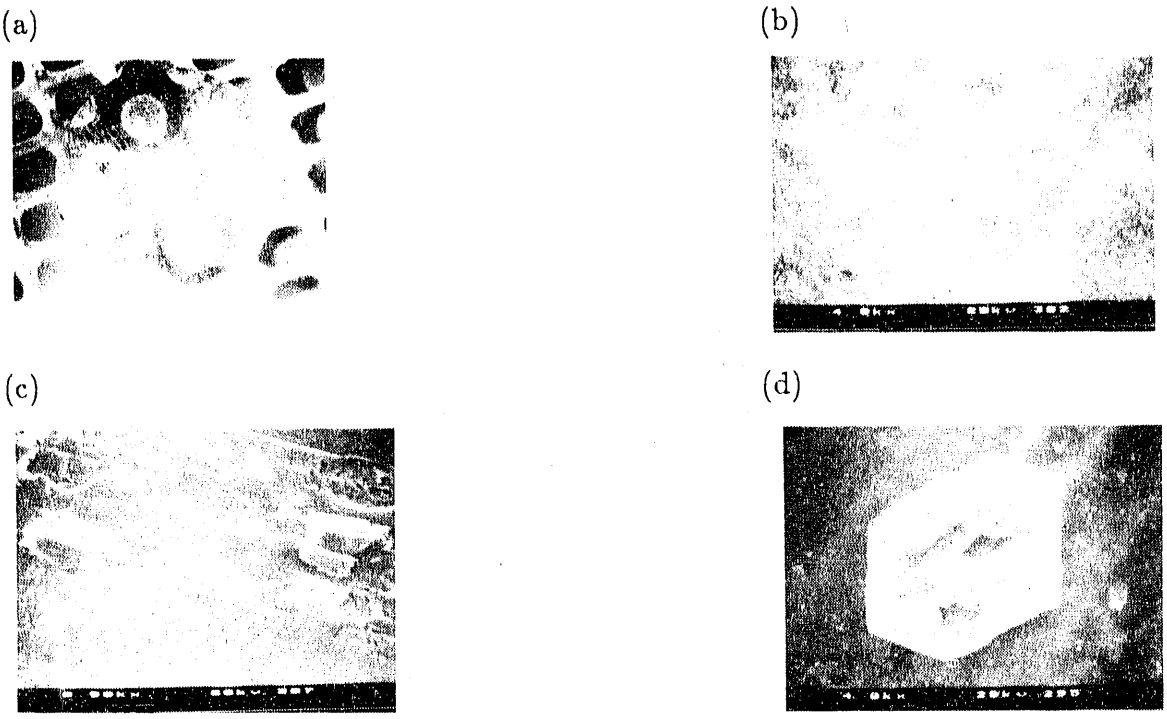

Fig. 29. SEM Micrographs Showing the General Surface Features on the Top of P-V-6. (a) ~6X, (b) 4000X, (c) 500X, and (d) 4000X (see text)

In contrast with all the other samples in the P-V series, no $CaSO_4$ is present. Instead, $CaCO_3$ occurs in fine fluffy masses and as fairly large (up to 20 μ) euhedral grains (Fig. 29d). The large euhedral grains show evidence of having undergone an episode of dissolution. As $CaCO_3$ has retrograde solubility, this may have occurred when the sample was cooled during termination of the experiment. The only other secondary phase is Cr-Mn±Fe oxide or hydroxide. These occur as fine grains distributed across the surface and sometimes in small colonies similar to P-V-7 (see Fig. 30d). In some places, small clusters of grains occur within the layer which imparts a mottled appearance, similar to that observed on the top of P-V-4.

e. P-V-7, 254-Week Sample

This sample is from the longest duration batch experiment. The top surface is similar to the other P-V experiments except that no saw marks are present. There are two well-defined regions, one which is brown-black and another which has a light blue-gray cast. The noncontact areas are poorly discernible. In two of these areas, there are small masses of milky-blue precipitates. There are a number of string-shaped deposits in the contact area (see below). In two noncontact areas and near the edge of the glass, there are patches of large prismatic grains, which EDS analyses suggest are calcite (see below).

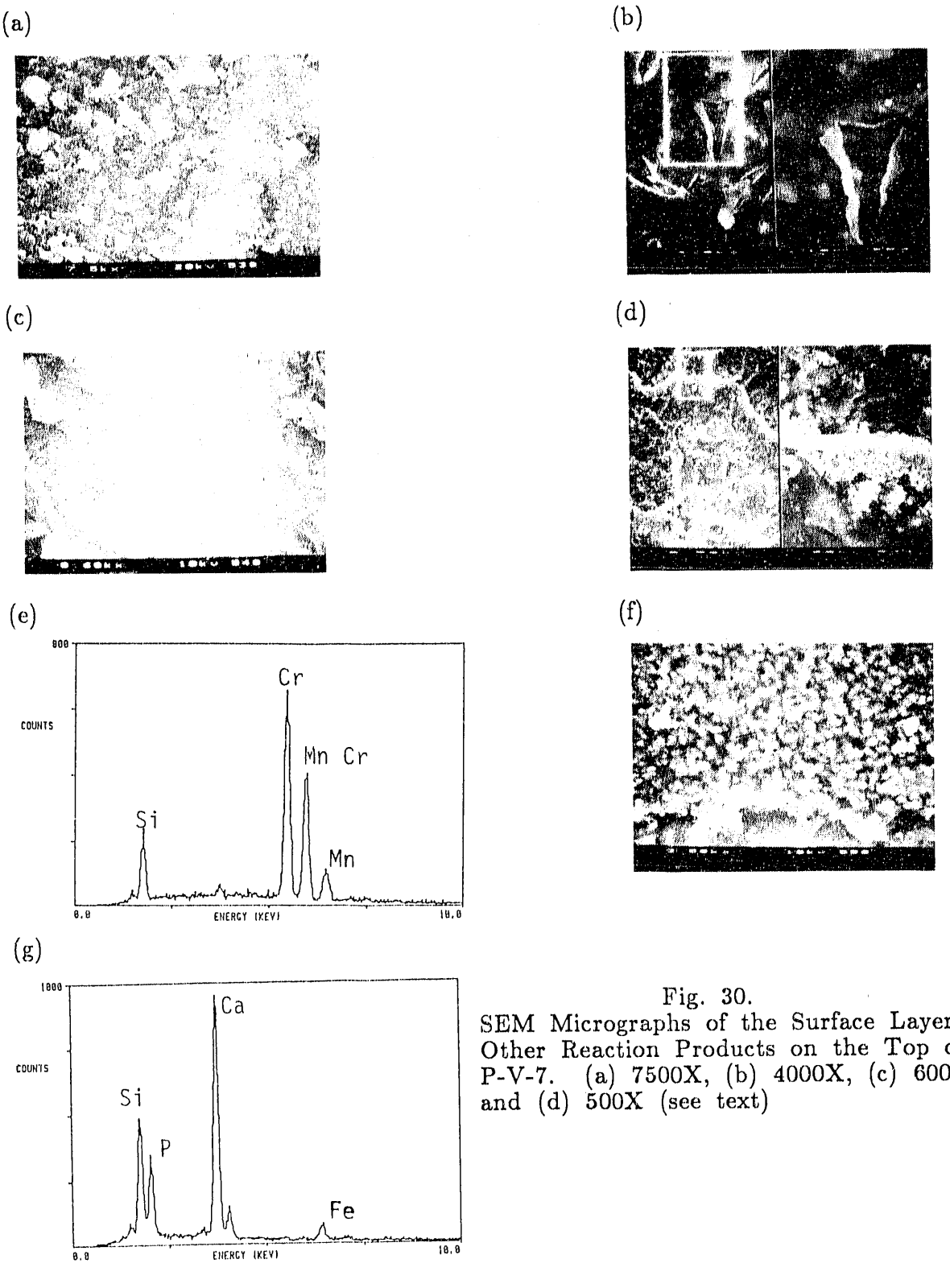

Fig. 30.
SEM Micrographs of the Surface Layer and Other Reaction Products on the Top of P-V-7. (a) 7500X, (b) 4000X, (c) 600X, and (d) 500X (see text)

A reacted layer has developed on the top surface, giving a fuzzy appearance at low magnification. The "as-cut" surface is generally preserved although the contours are noticeably rounded. At higher magnification the surface has a variably developed flaky texture similar to that observed on P-V-4 (Fig. 30a). The flaky texture is generally coarser in the noncontact areas. A hummocky appearance has developed, indicating local variations in layer thickness. The flaky texture and composition suggest the layer is composed of Fe-smectite.

A complex layer structure has locally developed in both the contact and noncontact areas. A thin, smooth layer is draped over the flaky textured material. This deposit is frequently cracked and split, revealing the coarser material from below (Fig. 30b). The smooth areas are somewhat enriched in Si relative to Al. Discontinuous sheets of precipitates have formed on top of the smooth layer, although to a lesser extent than that observed on P-V-4. It would seem, based on examination of the surfaces only, that the top of P-V-4 has evolved to a greater extent even though it was terminated after only 52 weeks. There is no evidence of large-scale exfoliation; however, there are many places where the layer has cracked and pieces have raised up from the surface. The lack of considerable exfoliation may be attributable to the absence of rough saw-marked regions on the surface.

Calcite is abundant, especially in the noncontact areas. Several colonies of large (~60 μm) etched prismatic grains are present (Fig. 30c). Small isolated grains of calcite are also present, often associated with other secondary phases. Fine Cr- and Mn-rich grains, presumably oxide or hydroxide, occur as small clusters and as large colonies (Figs. 30d and 30e/EDS). This phase is responsible for the string-shaped deposits observed under the optical microscope. Both calcite and the Cr-Mn-rich phase were observed on P-V-6. Other colonies on the top glass are composed of Ca- and P-bearing grains (Figs. 30f and 30g/EDS). These may very well be apatite. Rare Ti-rich grains are present which may be anatase (TiO_2).

The bottom glass surface is similar to the other P-V samples. The noncontact areas are well marked and the light gray coloration extends into the adjacent contact area. The contact area is brown-black with some light-colored speckles. The surface layer appears to be pulling away from the glass but no exfoliation is apparent.

The bottom surface has a fuzzy surface at low magnification under the SEM. The "as-cut" contours are partially obscured. In detail, the surface layer is quite different compared to the top. Two distinct layers are apparent, although the upper layer is discontinuous (Fig. 31a). The upper layer has a "cardhouse" texture indicative of precipitated smectite. Its composition is consistent with this interpretation. In some places, it seems as though the upper layer has only partially formed (Fig. 31b), while elsewhere it appears to have formed and exfoliated (Fig. 31a). The lower layer has a bumpy texture with the individual bumps ~0.5 μm across (Figs. 31b and 31c). Locally there is a preferred orientation to the bumps, possibly related to the presence of stress marks on the original glass surface. The alignment is apparent particularly in

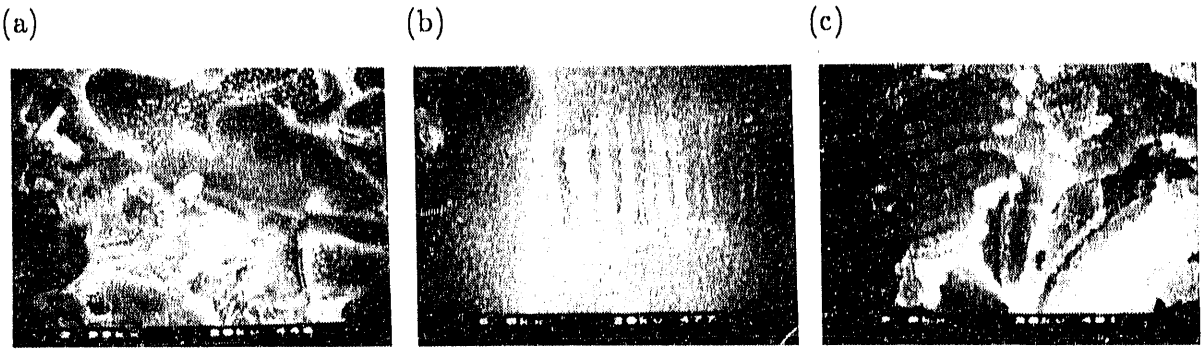

Fig. 31. SEM Micrographs of Surface Layer Features on the Bottom of P-V-7. (a) 2900X, (b) 6000X, and (c) 9000X (see text)

Fig. 31c but is also visible in Fig. 31b. Preferential precipitation of the Si-rich "clay" occurs on these aligned bumps. The lower layer shows extensive cracking and puckering from the surface; however, no complete exfoliation has occurred. There are very few precipitated grains on the surface aside from the Si-rich "clay". Traces of S and Cl are occasionally detectable in EDS analyses of the surface layer.

3. Solution Analyses

Elemental releases from the P-V-1 continuous experiment are shown in Fig. 32 and normalized releases for Li, B, and U are given in Table 13. The raw data and background subtracted cumulative releases are included in Appendix I for both the continuous and batch experiments.

The P-V experiments have the smallest element release of any of the parametric experiments. There are, however, several factors that hamper interpretation of the solution data. The most significant problem results from the lack of recovered solution during sampling. When the solution was diluted to obtain enough for chemical analysis (usually 20 times the original volume), many elements including Li, B, and U were sometimes below the level of detection. For the P-V-1 experiment B was below the detection limit on nine occasions (out of a total of 17), while Li and U were below the limit three times. Since the detection limit value is used when computing cumulative release, the magnitude of release must be viewed as a maximum. Similarly, trends also represent maximum rates of release. Another problem involves the observed extrusion of the silicone rubber gaskets into the vessels. It is unknown what contribution, if any, the gaskets made to the amount of Si in solution, but the reported Si values must be suspect for the first 26 weeks.

The concentrations of Ca and Na were always above the detection limit even though both have a net negative cumulative release. This corresponds to the precipitation of Ca- and Na-bearing phases on the WPA. The erratic behavior of Na suggests that precipitation of an Na-bearing phase occurs when little water is available and it is subject to dissolution when more water is present.

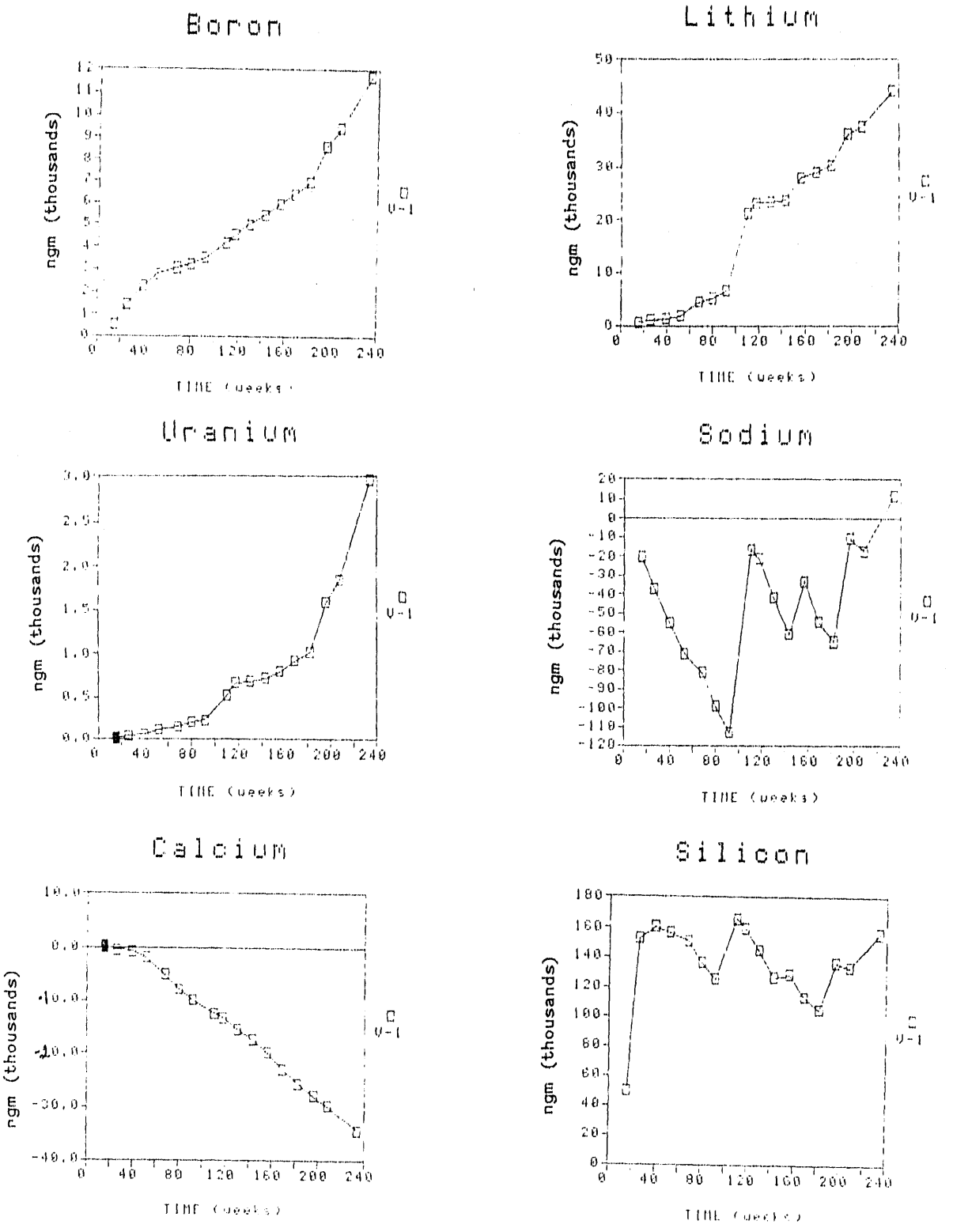

Fig. 32. Cumulative Releases of Selected Elements from the P-V-1 Continuous Experiment

Table 13. Normalized Elemental Release for the P-V Series

Test #	Period (weeks)	Normalized Release (g/m^2)		
		B	Li	U
P-V-3	26	0.2	0.6	0.1
P-V-4	52	0.4	1.1	0.3
P-V-5	52	0.3	1.0	0.2
P-V-6	110	0.2	0.9	0.1
P-V-1	26	0.1	0.0	0.0
	52	0.1	0.1	0.0
	110	0.2	0.8	0.1
	156	0.2	1.1	0.1
	182	0.2	1.1	0.1
	208	0.3	1.4	0.2
	234	0.4	1.7	0.3
P-V-2	26	0.1	0.1	0.0
	39.5	0.1	0.5	0.1

[a]Values are affected by the Si contributed by the silicone rubber gasket.

4. Discussion

The P-V samples appear to have undergone less alteration compared with the other experiments. This conclusion is based on the smaller quantity of precipitates on the surfaces and the low measured element releases. These samples provide insight into the initial stages of surface layer formation. Initial alteration (hydration and leaching) of the glass surface is nonuniform and may be influenced by the surface roughness. Like the glass, there is no fine-scale texture in altered areas; however, the surface does appear somewhat fuzzy and stress marks are absent. Precipitation of a Si-rich "clay" mat begins at an early stage, even before a continuous hydrated glass layer is completed. This signals the beginning of what will become a composite surface layer. Sample P-V-3 is at this early stage, while P-V-4 already has a partially developed composite layer. The altered layer begins to crack and pull away from the glass. This marks the onset of the process that leads to exfoliation. It is important to note that this process can commence even before the altered layer has completely developed across the surface. Precipitation of the Si-rich "clay" layer appears to be independent of this process. The original surface roughness may be an important factor in the pace and location of exfoliation. Cracks seem to develop first in the rough regions associated with the saw marks. For example,

on the top of P-V-6, where the surface is generally quite smooth, cracking and puckering of the surface layer is restricted to the striations and shallow saw mark traces. As the surface layer ages, coarsening of its texture is apparent. This is particularly noticeable for P-V-7, the 254-week duration experiment. This coarsening may correspond to progressive crystallization of an amorphous layer, but, this is not revealed at the resolution of the SEM.

The top of P-V-6 appears much less reacted than the top of P-V-4 even though its duration was twice as long. This may be the result of the smoother surface on P-V-6 impeding reaction but this is only a hypothesis. The lack of reaction might also result from less water-glass contact during the experiment, perhaps due to evaporation during the experiment.

In all the P-V experiments, Ca is removed from the EJ-13 water. This is consistent with the presence of Ca-bearing phases on the batch samples. On samples P-V-3 and P-V-4 $CaSO_4$ (either gypsum or anhydrite) is ubiquitous. On samples P-V-6 and P-V-7 calcite is abundant and $CaSO_4$ is absent. While the availability of sulfate is not well understood, it is unknown why such a difference in mineral occurrence should happen between these samples.

E. P-VIII Experiments

The purpose of these experiments is to examine the effect of sensitization of the stainless steel components on metal-glass-fluid interactions. As the stainless steel pour canisters are anticipated to be exposed to elevated temperatures during filling, the behavior of heat-sensitized steel has direct relevance to waste form performance in the proposed geologic repository.[3] The stainless steel used in the experiments is from heat #22841 which contains 0.016 wt% carbon. The components were held at 550 ± 20°C for 24 hours and were then slowly cooled to room temperature by turning off the furnace. This steel proved very difficult to sensitize, owing to its low carbon content.[13] The degree of sensitization to the actual samples, while believed to be low based on testing of heat-treated but unreacted steel, has not been measured.

The experiments were initiated on 2/27/86 and have been completed through 195 weeks. Batch experiments were terminated after 13, 26, 39, 52, and 104 weeks. Continuous experiment P-VIII-2 was terminated after 170 weeks because the WPA tipped and would no longer remain upright. The batch sample P-VIII-8, which was first sampled after 104 weeks, is presently being treated as a continuous experiment.

1. General Observations

The WPA had a similar appearance in all the experiments during sampling. The top surface was always dry with some light-colored precipitates often present on the glass in the noncontact areas. Some precipitation of secondary phases occurred on the metal. The bottom surface was always wet with some standing water around the circumference of the glass (sample P-VIII-4 was dry upon termination, however). The extent of standing water was variable.

At termination of P-VIII-7 (104 weeks), the water was about at the level of the bottom of the glass. When P-VIII-8 was first sampled after 104 weeks, the water level was halfway up the side of the WPA indicating that the bottom had been inundated for a significant period of time. These observations must be considered when interpreting the solution composition data from these experiments.

The metal components from all the terminated experiments experienced approximately the same amount of weight gain (Table 14). This is consistent with the observation of secondary phases on the metal. The glass in the short-term experiments (≤26 weeks) gained a small amount of weight, while there was a net decrease in the longer experiments proportional to the experiment duration.

2. Component Analyses

The glass from all the terminated batch experiments was examined optically. The top surface of P-VIII-4 and the top and bottom surfaces of P-VIII-6 and P-VIII-7 were investigated by SEM/EDS. The metal components from P-VIII-6 and P-VIII-7 were also examined by SEM/EDS.

a. P-VIII-3, 13-Week Sample

The noncontact areas on the top surface are rather discrete. They have a light gray tint which is in contrast with the brownish background of the contact areas. The central noncontact area, however, has a bluish cast. There are three small light-colored areas, in the contact area, suggesting localized precipitation has occurred.

The bottom surface has a uniform gray color and the noncontact areas are not discernible. There is one light-colored area at the edge of the glass which is similar to the patches on the top surface. Saw marks are readily visible as light-colored streaks on both the bottom and top surfaces. Rougher regions are associated with the saw marks which have a coarse speckled appearance. Finer speckling is visible in the smooth regions at higher magnification.

b. P-VIII-4, 26-Week Sample

Several features stand out on the top surface. Part of the surface has a light gray-blue tint which is mostly associated with the central noncontact area. White precipitates are present in the bluish regions. The other noncontact areas are poorly marked. These are somewhat lighter in color with some white precipitates at their margins. The contact area is generally brownish but light gray tinting occurs around the edge of the glass. Saw marks, visible as white streaks, are present over much of the surface, imparting a coarse-speckled appearance.

Table 14. Experimental Matrix and Weight Change Results for the P-VIII Series

Test No.	Test Period (weeks)	Date Started	Date Stopped	Initial Glass Mass (gm)	Final Glass Mass (gm)	Δ Mass ($gmx10^{-5}$)	SA Glass (cm^2)	Initial Top Canister Mass (gm)	Final Top Canister Mass (gm)	Δ Mass ($gmx10^{-5}$)
P-VIII-1[a]		2/27/86	in progress	10.50533			13.88	2.34774		
P-VIII-2[a]	170	2/27/86	6/01/89	9.99264			13.35	2.37578		
P-VIII-3	13	2/27/86	5/28/86	10.23029	10.23050	210	13.81	2.35705	2.35720	150
P-VIII-4	26	2/27/86	8/28/86	10.37222	10.37225	30	13.86	2.36451	2.36462	110
P-VIII-5	39	2/27/86	11/26/86	10.17771	10.17515	(256)	13.52	2.37383	2.37400	170
P-VIII-6	52	2/27/86	2/26/87	10.27582	10.27524	(580)	13.63	2.36734	2.36774	400
P-VIII-7	104	2/27/86	2/29/88	10.30219	10.30102	(1170)	13.69	2.35248	2.35271	230
P-VIII-8[b]		2/27/86	in progress	10.37649			13.78	2.37175		

[a]Continuous experiments.
[b]Treated as a batch experiment up to 104 weeks. Thereafter treated as a continuous experiment.

Cont'd

Table 14 (Cont'd)

Initial Bottom Canister Mass (gm)	Final Bottom Canister Mass (gm)	Δ Mass ($gm \times 10^{-5}$)	Initial Total Vessel Mass (gm)	Final Total Vessel Mass (gm)	Δ Mass ($gm \times 10^{-5}$)	Water Added During Testing
3.35091			320.19			
3.34846			327.34			
3.33102	3.36114	120	325.59	327.18	1.59	1.95
3.33765	3.33776	110	320.56	323.70	3.14	3.90
3.35271	3.35291	200	324.34	328.96	4.62	5.85
3.39773	3.39823	500	325.82	331.74	5.92	7.80
3.35328	3.35359	310	325.71	336.98	11.27	15.60
3.35672			325.71			

The bottom surface has a rather uniform dark gray color. The noncontact areas are marked by somewhat lighter colored rings around a central region that looks much like the contact area. There is a patch of whitish precipitates, similar to that observed on P-VIII-3. Saw marks give a coarse-speckled appearance to approximately one quarter of the surface.

Only the top surface was investigated by SEM/EDS. The general appearance is similar to the P-IV experiments. The "as-cut" contours are clearly visible, however, the surface has a fine-scale texture at high magnification indicating that reaction has occurred (Fig. 33a). A Si-rich alteration layer has developed across the glass surface. Its composition is essentially the same as observed for the other experiments. Small precipitates of similar composition occur on the surface (Fig. 33a). In some parts, coverage is extensive, forming a discontinuous upper layer upon the altered surface. That the glass has reacted is also indicated by the preferential etching of stress marks. Short cracks have locally developed in the layer and small portions have raised up from the glass. This phenomenon occurs in both the contact and noncontact areas.

Aside from the Si-rich layer, there are several other secondary phases that have precipitated on the surface. There are colonies of small (<0.5 μm) spherical grains distributed over the entire surface (Fig. 33b). These areas are enriched in Fe relative to the surface layer and EDS analyses suggest a very fine-grained mixture of Si-rich "clay" and Fe ± Mn ± Ni oxide or hydroxide (Fig. 33c/EDS). This is based on the observation that the Si, Al, and Ca peaks have relative intensities approximately equal to precipitated Si-rich "clay" (compare Fig. 33c with Fig. 34c). The Fe peak intensity varies from spot to spot, suggesting its signal is independent of Si, Al, and Ca and that this results from variable proportions of two phases being detected. The phenomenon of coprecipitation is well known.[14,15]

Other irregular-shaped grains contain Ca and S and are probably either gypsum or anhydrite (see above). A number of large (up to 180 μm) prismatic grains are present whose EDS spectrum consists of only a Ca peak suggesting it is calcite. Several irregular fluffy masses occur with only Si, Al, and K detectable by EDS (Figs. 33d and 33e/EDS). Their approximate stoichiometry is consistent with K-feldspar, but they have not been analyzed by XRD.

c. P-VIII-5, 39-Week Sample

The noncontact areas on the top surface are easily visible owing to a rather heavy coverage of whitish-gray precipitates. The central noncontact area is gray, and extends into the adjacent contact area. Exfoliation of the altered layer is apparent in the middle of several noncontact areas. The contact areas are brown except in the saw marked regions which have light-colored speckles as observed on most other P-VIII samples. The bottom surface is similar to the top of P-VIII-3. Most of the noncontact areas are only faintly visible with a slight grayish tone. Saw marks and a corresponding rough-speckled appearance covers approximately half the surface.

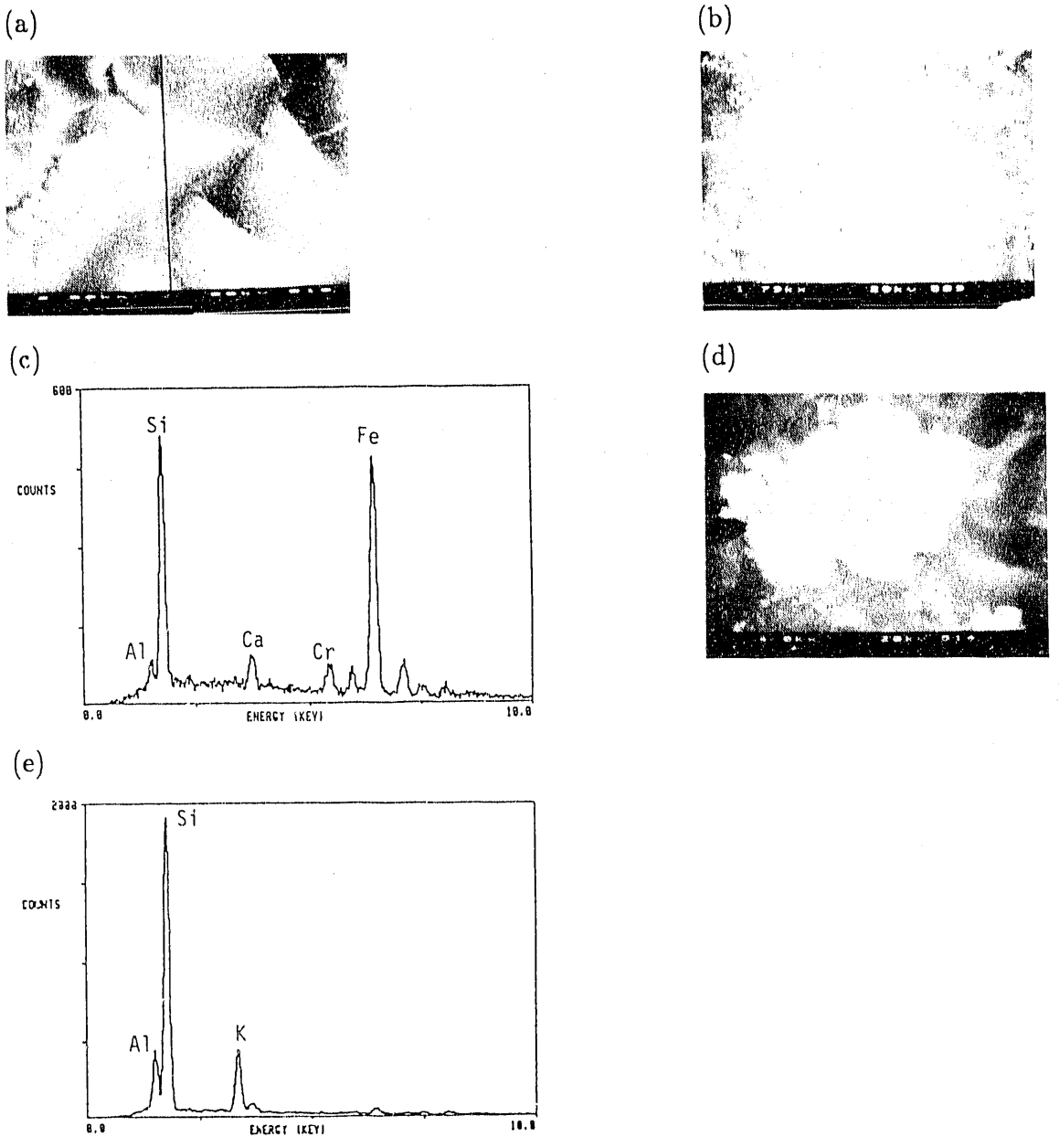

Fig. 33. SEM Micrographs and EDS Spectra from the Top of P-VIII-4. (a) 2500X, (b) 1790X, (c) EDS spectrum of material shown in (b), (d) 4000X, and (e) EDS spectrum of grain shown in (d)

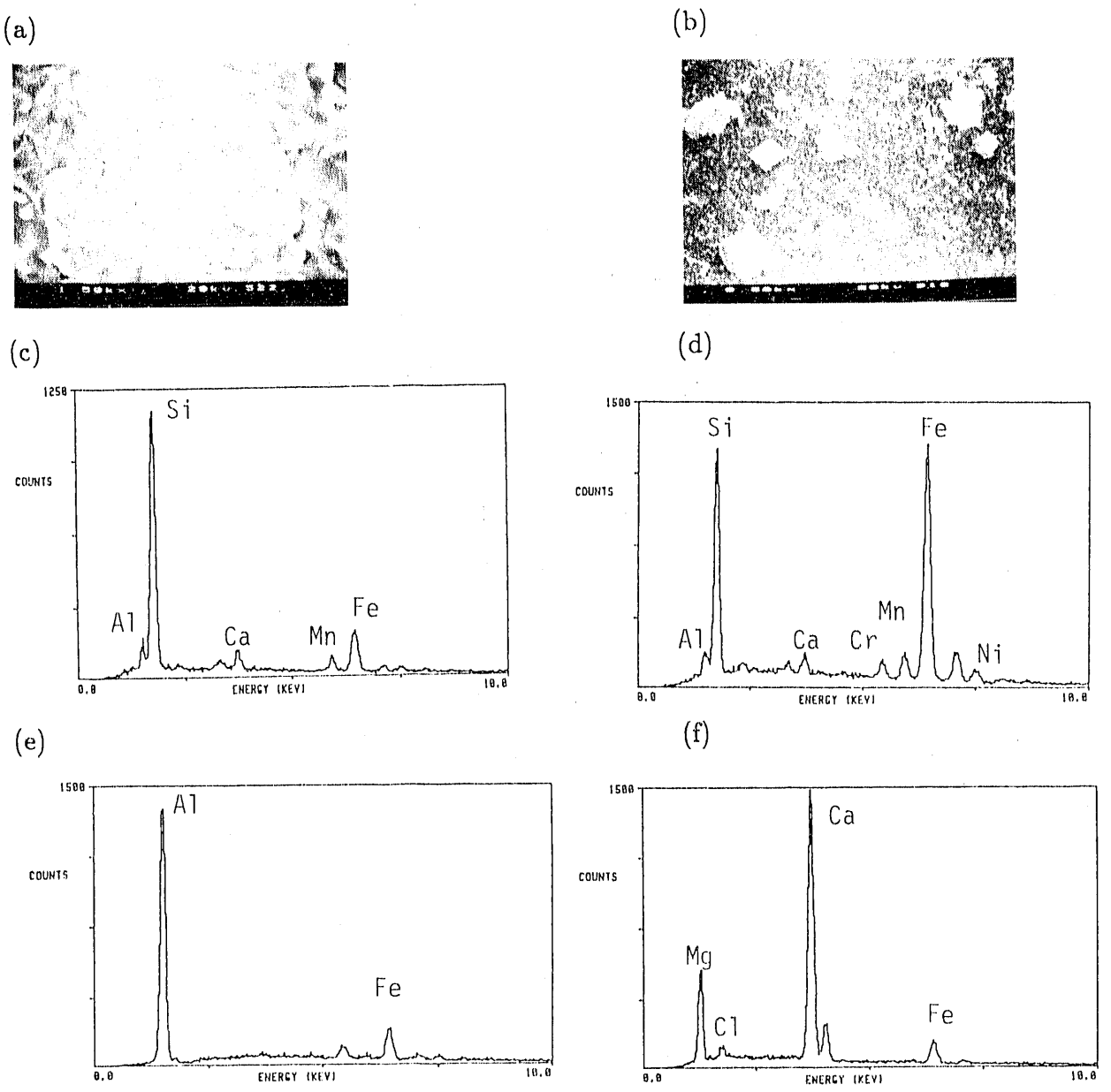

Fig. 34. SEM Micrographs and EDS Spectra from the Top of P-VIII-6. (a) 1500X, (b) 300X (see text)

d. P-VIII-6, 52-Week Sample

The glass and metal components were examined optically and by SEM/EDS. Two precipitates were also analyzed by XRD.

(1) Glass

The top portion of the glass has clearly marked contact and noncontact areas. The noncontact areas are lighter in color than the contact areas, being tan rather than gray. This is due to heavier precipitate coverage in the noncontact areas. Some saw marks appear as light-colored, discontinuous streaks. Close optical inspection suggests the color difference is mostly due to the partial separation of the surface layer from the glass in the saw grooves. One region, encompassing approximately one-third of the top surface, has a rusty appearance and seems to have more precipitates on it.

The "as-cut" contours are preserved, although they are subdued (Fig. 34a). The surface has a poorly developed flaky texture at high magnification like that on P-VIII-4, indicating the presence of an altered layer (see Fig. 33a). A coarsening of this texture is locally observable, but this may be the result of precipitation. The layer composition is the same as for samples from other experiments; it is Si rich with some Al, Ca, Fe, ± Mg ± Mn ± Ni, ±Na. Only minor cracking of the surface layer is apparent, although such features are present in both the contact and noncontact areas (Fig. 34a). Where cracking has occurred, small pieces of the adjacent layer have raised up from the glass.

There are a number of secondary phases present. The most abundant is a Si-rich material which occurs in numerous morphologies including: ribbons, round grains with flaky surfaces, string-shaped masses, and fine fromboidal masses (Figs. 34b and 34c/EDS). This material has the same composition as the surface layer. The relative uniform Al-to-Si ratio suggests this is a crystalline phase and its composition is consistent with smectite. The Fe, Mn, and Ni contact can be quite variable; sometimes Ni content can exceed that of Fe.

The next most abundant phase is Fe oxide or hydroxide which is especially abundant in the rusty region. It occurs as irregular-shaped grains; however, some possess a good geometric form, like the diamond-shaped grain in the left center of Fig. 34b. Fe-rich material is also associated with many of the fine-grained precipitates that are present all over the surface. This may explain, in part, the apparent variability in Fe content of the Si-rich precipitates. Along with Fe, a small amount of Mn is almost always present and Cr and Ni are locally important components (Fig. 34d/EDS).

A Ca- and S-bearing phase, most probably anhydrite or gypsum, is ubiquitous on the glass surfaces It occurs as very fine fromboidal grains that grow on other phases and are often intimately intermingled with these phases. For example, fromboids are growing on the Fe-rich grain in Fig. 34b.

Several other phases are present in minor quantities which are worthy of note. A silica phase, presumably either quartz or opal, is present as small angular grains. An Al-rich phase occurs in several places. The absence of any other detectable elements, along with its flaky appearance, suggest it is gibbsite or some other Al-hydroxide (Fig. 34e/EDS). Another Ca-rich phase containing Mg and Fe is present which is probably a high-Mg calcite or possibly dolomite (Fig. 34f/EDS). In rare instances, Cl is detectable. These grains often have a complex composition suggesting the presence of numerous phases.

The surface layer and precipitates are well developed on the bottom glass surface. There is only a weak demarkation between the contact and noncontact areas. This is in contrast to the top surface where contact-noncontact areas are well delineated. Saw marks are clearly visible on the bottom surface, marked by light-colored streaks. As with the top layer, this color difference seems to result from buckling and separation of the surface layer from the glass.

The "as-cut" contours are mostly obscured and the surface has a flaky appearance that is much coarser than observed on the top surface (Fig. 35a). This suggests that much of the visible surface may have formed by precipitation, masking the original surface topography. The composition is typical of the altered layer and is probably smectite. An extensive network of cracks has developed across the surface (Fig. 35a). Most have the appearance of shrinkage cracks caused by dessication, presumably after termination of the experiment. However, the glass exposed within the cracks looks altered and has some fine precipitates on it. This suggests cracking must have begun during the experiment. The cracks would then become enlarged as the layer dried after termination of the experiment. Other cracks, where the surface layer has raised up, are associated with the saw marks (Fig. 35b). This represents the initiation of exfoliation of the surface layer.

The types of precipitated phases are essentially the same as described for the top surface with a couple of minor additions. A Ca-bearing phase without any Mg or Fe is present and is probably calcite. One analyzed grain contains only Si, Al, and Na, with Al exceeding the amount found in the surface layer (Figs. 35c and 35d/EDS). It does not have a distinctive morphology, but its composition suggests it is analcime.

(2) Metal Components

The top and bottom steel components generally have the same appearance. They have a dull rusty color where they were in contact with the glass during the experiment. Along the rims and the sides facing away from the glass, little reaction has occurred. There are some small irregular-shaped patches of corrosion on these surfaces. There are, however, small patches of thick precipitates that have developed in both the contact and noncontact areas on the side facing the glass. These are mostly intimate mixtures of Si-rich material, probably smectite clay, and Fe-oxide or hydroxide. The clumps can be stringy in form, similar to that observed on the glass.

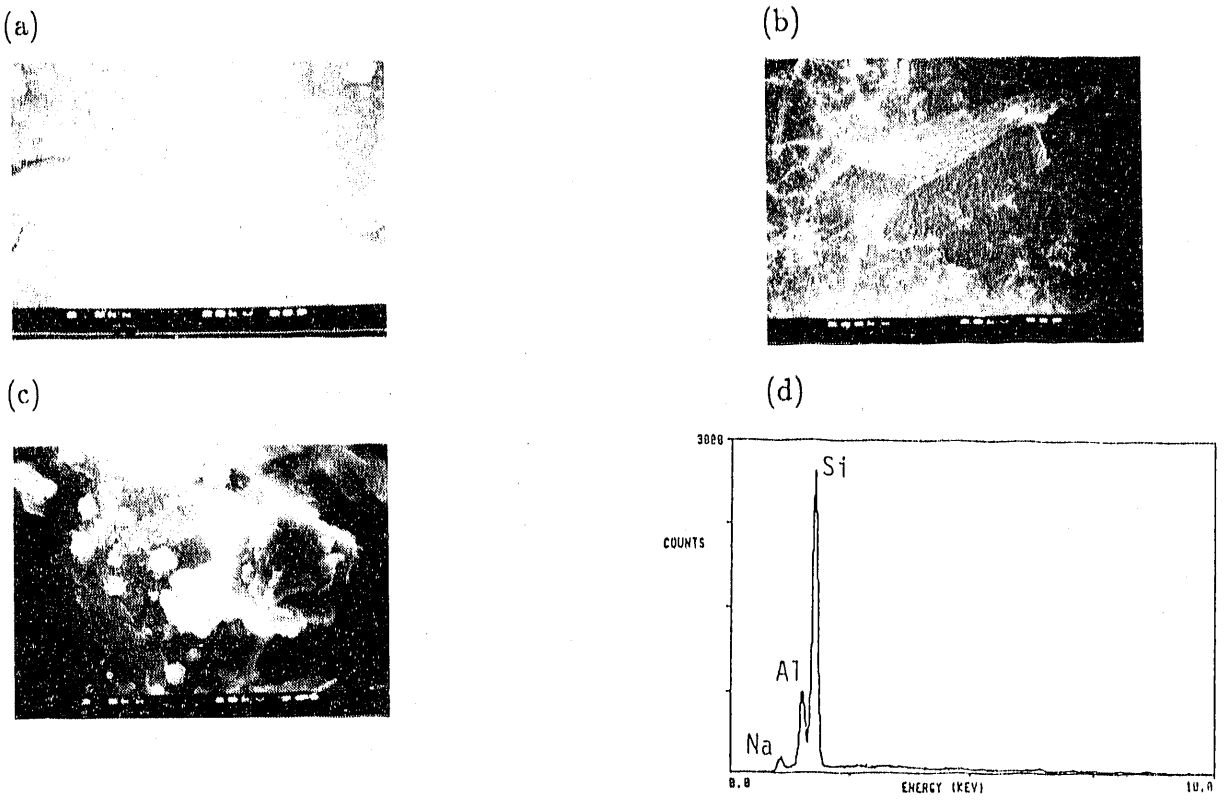

Fig. 35. SEM Micrographs of Surface Layer Features from the Bottom of P-VIII-6. (a) 2500X; (b) 200X; (c) a small grain on the surface that contains only Si, Al, and Na (3500X); and (d) EDS spectrum from grain shown in (c)

On the bottom metal piece, there are numerous honey-colored precipitates. These are shaped like open cylinders and cones (Fig. 36a). Analysis of this material by XRD suggests that it is hematite. They occur on both sides of the metal but are most abundant along the edges on the side facing away from the glass. In general, there are more precipitates on the surfaces facing the glass than on the other side. Unlike the glass, there is no complete surface coating on the metal.

Virtually all the phases identified on the glass are also present on the metal components. The most common phases on the metal are the Si-rich clay, Fe-oxide or hydroxide, and calcium sulfate. These are often intimately intergrown with each other. The Si-rich material has the same composition as that found on the glass except that it is generally very poor in Ni. Fe-oxide or hydroxide occurs as the material covering the surface and as open cylinders and cones (Fig. 36a). Tiny dots of gypsum or anhydrite occur all over the metal surface. Chloride-rich grains are present, mostly associated with the welded regions. These grains may contain Na, K, and Ca. XRD analysis confirms the occurrence of NaCl. There is a Cr-rich substance present on both metal components that was not observed on the glass. While spectra from this

(a)

(b)

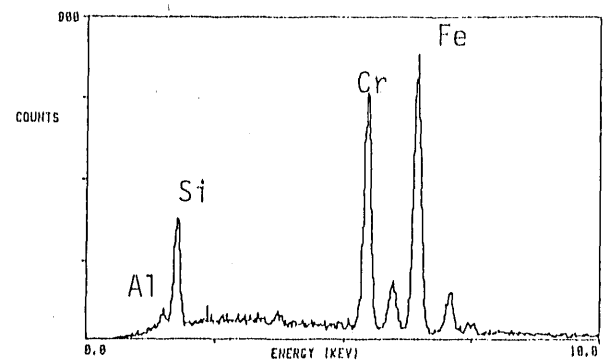

Fig. 36. SEM Micrograph (250X) and EDS Spectrum of Fe- and Cr-Rich Deposit on the Bottom Surface of the Metal Component on P-VIII-6

material resemble the metal and Fe-hydroxide, the Cr content is very high (Fig. 36b/EDS). This may be Fe-hydroxide that is for some reason locally very rich in Cr. Considering that the source of the Cr is the metal, the absence of Cr-rich material on the glass suggests that Cr is not very mobile under the conditions of the experiments.

e. P-VIII-7, 104-Week Sample

The glass and metal components were examined optically and by SEM/EDS/WDS.

(1) Glass

The top glass has a general medium gray tone with a smooth, evenly colored region and a rough, mottled region. The roughness is from the saw blade during cutting of the glass cylinder. There is a distinction between the contact and noncontact areas but it is not very pronounced. Precipitates are sparsely scattered over the noncontact areas. A honey-colored mark and a concentration of precipitates are present in one small portion of the contact area, near the edge of the glass.

A well-developed altered layer is present over the entire surface. The "as-cut" contours are not preserved and the layer has a "cardhouse" type morphology reminiscent of clay (this is consistent with its composition). Masking of the contours suggests at least a portion of the layer formed by precipitation, filling in depressions on the rough surface. The surface layer is cracked in many places and appears to be pulling away from the glass (Fig. 37a). Some of the cracks expose etched glass from below. The presence of precipitates bridging the cracks suggests the cracks began to form during the experiments. Some shrinkage after termination of the experiment may have enlarged the cracks. The pulling away of the surface layer from the glass is more pronounced in the rough region. Here, it appears that the layer has variable thickness.

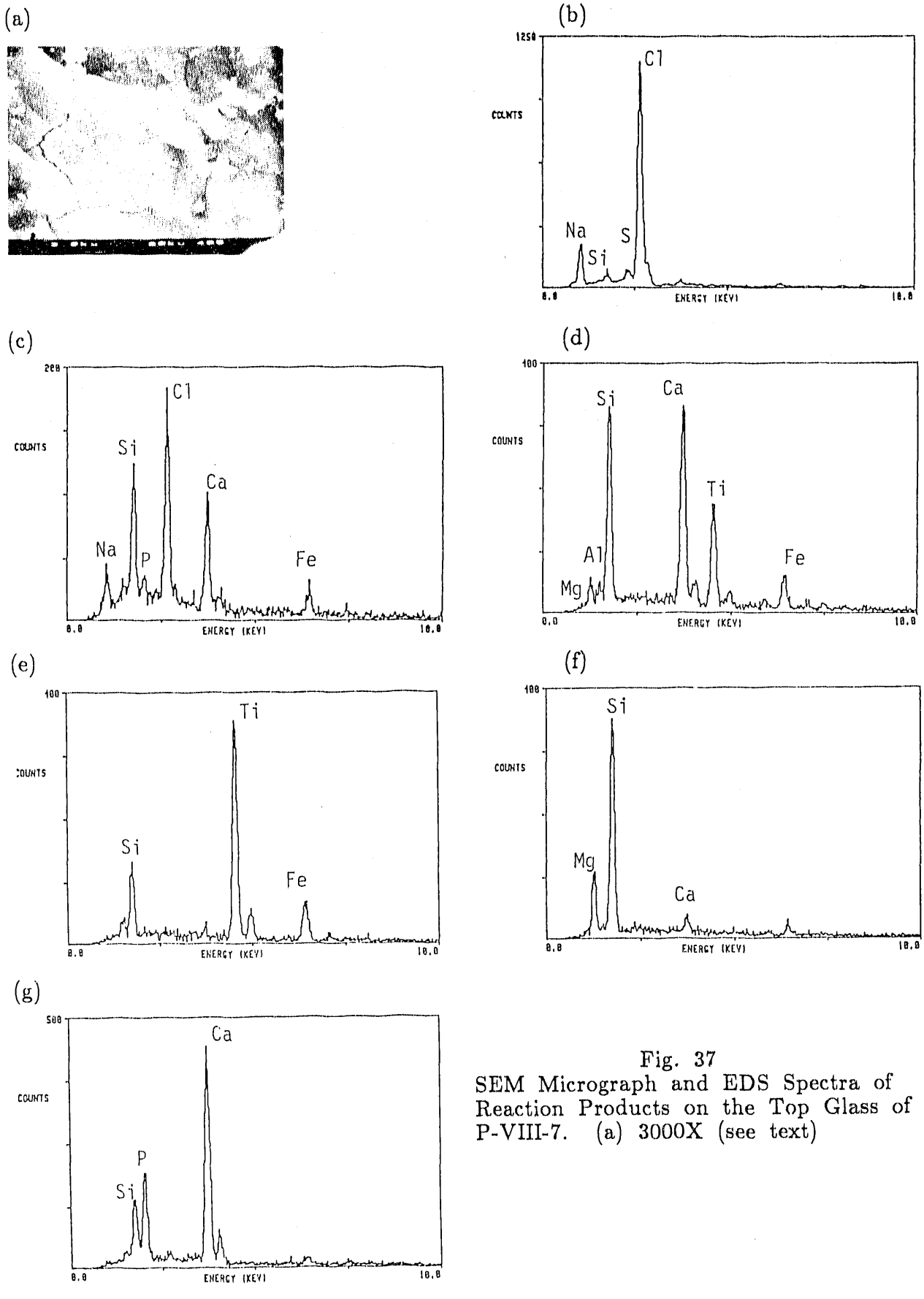

Fig. 37
SEM Micrograph and EDS Spectra of Reaction Products on the Top Glass of P-VIII-7. (a) 3000X (see text)

The most abundant precipitated phase is Si-rich which also contains Al, Ca, Fe, Mn, ± Mg ± Ni, ± Na, ± K, in proportions similar to the average surface layer. It occurs as ribbons, flaky grains, and fluffy textured masses of variable size (Fig. 37a). At high magnification, the small fluffy masses have the same "cardhouse" type morphology as the top of the surface layer which suggests that the visible portion of this layer may also have formed by precipitation. The next most abundant phase is very Fe rich and is probably Fe-oxide or hydroxide. This material occurs as irregular-shaped grains and is almost always intergrown with Si-rich "clay". It is otherwise generally quite pure with only a small amount of Mn present.

Other precipitated phases include Ca-rich grains, presumably calcite, which are fairly abundant Some Ca-bearing grains also contain Mg and Fe, indicative of dolomite. Some grains are very Al-rich and are possibly gibbsite (or bayerite?, or nordstrandite?). Variable small Si and Fe peaks on the spectra suggest this material is intermingled with Si-rich "clay". Tiny Cl- and S-rich grains occur on the surface layer and on many precipitates. Based upon numerous EDS analyses, the phases present are likely to be NaCl, Na_2SO_4, $CaSO_4$, and possibly $CaCl_2$ (Figs. 37b/EDS and 37c/EDS). Whether the sulfates are actually hydrated is impossible to determine by EDS. A number of grains contain significant Ti. When EDS spectra from several grains are compared, it is clear that they are a mixture of phases (Figs. 37d/EDS and 37e/EDS). For example, while the spectrum in Fig. 37d has large Si and Ca peaks, that in Fig. 37e has a much smaller Si peak and virtually no Ca. This suggests that the Ti-bearing phase does not contain either of these elements. A plausible interpretation is that these grains contain TiO_2, anatase?, along with Si-rich "clay" and calcite.

Several other phases, while occurring rarely, are worthy of note. A couple elongate, layered grains are present which contain only Si and Mg (Figs. 37f/EDS). Their morphology and composition suggest they are serpentine. Ca-phosphate grains presumably apatite, occur sparingly (Fig. 37g/EDS). Silica, possibly quartz or opal occur very rarely.

The bottom surface has a medium gray color with smooth and rough cut regions. The noncontact areas are generally poorly defined, being only slightly darker gray than the adjacent contact areas. Under the SEM, the surface has a similar texture to that observed on the top surface. Small precipitated grains have the same "cardhouse" type texture and composition as the surface layer. An extensive network of cracks is present and, in places, pieces of the layer have exfoliated, exposing etched glass below (Fig. 38a). It is clear that exfoliation occurred during the experiment because of the presence of fine NaCl threads in some of the cracks and Si-rich precipitates on some of the freshly exposed surfaces (Figs. 38a and 38b). In these exfoliated regions there is a continuum of surface appearance from fresh etched glass, to glass with a few precipitates, to glass with a heavy cover of precipitates. This suggests that exfoliation occurred over a period of time up to the termination of the experiment. In one location, it is apparent that the surface layer is actually composed of two layers (Fig. 38b). Here, a flake of the upper portion of the layer has spalled off, exposing a lower layer which in turn is also in the process

(a) (b)

Fig. 38. SEM Micrographs of Surface Layer Features on the Bottom of P-VIII-7. (a) 1600X, irregular-shaped grain in NaCl; and (b) 2000X (see text)

of exfoliating. The glass below has many small dots on it either from precipitation or alteration. Based upon several EDS analyses, there are no significant compositional differences between the two layers. The lower layer is finer grained; however, it has the same texture as the upper layer when viewed at high magnification.

Like the other samples, the surface layer and associated Si-rich precipitates form the dominant alteration product on the bottom surface. The texture and composition is consistent with it being Fe-smectite. The next most abundant phase is NaCl. It occurs as fine threads and blocky grains and may also be intimately associated with the Si-rich "clay". It often occurs with Na_2SO_4 and $CaSO_4$ (whether these sulfates are hydrated is uncertain). These phases, along with $CaCO_3$, calcite, are frequently intergrown with the Si-rich "clay" at a very fine scale. Fe-rich material is also present as irregular blobs on the surface which may contain minor Mn and Ni. This is probably Fe-oxide or hydroxide, although the XRD results from P-VIII-6 suggest it is an oxide.

(2) Metal Components

There is an extensive deposit of precipitates on the metal components. Small patches of corrosion are associated with the welds. Most of the phases found on the glass are also present on the metal. There are two predominant phases: Si-rich "clay" and Fe-oxide or hydroxide. There is a thin Si-rich "clay" mat on the bottom component, but for the most part, the "clay" occurs in clumps with a fluffy texture. The clumps occur on both sides of the components indicating an origin by precipitation. The EDS spectra are often enriched in Fe (and not Cr) suggesting that the clay is intergrown with Fe-oxide or hydroxide, as was observed on the glass. Fe-oxide or hydroxide occurs in irregular clumps and as tiny balls and open cylinders (see Fig. 36a from P-VIII-6).

Ca-rich phases, presumably calcite and dolomite, are quite abundant. Some grains have a rhombohedral form which is characteristic of calcite. Many Si-rich "clay" clumps have detectable Ca and S suggestive of gypsum or anhydrite.

Very Al-rich grains are abundant on the top component. These grains are generally only a few microns across with only Al in their EDS spectra, suggestive of Al-hydroxide (Fig. 39a/EDS). Ti-rich grains, which are possibly mixtures of clay and TiO_2, are also present on the top metal piece. A rare Cr-Mn phase is associated with the metal grain boundaries and is probably the result of corrosion (Fig. 39b/EDS).

3. Solution Analyses

Elemental releases from the continuous experiments are shown in Fig. 40, and the normalized releases of B, Li, and U are presented in Table 15. The raw data and the background subtracted cumulative releases are included in Appendix I for both the continuous and batch experiments. Continuous experiment P-VIII-2 was terminated after 170 weeks because the WPA would not remain in an upright position. Batch experiment P-VIII-8 is currently being treated as a replacement for P-VIII-2, but the data are not presented as such in Fig. 40.

There is good agreement in the trends and magnitudes of elemental release between the two continuous experiments, P-VIII-1 and P-VIII-2. Overall release is low and is comparable to the P-V experiments. The last sampling of P-VIII-2, at 170 weeks, showed a sharp change in all element releases (Fig. 40). The tipped WPA may, in some way, have caused this accelerated behavior. The release from P-VIII-8 is significantly greater than the other two continuous experiments. This is probably attributable to the period prior to the 37-week sampling when the bottom of the WPA was submerged. Comparison of the last two solutions, collected at 170 and 195 weeks, suggests a sharp reduction in the rate of release.

The relative magnitudes of release are Li $>$ B $\geq$ U (Table 15). There is a net negative release of Ca and Mg in all three experiments. This indicates that these elements have been removed from the EJ-13 water and incorporated in secondary phases on the WPA. This is consistent with the occurrence of $CaSO_4$ and calcite on the batch samples. Release of Si is negative in the P-VIII-1 and P-VIII-2 experiments. It is positive in P-VIII-8, however, the most recent sampling at 195 weeks shows a minor net negative release. The negative Si release correlates with the extensive amount of precipitated clay on the glass and metal components in the batch experiments. Release of Na is erratic in P-VIII-1 and P-VIII-2 which is similar to that observed in the P-II and P-III experiments. Release of Na in P-VIII-8 is positive and mirrors that of Li, B, and U. The erratic behavior of Na is attributable to periodic precipitation of NaCl or Na_2SO_4 followed by subsequent redissolution during later sampling intervals. These Na-bearing phases are commonly observed on the batch experiments.

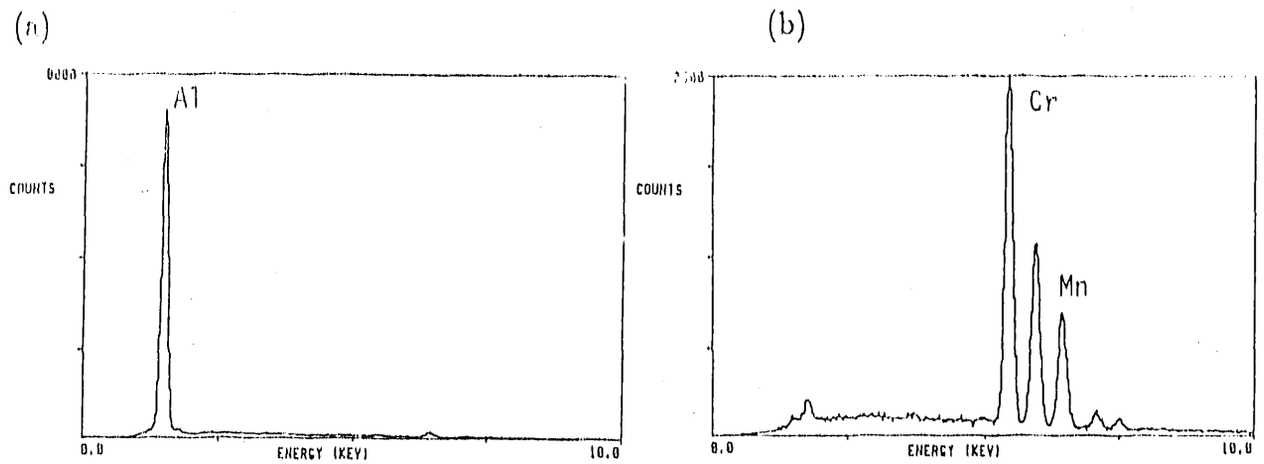

Fig. 39. EDS Spectra of Precipitates on the Top Metal Component of P-VIII-7

Table 15. Normalized Elemental Release for the P-VIII Series

Test #	Period (weeks)	Normalized Release (g/m^2)		
		B	Li	U
P-VIII-3	13	0.1	0.4	0.10
P-VIII-4	26	0.2	0.9	0.10
P-VIII-5	39	0.2	0.4	0.09
P-VIII-6	52	1.2	2.1	1.24
P-VIII-7	104	1.5	2.6	1.54
P-VIII-8	104*	2.6	4.8	1.63
	170	5.1	8.3	3.17
	195	5.4	8.8	3.40
P-VIII-1	52	0.1	1.0	0.07
	104	0.2	1.4	0.11
	143	0.2	1.6	0.12
	170	0.2	1.8	0.12
	195	0.2	2.0	0.13
P-VIII-2	52	0.2	0.6	0.05
	104	0.2	1.0	0.07
	143	0.2	1.2	0.18
	170	0.3	1.5	0.29

*P-VIII-8 was treated as a batch experiment up to 104 weeks.

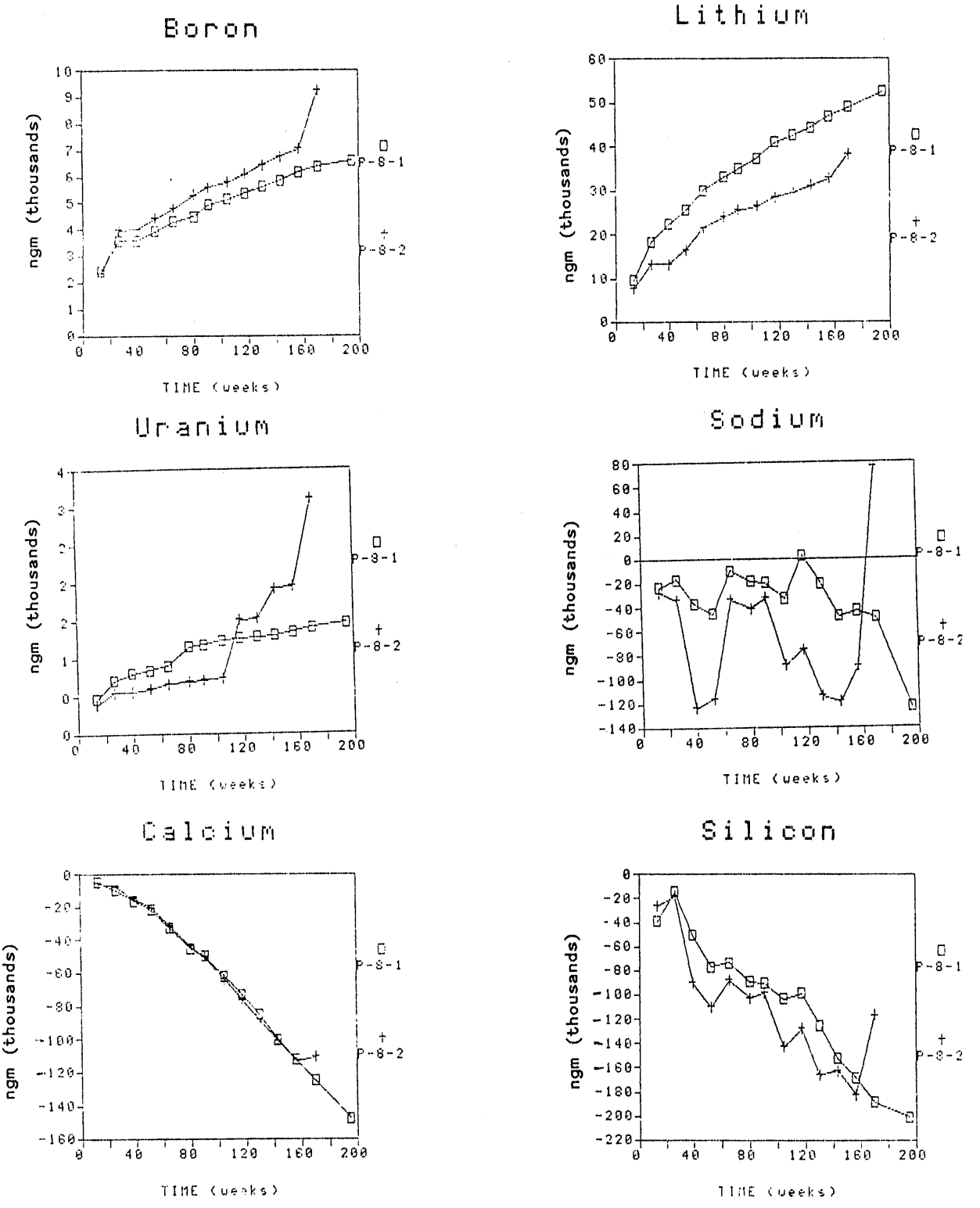

Fig. 40. Cumulative Release of Selected Elements from the P-VIII-1 and P-VIII-2 Continous Experiments

4. Discussion

There are several observations that can be made about the nature of reaction during the experiments. Despite the apparent difference in the conditions between the top and bottom surfaces (i.e., the top may have undergone wet/dry cycling, whereas the bottom remained wet at all times), the secondary phases are the same. The only difference is that the bottom appears to have undergone somewhat more reaction. The bottom has more precipitates and the surface layer may be a little thicker. The Si-rich "clay" is present as the reacted surface layer and as discrete grains on the glass and metal components. This indicates that the Si-rich material forms by both in situ transformation of hydrated glass and by precipitation. Its composition is consistent with Fe-smectite. The flaky texture of the glass surface is the same as observed on the metal which suggests that much of what is visible on the glass developed by precipitation. Most of the precipitates are composed of a very fine scale mixture of Si-rich "clay," Fe-oxide or hydroxide, and gypsum or anhydrite. This suggests that coprecipitation has occurred which lends support to the interpretation that the visible surface formed by precipitation. There appears to be more Fe-oxide or hydroxide associated with the P-VIII experiments indicating that presensitizing the stainless steel has had an influence on the observed secondary phases. However, the amount of metal corrosion is slight.

The structure of the surface layer undergoes changes upon aging. A network of cracks forms and parts of the layer begin to pull away from the glass. As this process continues, pieces of the layer exfoliates and precipitates form on the freshly exposed glass surfaces. The surface layer also seems to have a complex internal structure of multiple layers. These may correspond to portions formed through glass transformation and precipitation.

IV. DISCUSSION AND CONCLUSIONS

A. Parametric Effects

The series of five parametric experiments were designed to investigate the effect of various parameters on the rate of glass reaction. Overall element release is generally similar for the experiments suggesting that release is relatively insensitive to these parameters. However, there are differences in release and the observed extent of reaction which can, at least in part, be attributed to the varied parameters. The normalized releases of Li, B, and U are summarized in Fig. 41 for all the parametric experiments and the N2 standard Unsaturated Test using SRL 165U glass.[6] Relative release for all the experiments except P-II is Li > B ~ U which suggests either nonstoichiometric dissolution of the glass or that B and U are accommodated in secondary phases. The SIMS profiles from the P-III experiments indicate that B is depleted on the surface and within the altered layer, favoring nonstoichiometric dissolution as the explanation for the observed release behavior (Figs. 10, 17, and 19).

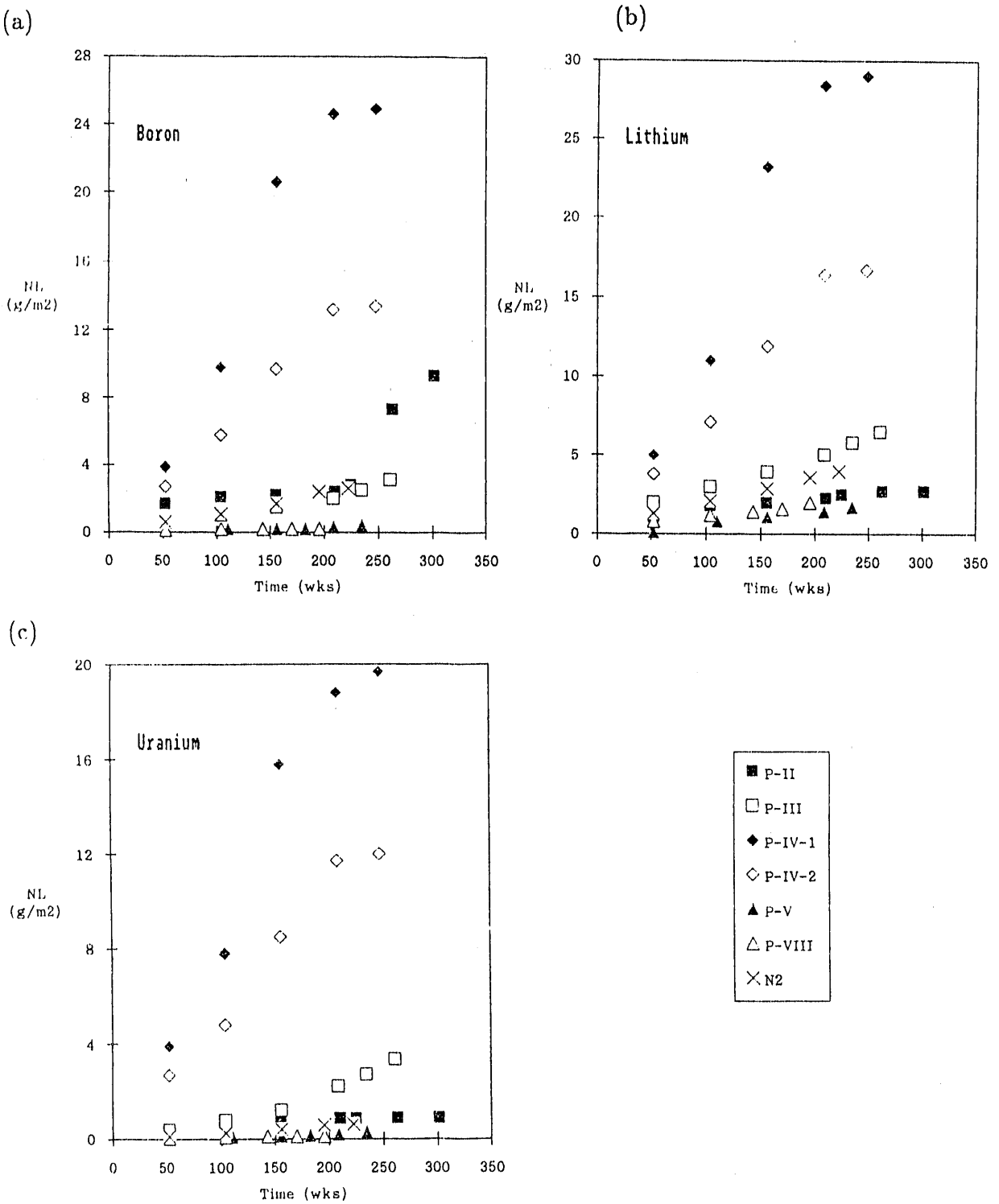

Fig. 41. Normalized Releases of B, Li, and U for the Parametric and "Standardized" N2 Unsaturated Experiments

The behavior of the experiment without the metal retainer (P-II) is similar to the N2 Test. The major difference between the P-II and the other experiments is the abundance of secondary phases that formed by evaporation (e.g., NaCl) and that B release exceeds Li release. Without the metal component, the glass surface may be more prone to drying out between injections, however, a direct cause and effect is not possible, because of problems with water retention in the vessels during the experiments. These problems may also be the cause of the reversed element release.

The reduction of glass surface area (experiments P-III and P-IV) gives an apparent small increase in the normalized release of Li and U relative to the N2 test (Fig. 41). This is an apparent increase because the geometric surface area was used in the normalization procedure, rather than an effective surface area. Visual observations and the results from SEM/EDS and SIMS examinations all indicate a variable extent of reaction between the top, bottom, and side surfaces, with the sides showing the least reaction. Since the surface area was reduced by shortening the sides of the glass cylinder, the change in the effective surface area (i.e., that part of the surface where reaction takes place) should be minimal. Therefore, the normalized releases for the P-III and P-IV experiments are exaggerated by close to a factor of two relative to the other parametric experiments. This must be considered when comparing releases from different experiments. As the effective surface area is smaller than the geometric surface area, the reported normalized releases for all the parametric experiments, especially those with the "full size" glass, will be underestimates of the "true" release. This must also be accounted for when comparing with other types of experiments such as leach tests where geometric surface area is equal to the effective surface area.

The P-IV experiments have anomalously high element release. There are two modified parameters in these experiments: a reduction in surface area and a reduction in the volume of water injected. Even if account is taken of the effective surface area (see above), the normalized releases are still significantly greater than any of the other experiments. The high release correlates with the extensive reaction observed on the surfaces by SEM. The reason for this anomalous behavior is uncertain. A reduction in injected water volume would seem to be an unlikely cause for a sharp increase in release. Conceivably, reaction could be enhanced by precipitation from a smaller fluid volume that would become rapidly saturated. However, the amount of precipitates on the P-IV samples is not noticeably greater than on samples from other experiments such as P-VIII. The observation that the WPAs in the P-IV experiments were always wet during sampling may provide a clue to the accelerated behavior, but, the reason why these experiments remained wettest is not known. In general, while the extent of reaction in these experiments was large, there was considerable variance in the batch and continuous test results.

Extension of the injection interval from 3-1/2 to 14 days reduces the element release and apparent extent of glass reaction. Observation of dry surfaces during sampling suggest that water is virtually absent for prolonged periods between injections. Consequently, elemental release from the glass is limited to short periods directly following injection.

The fifth parameter investigated is the effect of sensitizing the metal components. Assessment of this parameter is hampered by the poorly constrained degree of sensitization of the stainless steel. The stainless steel used in the P-VIII experiments has a lower C content (0.016 wt %) than the steel used in the standard N2 tests (0.022 wt %) which reduces the ability of the steel to become sensitized (Table 5).[6,16] In the N2 tests, pervasive metal reaction was observed.[6] However, in the P-VIII experiments, corrosion of the metal components is of a localized nature suggesting incomplete sensitization. Release is marginally greater for the experiments that exhibit metal reaction, but this is not definitive as these are also longer duration experiments. In addition, element release is much lower than in other experiments where unsensitized metal was used (compare P-VIII release and P-III, P-IV releases in Fig. 41). It is not clear that metal corrosion has any significant influence on glass reaction. At most it appears to be a second order effect. The metal components do act as sites for secondary phase precipitation and probably help to maintain water in contact with the glass by capillary action. These physical effects should act to enhance glass reaction.

B. The Surface Layer and Secondary Phases

The variation in the extent of reaction between individual parametric experiments provides the opportunity to investigate the evolution of the glass surface during reaction. The following discussion is limited because it is based only on SEM examination. Abrajano et al.[11] have demonstrated that Analytical Electron Microscopy (AEM) is required to achieve the resolution necessary for thorough characterization of the alteration layer and its relation to the glass surface. Several samples from the parametric experiments are being prepared for AEM examination, and preliminary results are presented in the Addendum. To help track the phases tentatively identified on the reacted test components, Table 16 provides a listing of phases discussed in the text.

An altered layer develops on the glass surface, presumably resulting from hydration and leaching of the glass. Initially, there is very little structure to this layer at least up to 15,000X magnification. Over time there is a progressive coarsening of the layer texture creating a bumpy or flaky surface. This layer is Si-rich and contains Fe, Ca, ±Mg, ±Na, ±Mn, ±Ni. It is similar in composition to Fe-smectite and to an amorphous phase called hisingerite. Eggleton et al. indicate that Fe-smectite crystallizes from hisingerite upon aging. It is conceivable that this may also occur in the altered layer. The progressive coarsening of the layer with time supports this hypothesis.

Investigation of extensively reacted samples reveals a complex structure with two to four discrete components to the altered layer. The outermost layer usually has a "cardhouse" or coarse flaky texture and is often not continuous across the surface suggesting it formed by precipitation. Its composition is essentially the same as the other parts of the altered layer, although other phases such as $CaSO_4$ and Fe-oxide or hydroxide are detectable in some EDS analyses. This intimate mixture of phases is consistent with the interpretation that the outermost layer formed by precipitation because the source for most of the Ca is the EJ-13 water. The lower portions of the altered layer have a variable texture as discussed above. The origin of these sublayers is not clear and awaits AEM examination.

Table 16. Summary of Phases Tentatively Identified in the Parametric Tests

Test #	Time of Reaction	Tentative Phase
P-II	26	Si-rich layer (smectite) Smooth layer (similar to glass composition) Gypsum or anhydrite ($CaSO_4$) Calcite ($CaCO_3$)
	52	Si-rich layer (smectite) Calcite Gypsum or anhydrite NaCl
P-III	13	Si-rich layer (smectite) NaCl Na_2SO_4 Na_2CO_3
	26	Si-rich layer (Ca smectite) Gypsum or anhydrite U, Si, Ca grain (uranophane) Na, Ca, S, Cl grains
	39	Si-rich layer Mn, Cr, Fe, Si grains Fe, Mn oxides/hydroxides Gypsum or anhydrite TiO_2 (anatase)
	52	Si-rich layer (smectite) NaCl Gypsum or anhydrite $CaCl_2$ Fe, Mn oxide/hydroxide
P-IV	25.5	Si-rich layer (smectite) Silica (opal/quartz) Calcite Cr, Fe, Mn oxide/hydroxide
	52	Si-rich layer (smectite) Gypsum/anhydrite Cr, Mn, Fe, Ni oxide/hydroxide

Cont'd

Table 16 (Cont'd)

Test #	Time of Reaction	Tentative Phase
P-V	26	Si-rich layer (smectite) Gypsum/anhydrite Fe, Cr, Mn oxide/hydroxide Silica (opal/quartz) Al-rich grains KCl Calcite Ca-P grains (apatite) Dolomite Mixed Ti-rich grains
	52	Si-rich layer (smectite) Cr, Mn, Fe, Ni oxide/hydroxide
P-VIII	26	Si-rich layer (smectite) Fe-rich grains with Mn, Ni Gypsum/anhydrite Calcite Si-Al-K grains (K-feldspar)
	52	Si-rich layer (smectite) Fe, Mn, Cr, Ni oxide/hydroxide Anhydrite/gypsum Silica (quartz/opal) Al-rich phase (gibbsite or Al-hydroxide) High-Mg calcite (dolomite) Calcite Cl-rich phase Na-Al-Si grain (analcime) NaCl
	104	Si-rich layer (Fe-smectite) Fe oxide/hydroxide Calcite, with Mg/Fe (dolomite) Al-rich grain (gibbsite, bayerite, nordstrandite) Cl- and S-rich grains NaCl, Na_2SO_4, CaSO, $CaCl_2$ Ti-rich phase (anatase) (Serpentine) (Apatite) Silica (quartz, opal)

The discontinuous nature of the precipitated layer along with its porous appearance of loosely intergrown grains indicate that the precipitates do not form a reliable barrier to fluid infiltration. While the precipitates will influence the local fluid chemistry, they do not physically impede fluid-glass interaction.

The surface layer undergoes other changes upon aging. A network of cracks form and parts of the layer begin to pull away from the glass. Cracking begins as a localized phenomenon even before the layer has fully developed across the surface. This process, sometimes referred to as crazing, has been observed during leaching of simple alkali-silicate glasses.[17] The inception of cracking may be influenced by the surface topography. The cause of cracking may be tensional forces at the interface between the hydrated altered layer and the glass. A contributing factor may also be volume changes and tensional forces within the layer as it begins to crystallize upon aging. Once a network of cracks is established, pieces of the layer begin to exfoliate from the surface, exposing patches of glass from below. Eventually, the exposed glass becomes covered with precipitates. The ubiquitous occurrence of cracks indicates that the surface layer cannot retard glass-fluid interaction to any large degree. While the intact layer may (or may not) act as a diffusion barrier, the cracks provide free access to the glass.

There are a number of secondary phases that have precipitated on the surface of both the glass and the metal components. The most common is Si-rich "clay" which has the same composition as the altered layer. Fe-oxide or hydroxide (XRD results suggest it is an oxide) is common especially on samples where the metal components have corroded. Some samples have a Cr- and Mn-rich phase, presumably an oxide or hydroxide. While the source of the Cr is probably the metal, no localized metal corrosion is observable on the samples where this phase occurs.

There are two common Ca-bearing phases: calcite and $CaSO_4$. They may occur together but generally only one is present. The net negative release of Ca in all the experiments indicates that Ca is removed from the EJ-13 water. Furthermore, the Ca depletion indicates that $CaSO_4$ precipitated during the experiment rather than upon cooling during sampling. Being the stable phase at 90°C, anhydrite must have precipitated. This demonstrates the influence of the EJ-13 water composition on the formation of secondary phases. Sodium-bearing phases are abundant on some samples but absent on others. Their occurrence is presumably linked to the availability of water. Phases tentatively identified include: NaCl, Na_2SO_4, and Na_2CO_3.

A U-bearing phase was observed on the metal components of the P-III-6 batch experiment. The small clusters of acicular grains contain Si and Ca which is suggestive of uranophane. This is the only observed occurrence of an U-bearing phase in any of the parametric experiments, although U-bearing phases are observed in the N2 tests.[6]

In order to assess the relative effects of an unsaturated environment where water drips onto the waste form, it is informative to compare this study's results with other types of experiments. Two short-term leaching experiments have been performed at 90°C using the same SRL 165U glass.[18,19] In these experiments, the glass was submerged in EJ-13 water and run both with and without an imposed γ-radiation field. The experiments of Ebert were performed at 0 and 1 x 10^{-3} rad/hr up to 278 days and those of Abrajano had a 1 x 10^{-4} rad/hr radiation field and a maximum duration of 182 days.

The normalized releases of B, Li, and U in the 278-day experiments of Ebert are presented in Table 17 along with the releases from selected batch and continuous experiments of similar duration. Element releases in the leaching experiments are only slightly greater than in the P-IV continuous and P-III batch experiments (by less than a factor of two). This difference is much less than

Table 17. Comparison of Normalized Release of B, Li, and U between the Leaching Experiments of Ebert and the Parametric Experiments

Test #	Time (weeks)	Normalized Release (g/m^2)		
		B	Li	U
G308[a]	39.7	4.93	6.98	4.38
G309[a]	39.7	4.80	6.89	4.17
G350[b]	39.7	3.61	5.87	3.56
G351[b]	39.7	4.08	5.97	3.51
	Parametric Experiments			
P-II-1	39	2.2	0.9	0.29
P-II-2	39	1.0	1.1	0.24
P-II-6	39	0.8	1.1	0.27
P-III-1	39	0.5	1.8	0.46
P-III-2	39	0.4	1.6	0.34
P-III-7	39	3.1	4.2	2.11
P-III-8	39	2.0	3.3	1.48
P-IV-1	39	2.9	3.8	2.88
P-IV-2	39	2.2	3.2	2.10
P-V-1	39.5	0.1	0.0	0.00
P-V-2	39.5	0.1	0.5	0.06
P-VIII-1	39	0.1	0.8	0.07
P-VIII-2	39	0.1	0.5	0.05
P-VIII-5	39	0.2	0.4	0.09

[a]90°C leach test of Ebert with 1 x 10^{-3} rad/hr γ-radiation.
[b]90°C leach test of Ebert with no radiation.

the order of magnitude range in release obtained for the set of parametric experiments. Furthermore, the normalization procedure underestimates release only for the parametric experiments because the geometric and effective surface areas are equal in the leaching experiments (see above). This suggests that true normalized releases, based upon the effective surface area, would be in even closer agreement between the parametric and leaching experiments.

The release trends of the leaching and parametric experiments do appear to differ. The rates of release in the leaching experiments become progressively reduced through 39 weeks. In contrast, the release rates remain relatively constant in the parametric experiments for at least 300 weeks. This differing behavior may be attributable to the dripping environment where fresh water is periodically added and where evaporation can occur.

Relative release for the leaching (complete liquid submersion) and parametric (drip) experiments is Li > B ~ U (except for P-II) suggesting a similar mechanism of glass reaction for both types of experiments. In the leaching experiments Na and Mg exhibit large positive releases but Ca has only a very small release. In the parametric experiments Na release is often erratic and Mg and Ca have net negative releases. This contrasting behavior is most likely attributable to differences in the secondary phases that precipitate on the glass. Aside from an Fe-smectite-like surface layer, precipitation in the leach experiments is not very extensive. Some Ca-rich precipitates such as calcite are reported by Ebert along with a U-silicate, an Al-rich phase, and rare NaCl. In contrast, precipitates are generally much more abundant in the drip experiments. Ca-rich precipitates such as calcite or anhydrite are common as is NaCl. It appears that in the unsaturated environment of the parametric experiments precipitation is more extensive, which in turn influences the solution chemistry. The development of a clay-like surface layer is common to both types of experiments and the behavior of the elements most indicative of glass reaction (Li, B, and U) is the same.

V. ACKNOWLEDGMENTS

Work supported by the U.S. Department of Energy, Office of Civilian Radioactive Waste Management, Yucca Mountain Site Characterization Project, under subcontract to Lawrence Livermore National Laboratory, SANL 910-005.

VI. REFERENCES

1. J. K. Bates and T. J. Gerding, "NNWSI Phase II Materials Interaction Test Procedure and Preliminary Results," Argonne National Laboratory report ANL-84-81 (1984).

2. J. K. Bates and T. J. Gerding, "One-Year Results of the NNWSI Unsaturated Test Procedure: SRL 165 Glass Application," Argonne National Laboratory report ANL-85-41 (1986).

3. Site Characterization Plan, U.S. Department of Energy, Office of Civilian Radioactive Waste Management, DOE report DOE/RW-0199 (1988).

4. W. L. Bourcier, D. W. Peiffer, K. G. Knauss, K. D. McKeegan, and D. K. Smith, "A Kinetic Model for Borosilicate Glass Dissolution Based on the Dissolution Affinity of a Surface Alteration Layer," Mat. Res. Soc. Symp. Proc. 176, 209-216 (1990).

5. C. J. Bruton, "Geochemical Simulation of Dissolution of West Valley and DWPF Glasses in J-13 Water at 90°C," Lawrence Livermore National Laboratory preprint UCRL-96703 (1987).

6. J. K. Bates and T. J. Gerding, "Application of the NNWSI Unsaturated Test Method to Actinide Doped SRL 165 Type Glass," Argonne National Laboratory report ANL-89/24 (1990).

7. G. T. Chandler, G. G. Wicks, and R. M. Wallace, "Effects of SA/V and Saturation on the Chemical Durability of SRP Waste Glass," Savannah River Laboratory report DP-MS-86-56 (1986).

8. "DWPF Waste Form Compliance Plan," U.S. DOE report DPST-86-746 (1988).

9. C. M. Jantzen and M. J. Plodinec, "Thermodynamic Model of Natural, Medieval, and Nuclear Waste Glass Durability," J. Non-Cryst. Sol. 67, 207-223 (1984).

10. W. A. Deer, R. A. Howie, and J. Zussman, An Introduction to the Rock-Forming Minerals, Longman, London, 528 pp. (1966).

11. W. L. Ebert, J. K. Bates, and W. L. Bourcier, "The Hydration of Borosilicate Waste Glass in Liquid Water and Steam at 200°C," accepted for publication in Waste Management.

12. T. A. Abrajano, Jr., J. K. Bates, A. B. Woodland, J. P. Bradley, and W. L. Bourcier, "Secondary Phase Formation during Nuclear Waste-Glass Dissolution," Clay and Clay Min. 38, 537-548 (1990).

13. J. K. Bates, T. J. Gerding, W. L. Ebert, J. J. Mazer, and B. M. Biwer, "NNWSI Waste Form Testing at Argonne National Laboratory, Semiannual Report, July-December 1987," Lawrence Livermore National Laboratory report UCRL-21060-87-2 (1989). NNA.881115.0026

14. A. E. Nielsen, Kinetics of Precipitation, MacMillan Co., New York, pp. 72-85 and 108-119 (1964). NNA.910903.0118

15. W. Stumm and J. J. Morgan, Aquatic Chemistry, An Introduction Emphasizing Chemical Equilibria in Natural Waters, 2nd Edition, J. Wiley and Sons, New York, NY, 230-319 (1981). NNA.910903.0117

16. R. L. Cowan and C. S. Tedman, Jr., "Intergranular Corrosion of Fe-Ni-Cr Alloys," in Advances in Corrosion Science and Technology, Vol. 3, M. G. Fontana and R. W. Staehle, eds., Plenum Press, New York, 292-400 (1973). NNA.890921.0111

17. B. C. Bunker, G. W. Arnold, E. K. Geauchamp, and D. E. Day, "Mechanisms for Alkali Leaching in Mixed Na-K Silicate Glasses," J. Non-Cryst. Sol. 58, 295-322 (1983). NNA.910215.0015

18. T. A. Abrajano, Jr., J. K. Bates, T. J. Gerding, and W. L. Ebert, "The Reaction of Glass during Gamma Irradiation in a Saturated Tuff Environment, Part 3: Long-Term Experiments at 1 x 10^4 Rad/Hour," Argonne National Laboratory report ANL-88-14 (1988). HQX.880721.0013

19. W. L. Ebert, J. K. Bates, and T. J. Gerding, "The Reaction of Glass during Gamma Irradiation in a Saturated Tuff Environment, Part 4: SRL 165, ATM-1c, and ATM-8 Glasses at 1E3 R/h and 0 R/h," Argonne National Laboratory report ANL-90/13 (1990). NNA.900509.0197

20. J. P. Bradley and J. K. Bates, "Leached Nuclear Waste Glasses: Ultramicrotomy and Electron Microscopic Characterization," Proc. of the 12th Mtg. of the Microbeam Analysis Soc. (1990). NNA.910903.0119

ADDENDUM

While the SEM provides important information about the nature of glass reaction, it lacks the requisite resolution to understand the detail of alteration layer development. Analytical electron microscopy (AEM) may provide the key to unravelling this process. For example, the AEM study by Abrajano et al. of leached SRL 131 glass reveals a reaction layer with a complex structure, composed of six distinct sublayers and a mixture of amorphous material and crystalline phases.[12] At present two samples from the parametric experiments have been prepared. The following a very brief description of these samples. A thorough AEM investigation will be the subject of a future topical report.

A section through the reacted layer from the bottom glass surface of P-VIII-7 (104 weeks) is presented in Fig. 42. As there is no accompanying glass in this sample, this must be viewed as only a partial section through the upper part of the layer. This part has a complex structure of repeated bands only partially attached to one another. Each band has a fine-grained Fe-rich element with an epitaxial growth of smectite on either side. The structure of the individual bands is reminiscent of that observed for the same glass after 280 days in static MCC-1 leach tests.[20] The origin of the multiple bands is uncertain at this time.

A sample from the side of P-III-10 (52 weeks) was taken from near the top surface where prolonged water contact had occurred during the experiment. There is a layer of coarse, loosely packed smectite grains which lies above the glass surface (Fig. 43). No Fe-rich band is observed here. The smectite may have formed by precipitation on the glass. However, etching has caused retreat of the glass surface, resulting in a gap between the smectite layer and the glass.

Much more work needs to be done; however, it is clear that the AEM is an extremely useful tool for investigating the mechanisms of glass alteration. This work is underway. It is comforting that some of the interpretations based on SEM observations are confirmed by the preliminary AEM results.

Fig. 42. TEM Micrograph of the Layer from the Bottom of P-VIII-7. The scale is 7 mm = 500 nm

Fig. 43. TEM Micrograph of the Side of P-III-10. The scale is 9 mm = 200 nm

APPENDIX I

Raw data for the analyses of solutions from the parametric unsaturated experiments (continuous mode) are presented. The data presented include the test number, sample interval (in weeks; both the interval and cumulative time periods are given), sample identifier (TF #), the solution volume in mL submitted for analysis (the original solution volume is diluted with acidified DIW prior to analysis), and the volume of test solution added during the test period (water is injected throughout the test period and a specified volume of water is added to the bottom of the test vessel at the beginning of each test period. The water added at the beginning of the test period is DIW for the P-II experiments and EJ-13 for the other experiments. The volume given in the H_2O Added column is only the volume of EJ-13 or J-13 water and the value is used in the background subtraction process).

The composition of groundwater (ppm) added during the test is given in the first row(s) under the heading of elements. For each sampling period, generally three rows of data are presented. The first row is the total mass of each element in the diluted solution submitted for analysis, the second row is the total mass of each element in solution that can be attributed to the glass (the value is obtained by subtracting from the total elemental mass the mass attributed to groundwater added to the test. The value will be negative if elements are precipitated from solution). The third row is the cumulative mass of each element attributed to the glass.

Test #	Time Period	TF #	Solution Volume	H2O Added		Al	B	Ca	Fe	Li	Mg	Mn	Na	Ni	Si	U	K
					E-313	100	130	13600	10	49	2130	5	46700	28	30900	0	4450
PII-1a	6	TF-63	20.57	0.900		1650	18100	4300	2470	4320	1070	450	28400		9460	420	
						1560	17983	-7940	2461	4276	-847	446	-13630	-25	-18350	420	0
1b	7	TF-69	20.75	1.050		10375	16200	3940	2280	3110	930	280	28600	435	5800	504	
	13					10270	16064	-10340	2270	3059	-1306	275	-20435	496	-26645	504	0
						11830	34046	-18280	4730	7334	-2154	720	-34065	380	-44995	924	0
1c	6.5	TF-72	20.71	0.975		1035	9300	5200	1850	3300	970	410	30000	400	8300	460	
	19.5					938	9173	-8060	1840	3252	-1107	405	-15532	373	-21828	460	0
						12768	43220	-26340	6571	10587	-3260	1125	-49598	753	-66822	1384	0
1d	6.5	TF-79	20.52	0.975		1000	8600	2000	1370	5130	550	160	55880	400	4500	615	
	26					902	8473	-11260	1360	5082	-1527	155	10348	373	-25628	615	0
						13670	51693	-37600	7931	15669	-4787	1280	-39250	1126	-92450	1999	0
1e	7	TF-91	20.80	1.050		1500	6000	3950	1620	4035	330	395	44300	600	12200	565	
	33					1395	5864	-10330	1610	3984	-1906	390	-4735	571	-20245	565	0
						15065	57556	-47930	9540	19652	-6694	1670	-43985	1696	-112695	2564	0
1f	6	TF-97	24.92	0.900		1200	5200	2750	1050	4500	125	350	64000	2050	14000	570	
	39					1110	5083	-9490	1041	4456	-1792	346	21970	2025	-13810	570	0
						16175	62640	-57420	10582	24108	-8486	2016	-22015	3721	-126505	3134	0
1g	6.5	TF-111	21.28	0.975		1200	2800	2100	1600	1210	250	340	16400	425	7000	147	
	45.5					1102	2673	-11160	1590	1162	-1827	335	-29132	398	-23128	147	0
						17278	65313	-68580	12172	25271	-10312	2351	-51148	4119	-149632	3281	0
1h	6.5	TF-123	25.5	0.975		1300	2370	2500	5870	1000	180	870	19100		5360	242	
	52					1202	2243	-10760	5860	952	-1897	865	-26432	-27	-24768	242	0
						18480	67556	-79340	18032	26223	-12209	3216	-77580	4092	-174400	3523	0
1i	6.5	TF-141	20.57	0.975		1000	2900	11300	5140	1770	1200		27000		9050	245	
	58.5					902	2773	-1960	5130	1722	-877	-5	-18532	-27	-21078	245	0
						19382	70329	-81300	23162	27945	-13086	3211	-96112	4064	-195478	3768	0
1j	7	TF-152	21.11	1.05		1050	3800	7600	2100	3380	1370	510	103200		24700	443	
	65.5					945	3664	-6680	2090	3329	-866	505	54165	-29	-7745	443	0
						20328	73993	-87980	25252	31274	-13952	3716	-41948	4035	-203222	4211	0
1k	5.5	TF-180	20.44	0.825		2000	2250	2050	715	3470	350	960	81600		6100	382	
	71					1918	2143	-9170	707	3430	-1407	956	43072	-23	-19392	382	0
						22245	76136	-97150	25958	34703	-15360	4672	1125	4012	-222615	4593	0

Test #	Time Period	TF #	Solution Volume	H2O Added	Al	B	Ca	Fe	Li	Mg	Mn	Na	Ni	Si	U	K
1l	7.5	TF-203	16.13	1.125	1600	3200	1300	400	3550	260	145	77100	320	13400	448	
	78.5				1488	3054	-14000	389	3495	-2136	139	24562	288	-21362	448	0
					23732	79189	-111150	26347	38198	-17496	4811	25688	4300	-243978	5041	0
1m	5	TF-224	20.12	0.75	2000	1700	1600	1400	2150	260	260	47300	560	12100	356	
	83.5				1925	1602	-8600	1392	2113	-1338	256	12275	539	-11075	356	0
					25658	80792	-119750	27740	40311	-18833	5057	37962	4839	-255052	5397	0
1n	7.5	TF-237	22.33	1.125	2200	1500	1100	330	3750	200	130	94000	450	21900	431	
	91				2088	1354	-14200	319	3695	-2196	124	41462	418	-12862	431	0
					27745	82146	-133950	28058	44006	-21030	5192	79425	5258	-267915	5828	0
1o	6.5	TF-256	23.49	0.975	2300	700	1200	230	460	110	110	1200	460	2300	0	
	97.5				2202	573	-12060	220	412	-1967	105	-44332	433	-27828	0	0
					29948	82719	-146010	28279	44418	-22996	5297	35092	5690	-295742	5828	0
1p	6.5	TF-268	20.97	0.975	2100	1300	2700	1000	3550	300	400	101700	420	30000	0	
	104				2002	1173	-10560	990	3502	-1777	395	56168	393	-128	0	0
					31950	83892	-156570	29269	47921	-24773	5692	91260	6083	-295870	5828	0
1q	6.5	TF-290	15.71	0.975	2200	700	4400	1600	960	800	520	12100	520	10400		
	110.5				2102	573	-8860	1590	712	-1277	515	-33432	493	-19728	0	0
					34052	84465	-165430	30859	48833	-26050	6207	57828	6576	-315598	5828	0
1r	6.5	TF-316	19.13	0.975	1900	550	2900	950	520	460	80	10100	540	4200	384	
	117				1802	423	-10360	940	472	-1617	75	-35432	513	-25928	384	0
					35855	84888	-175790	31800	49305	-27666	6282	22395	7089	-341525	6212	0
1s	6.5	TF-334	17.69	0.975	1700	530	1900	800	1200	350	200	32500	350	8500	459	
	123.5				1602	403	-11360	790	1152	-1727	195	-13032	323	-21628	459	0
					37458	85292	-187150	32590	50457	-29393	6477	9362	7411	-363152	6671	0
1t	5.5	TF-349	20.46	0.825	2000	600	1100	600	2200	360	180	70000		9000	473	
	129				1918	493	-10120	592	2160	-1397	176	31472	-23	-16492	473	0
					39375	85784	-197270	33182	52617	-30790	6653	40835	7388	-379645	7144	0
1u	26	TF-317	15.55	3.900	1500	450	2300	800	420	370	140	8200	430	3400	312	
	155				1110	-57	-50740	761	229	-7937	120	-173930	321	-117110	312	0
					40485	85728	-248010	33942	52846	-38728	6774	-133095	7709	-496755	7456	0

Test #	Time Period	TF #	Solution Volume	H2O Added	Al	B	Ca	Fe	Li	Mg	Mn	Na	Ni	Si	U	K
1v	36.5	TF-501	22.71	5.475	2200	5320	6400	2200	11100	2140	840	319200	2400	175100	4434	26800
	191.5				1652	4608	-68060	2145	10832	-9522	813	63518	2247	5922	4434	2436
					42138	90336	-316070	36088	63677	-48249	7586	-69577	9956	-490832	11890	2436
1w	18.5	TF-577	21.17	2.775	100	44	250	47	34	31	5	1340	36	200	6.5	300
	210				2117	931	5292	995	720	656	106	28368	762	4234	105	6351
					1840	571	-32448	967	584	-5254	92	-101225	684	-81514	105	-5998
					43977	90906	-348518	37055	64261	-53504	7678	-170802	10640	-572346	11995	-3561
1x	14.5	TF-639	18.38	2.175	1800	12130	8500	800	1800	350	400	104400	680	22800	239	23200
	224.5				1582	11847	-21080	778	1693	-4283	389	2828	619	-44408	239	13521
					45560	102754	-369598	37833	65955	-57786	8067	-167975	11259	-616754	12234	9960
1y	11.5	TF-680	31.52	1.725	3200	146568	13200	1900	400	1000	600	7200	1000	32500	117	9500
	236				3028	146344	-10260	1883	315	-2674	591	-73358	952	-20802	117	1824
					48587	249097	-379858	39716	66270	-60461	8659	-241332	12211	-637556	12351	11784
1z	20.5	TF-748	34.26	3.075	3400	45600	7500	1300	3600	550	340	156200	690	79100	120	38000
	256.5				3092	45200	-34320	1269	3449	-1473	325	12598	604	-15918	120	24316
					51680	294298	-414178	40985	69720	-61933	8983	-228735	12815	-653474	12471	36100
1aa	5.5	TF-767	24.41	0.825	2400	10000	1500	800	390	270	120	16800	730	22400	24	6600
	262				2318	9893	-9720	792	350	-1487	116	-21728	707	-3092	24	2929
					53997	304190	-423898	41777	70069	-63421	9099	-250462	13522	-656566	12495	39028
1bb	13	TF-820	18.28	1.95	5500	5500	1300	3800	370	180	180	7100	1650	25800	12	16500
	275				5305	5246	-25220	3780	274	-3974	170	-83965	1595	-34455	12	7822
					59302	309437	-449118	45557	70344	-67394	9270	-334427	15117	-691021	12507	46851
1cc	26	TF-864	15.04	3.90*	1500	2250	1350	890	180	420	500	4210	450	25870	23	4510
	301				1400	2120	-12250	880	131	-1710	495	-42490	422	-5030	23	60
					60702	311557	-461368	46437	70475	-69104	9765	-376917	15539	-696051	12530	46911

Test #	Time Period	TF #	Solution Volume	H2O Added		Al	B	Ca	Fe	Li	Mg	Mn	Na	Ni	Si	U	K
					J-13	100	130	13600	10	49	2130	5	46700	28	30900	0	4450
PII-2a	6	TF-64	20.60	0.900		3900	8650	1850	1440	1100	560	160	8240		2680	250	
						3810	8533	-10390	1431	1056	-1357	156	-33790	-25	-25130	250	0
2b	7	TF-71	20.76	1.050		12250	5400	2000	1300	3100	460	150	23700		4150	378	
	13					12145	5264	-12280	1290	3049	-1776	145	-25335	-29	-28295	378	0
						15955	13796	-22670	2720	4104	-3134	300	-59125	-55	-53425	628	0
2c	6.5	TF-73	20.88	0.975		1040	6050	2100	1670	9200	540	100	71000	410	18150	837	
	19.5					942	5923	-11160	1660	9152	-1537	95	25468	383	-11978	837	0
						16898	19720	-33830	4381	13257	-4670	395	-33658	328	-65402	1465	0
2d	6.5	TF-80	20.99	0.975		2900	2500	2000	900	3800	340	100	31500	420	5700	233	
	26					2802	2373	-11260	890	3752	-1737	95	-14032	393	-24428	233	0
						19700	22093	-45090	5271	17009	-6407	490	-47690	721	-89830	1698	0
2e	7	TF-92	20.99	1.050		1600	4000	2300	2400	10500	480	300	118100	900	51400	865	
	33					1495	3864	-11980	2390	10449	-1756	295	69065	871	18955	865	0
						21195	25956	-57070	7660	27457	-8164	785	21375	1591	-70875	2563	0
2f	6	TF-98	22.40	0.900		1100	1120	2200	1650	1200	150	100	24400	450	2900	73	
	39					1010	1003	-10040	1641	1156	-1767	95	-17630	425	-24910	73	0
						22205	26960	-67110	9302	28613	-9930	881	3745	2016	-95785	2636	0
2g	6.5	TF-112	19.08	0.975		950	860	1900	800	1240	170	115	23100	400	7100	66	
	45.5					852	733	-11360	790	1192	-1907	110	-22432	373	-23028	66	0
						23058	27693	-78470	10092	29806	-11837	991	-18688	2389	-118812	2702	0
2h	6.5	TF-124	25.15	0.975		1300	900	4000	1500	1400	500	1500	27400		7000	101	
	52					1202	773	-9260	1490	1352	-1577	1495	-18132	-27	-23128	101	0
						24260	28466	-87730	11562	31158	-13414	2486	-36820	2362	-141940	2803	0
2i	6.5	TF-140	20.24	0.975		1200	770	3240	3440	1500	485		22500		9300	79	
	58.5					1102	643	-10020	3430	1452	-1592	-5	-23032	-27	-20828	79	0
						25362	29109	-97750	15012	32610	-15006	2481	-59852	2334	-162768	2882	0
2j	7	TF-153	20.48	1.05		1020	610	7800	2250	1820	1660	1150	67400		23600	108	
	65.5					915	474	-6480	2240	1769	-576	1145	18365	-29	-8845	108	0
						26278	29583	-104230	17252	34379	-15582	3626	-41488	2305	-171612	2990	0

Test #	Time Period	TF #	Solution Volume	H2O Added	Al	B	Ca	Fe	Li	Mg	Mn	Na	Ni	Si	U	K
2k	5.5	TF-181	19.25	0.825	1900	620	2700	2300	2900	500	620	70800		11550	179	
	71				1818	513	-8520	2292	2860	-1257	616	32272	-23	-13942	179	0
					28095	30096	-112750	19544	37238	-16840	4242	-9215	2282	-185555	3169	0
2l	7.5	TF-204	16.77	1.125	1700	855	4700	600	3520	440	130	78500	340	13600	116	
	78.5				1588	709	-10600	589	3465	-1956	124	25962	308	-21162	116	0
					29682	30804	-123350	20132	40703	-18796	4366	16748	2590	-206718	3285	0
2m	5	TF-223	20.64	0.75	2000	660	1900	370	660	270	190	14700	600	4300	31	
	83.5				1925	562	-8300	362	623	-1328	96	-20325	579	-18875	31	0
					31608	31367	-131650	20495	41326	-20123	4462	-3578	3169	-225592	3316	0
2n	7.5	TF-238	22.69	1.125	2200	680	1300	250	450	230	110	8200	450	2300	22	
	91				2088	534	-14000	239	395	-2166	104	-44338	418	-32462	22	0
					33695	31900	-145650	20734	41721	-22290	4567	-47915	3583	-258055	3338	0
2o	6.5	TF-257	22.84	0.975	2300	690	1800	250	460	500	110	23100	460	2300	0	
	97.5				2202	563	-11460	240	412	-1577	105	-22432	433	-27828	0	0
					35898	32464	-157110	20974	42133	-23866	4672	-70348	4020	-285882	3338	0
2p	6.5	TF-269	21.51	0.975	2200	1600	5800	1660	5160	860	430	185000	420	74900	0	
	104				2102	1473	-7460	1650	5112	-1217	425	139468	393	44772	0	0
					38000	33937	-164570	22624	47246	-25083	5097	69120	4413	-241110	3338	0
2q	6.5	TF-291	15.71	0.975	1700	1020	2400	850	740	360	190	23600	380	12400		
	110.5				1602	893	-10860	840	692	-1717	185	-21932	353	-17728	0	0
					39602	34830	-175430	23464	47938	-26800	5282	47188	4766	-258838	3338	0
2r	6.5	TF-317	22.65	0.975	2200	450	1700	900	680	320	110	10900	450	5000		
	117				2102	323	-11560	990	632	-1757	105	-34632	423	-25128	0	0
					41705	35154	-186990	24354	48570	-28556	5387	12555	5189	-283965	3338	0
2s	6.5	TF-335	18.92	0.975	1900	570	2100	700	380	380	230	4900	380	3600	989	
	123.5				1802	443	-11160	690	332	-1597	225	-40632	353	-26528	989	0
					43508	35597	-198150	25045	48902	-30253	5612	-28078	5541	-310492	4327	0
2t	6.5	TF-350	17.11	0.825	1700	500	20700	2000	800	1200	430	25200	670	9600	640	
	129				1618	393	9480	1992	760	-557	426	-13328	847	-15892	640	0
					45125	35990	-188670	27036	49662	-30810	6038	-41405	6388	-326385	4967	0

Test #	Time Period	TF #	Solution Volume	H2O Added	Al	B	Ca	Fe	Li	Mo	Mn	Na	Ni	Si	U	I
2u	26	TF-318	15.94	3.900	1600	320	1200	640	480	220	80	7700	320	3500	1190	
	155				1210	-187	-51840	601	289	-8087	60	-174430	211	-117010	1190	0
					46335	35802	-240510	27639	49951	-38898	6099	-215835	6599	-443395	6157	0
2v	36.5	TF-502	17.91	5.475	1800	950	9700	8400	230	1250	1700	49600	3220	84100	150	5400
	191.5				1252	238	-54760	8345	-38	-10412	1673	-206082	3067	-85078	150	-18964
					47588	36041	-305270	35983	49912	-49309	7771	-421918	9666	-528472	6307	-18964
2w	18.5	TF-578	19.85	2.775	100	340	1220	110	190	50	15	12900	56	1970	14	420
	210				1985	6749	24217	2184	3772	993	298	256065	1112	39104	278	8337
					1708	6388	-13523	2156	3636	-4918	284	125473	1034	-46643	278	-4012
					49295	42429	-318793	38138	53548	-54228	8055	-295445	10700	-575116	6585	-22976
2x	14.5	TF-649	19.24	2.175												
	224.5				1900	14400	10400	2100	3800	900	290	215200	600	62700	231	25400
					1682	14117	-19180	2078	3693	-3733	279	114628	539	-4508	231	15721
					50978	56546	-337973	40217	57241	-57960	8334	-180818	11239	-579623	6816	-7254
2y	11.5	TF-681	31.20	1.725	3100	25600	4200	1000	3100	340	160	7500	620	29300	296	9400
	236				2928	25376	-19260	983	3015	-3334	151	-73058	572	-24002	296	1724
					53905	81922	-357233	41200	60257	-61294	8486	-253875	11810	-603626	7112	-5530
2z	20.5	TF-749	33.36	3.075	3300	20000	4000	700	500	330	160	12700	620	58700	37	10000
	256.5				2992	19600	-37820	669	349	-6220	145	-130902	534	-36318	37	-3684
					56852	101464	-401173	41864	60584	-68473	8628	-405792	12532	-653848	7149	-9214
2aa	5.5	TF-768	23.99	0.825	2400	6000	700	500	2400	240	120	6000	220	19700	24	4800
	262				2318	5893	-10520	492	2360	-1517	116	-32528	197	-5792	24	1129
					59170	107356	-411693	42356	62944	-69990	8744	-438320	12529	-659640	7173	-8086
2bb	13	TF-821	17.77	1.95	5300	96600	2300	22700	350	200	10000	8700	3000	35900	18	16000
	275				5105	96346	-24220	22680	254	-3954	9990	-82365	2945	-24355	18	7322
					64275	203703	-435913	65036	63198	-73944	18734	-520685	15474	-683996	7191	-763
2cc	26	TF-865	15.07	3.90	1500	8740	770	590	500	200	150	220000	450	104740	41	39480
	301				1110	8233	-52270	551	309	-8107	130	37870	341	-15770	41	22125
					65385	211936	-488183	65588	63507	-82050	18855	-482815	15815	-699766	7232	21362

						Al	B	Ca	Fe	Li	Mg	Mn	Na	Ni	Si	U		
					E-013	710	170	4100	10	71	370	5	46800	20	36900	4		
PIII-3	13.0	TF-128	28.56	1.95		1700	3450	4300	51700	13140	400	14900	113400	ND	[illegible]	691	ND	
						316	3079	-5695	51660	13002	-360	14870	22140	-39	-22255	664		0
PIII-4	15.0	TF-130	26.59	1.95		1860	4250	5050	42300	14900	560	29000	114900	ND	[illegible]	1239	ND	
						476	3918	-2945	42280	14762	-200	28990	23640	-39	4845	1232		0
PIII-5	26.0	TF-170	18.18	4.2	RINSE	900	1100	1600	545	2360	90	90	30900	360	18500	600	ND	
		TF-172	18.87		ACID SOAK	3000	10400	5100	26400	22300	630	11700	221000	5100	161500	4364	ND	
					TOTAL	3900	11500	9900	26945	24660	720	11790	251900	5460	180000	4964		0
						916	10786	-7320	26903	24362	-868	11769	55340	5376	25720	4949		0
PIII-6	28.0	TF-171	19.59	4.2	RINSE	1000	1700	2000	2150	2350	160	650	13700	450	15500	1042	ND	
		TF-173	16.56		ACID SOAK	13400	46400	9800	38300	57000	730	14200	399000	6500	453700	17340	ND	
					TOTAL	14400	48160	11800	40950	59350	890	14850	412700	6950	469200	18382		0
						11418	47446	-5420	40908	59052	-748	14829	216140	6866	314220	18367		0
PIII-7	39.0	TF-206	20.07	5.85	RINSE	2000	3010	2400	5600	3400	360	1500	26500	960	26500	1043	ND	
		TF-212	22.15		ACID SOAK	13700	43000	12600	86200	54300	930	21000	431700	7750	460900	15638	ND	
					TOTAL	15700	46010	15000	91800	57700	1290	22500	458200	8710	487400	16681		0
						11546	45016	-8985	91742	57285	-992	22471	184420	8593	271535	16660		0
PIII-8	39.0	TF-209	18.82	5.85	RINSE	1900	1730	940	2260	2500	120	530	26200	380	15800	621	ND	
		TF-213	20.97		ACID SOAK	7300	28300	12000	88300	42150	900	18200	385500	8000	338700	10778	ND	
					TOTAL	9200	30030	12940	90560	44650	1030	18730	412000	8380	354500	11399		0
						5046	29036	-11045	90502	44255	-1252	18701	136220	8263	138635	11388		0
PIII-9	52.0	TF-243	20.37	7.8		14300	54400	13900	69900	74400	1500	21000	607000	10000	513300	20044	ND	
						8762	53074	-18080	69822	73846	-1542	20961	241960	9944	225480	20016		0
PIII-10	52.0	TF-244	18.79	7.8		12200	54800	16500	62600	54100	1500	4100	464800	6400	392700	13822	ND	
						6662	53474	-15480	62522	53546	-1542	4061	119760	6244	104880	13294		0

Test #	Time Period	TF #	Solution Volume	H2O Added		Al	B	Ca	Fe	Li	Mg	Mn	Na	Ni	Si	U	K
					E-J13	710	170	4100	10	71	390	5	46800	20	36900	4	
					E-J13	240	161	7150	10	52	263	5	49200	20	34200	1	5600
PIII-1a	6.5	TF-114	20.33	0.975 *		1320	2440	3850	65700	6500	610	22600	38600	9150	28870	439	
						628	2274	-948	65690	6431	230	22595	-7030	9130	-7106	436	0
1b	6.5	TF-126	22.46	1.175		1100	1800	2700	20500	5200	280	4900	59100		39600	447	
	13					266	1600	-2118	20468	5117	-258	4894	4110	-24	-3758	442	0
						894	3874	-3065	86176	11547	-28	27469	-2920	9107	-10865	878	0
1c	6.5	TF-143	21.76	1.175		1100	1410	3700	10200	4350	175		65500		42900	496	
	19.5					266	1210	-1115	10188	4267	-283	-6	10310	-24	-458	491	0
						1159	5085	-4182	96367	15814	-312	27423	7593	9084	-11322	1369	0
1d	6.5	TF-156	21.19	1.250 **		1100	1020	3600	15000	2970	170	3180	58400	3600	36700	328	
	26					212	806	-1525	14988	2881	-318	3174	-2100	3575	-9425	324	0
						1372	5892	-5706	111354	18695	-629	30657	5290	12656	-20748	1693	0
1e	6.5	TF-187	16.94	1.175		1700	1100	4200	19100	3950	220	1400	64700	2900	42900	454	0
	32.5					866	900	-616	19086	2967	-238	1394	9710	2876	-458	449	0
						2236	6792	-6325	130442	21662	-868	32851	15000	15535	-21285	2142	0
1f	6.5	TF-210	21.36	1.175		2100	1070	3600	56000	2500	170	3800	69000	4900	41300	455	
	39					1266	870	-1218	55988	2417	-288	3794	5010	4876	-2056	450	0
						3503	7663	-7542	186431	24078	-1156	35345	28010	20412	-23262	2592	0
1g	6.5	TF-227	21.76	1.175		2200	1100	4100	12600	2600	195	650	63100	2000	42200	417	
	45.5					1366	900	-718	12588	2517	-263	644	8110	1976	-1158	412	0
						4869	8563	-8260	199819	26595	-1419	36470	28120	22388	-24420	3005	0
1h	6.5	TF-241	19.89	1.175		2000	1150	4000	17000	2200	300	1300	54100	2400	61000	350	
	52					1166	950	-818	16988	2117	-158	1294	-690	2376	17642	345	0
						6035	9513	-9078	218007	23711	-1577	37784	27250	24764	-6778	3350	0
1i	6.5	TF-252	21.44	1.175		2100	1070	2800	12900	1400	260	770	47200	1800	55700	643	
	58.5					1266	870	-2018	12888	1317	-198	764	-7350	1776	12342	638	3
						7300	10384	-11095	230896	30025	-1776	36542	19840	26541	5565	3988	4
1j	6.5	TF-274	12.22	1.175		1200	930	2900	9200	2000	250	400	52200	1000	120800	302	
	65					366	730	-1918	9188	1917	-225	394	-2750	976	77442	297	0
						7666	11114	-13012	240084	31945	-2004	38942	17050	27518	82006	4255	3

Test #	Time Period	TF #	Solution Volume	H2O Added	Al	B	Ca	Fe	Li	Mg	Mn	Na	Ni	Si	U	I
1k	6.5	TF-272	10.27	1.175	1000	1040	3000	11600	1200	250	360	54400	2500	66200	522	
	71.5				166	840	-1618	11588	1717	-178	354	-598	247e	22242	517	0
					7832	11954	-14630	251672	33661	-2122	3929e	164e8	29994	105850	4805	0
1l	6.5	TF-321	20.42	1.175	2000	940	3700	32700	2100	290	1700	64500	6200	125400	318	
	96				1166	740	-1118	32e88	2017	-168	1e94	9510	e27e	82042	313	0
					8998	12e94	-15942	284360	35678	-2350	48490	25970	36270	187892	5116	0
1m	13.0	TF-345	11.19	2.150	1450	1360	7550	23800	3700	680	1500	99800	3100	111700	866	
	91				-76	1454	-1315	23778	3547	-156	1469	-820	3157	38065	858	0
					6921	14169	-17262	308135	39225	-2509	42479	25150	39439	215951	5974	0
1n	13.0	TF-393	11.00	2.150	1650	1800	6800	40800	3300	540	1200	103000		78240	528	
	104				1134	1454	-8572	40778	3188	-25	1189	-2780	-45	6130	526	0
					10055	15643	-25835	348917	42413	-2534	43667	22370	39364	222068	6500	0
1o	13.0	TF-424	11.33	2.150	1100	1900	7000	5960	3700	260	600	120100	900	85000	998	
	117				584	1554	-8572	5878	3588	-305	589	14320	857	12350	996	0
					10639	17196	-34268	354796	46002	-2840	44258	36690	40242	234418	7496	0
1p	13.0	TF-453	15.24	2.150	1500	2300	7900	13000	3500	260	600	110200	1200	73300	7e6	14300
	130				984	1954	-7472	12978	3398	-305	589	4420	1157	630	764	3550
					11623	19150	-41680	367774	49390	-3145	44847	41110	41395	235048	82e0	3850
1q	14.0	TF-486	16.50	2.200	1700	1340	5400	4500	3500	80	450	90100	670	72800	607	13700
	144				1148	970	-11045	4277	3380	-525	418	-23060	824	-5860	605	2400
					12771	20120	-52725	372051	52770	-3670	45266	18050	42222	229186	8865	5950
1r	12.0	TF-529	19.05	2.000	1900	1500	5100	9100	2700	210	475	85400	1300	62200	487	8000
	156				1420	1178	-7200	9080	2576	-316	465	-13000	1260	-5e30	455	-2000
					14191	21299	-61925	381131	55366	-3986	45731	5050	43482	223583	9350	5950
1s	13.0	TF-560	20.25	2.150	130	47	130	220	89	20	9	2600	36	1400	21	300
	169				2825	952	2450	4455	1802	405	182	52650	729	28350	425	6075
					1509	606	-13742	4494	1650	-160	172	-53130	63e	-44320	425	-4675
					15700	21904	-74868	385565	57057	-4146	45902	-48080	44166	179268	9775	-725

Test #	Time Period	TF #	Solution Volume	H2O Added	Al	B	Ca	Fe	Li	Mg	Mn	Na	Ni	Si	U	K	
1t	13.0	TF-827	20.29	2.15													
	182				2000	3900	6100	3400	5300	200	180	111200	600	90300	1542	16000	
					1484	3554	-9272	3378	5188	-365	169	5420	557	17630	1540	5250	
					17164	25457	-84140	389943	62245	-4512	46071	-42660	44726	196898	11313	4525	
1u	13.5	TF-833	20.91	2.225													
	195.5				2100	3600	2500	5000	5400	200	190	116800	630	80100	1390	12800	9.33
					1566	3242	-13409	4978	5284	-365	179	9330	586	4895	1388	1675	
					18750	28699	-97549	393721	67529	-4697	46250	-33330	45511	201792	11310	6200	
1v	12.5	TF-783	22.17	2.075	100	160	260	270	250	10	12	4720	40	3380	62.2	59	
	208				2217	3547	5764	5986	5542	222	266	104642	887	74935	1379	13080	
					1719	3213	-9072	5965	5455	-324	256	2552	845	4800	1377	2705	
					20467	31712	-106621	399686	72964	-5221	46506	-30778	46156	206592	12687	8905	
1w	13	TF-771	20.97	2.15	2100	4600	6500	4400	5500	360	210	113900	1800	66500	1266	16800	
	221				1584	4254	-8872	4378	5388	-205	199	8120	1757	-7030	1264	6050	
					22053	36166	-115493	404265	78352	-5427	46705	-22656	47913	199562	13951	14955	
1x	13	TF-830	11.37	2.15	1950	5340	6370	6370	6250	295	455	114800	970	7530	1615	13870	
	234				1414	4994	-9002	6348	6136	-269	444	9020	927	-66000	1613	3120	
					23467	41160	-124496	410613	84490	-5676	47149	-13638	48840	132562	15564	16075	
1y	26	TF-866	17.56	4.1	3160	11080	7200	4050	13540	316	229	299200	1580	149600	3709	26830	
	260				2176	10420	-22115	4009	13327	-762	208	7480	1498	9380	3705	8330	
					25643	51556	-146611	414622	97817	-6[illegible]2	47355	-6158	50336	142542	19269	26405	

						Al	B	Ca	Fe	Li	Mg	Mn	Na	Ni	P	U	V
					E-J13	710	170	4100	10	71	390	5	46800	20	[illegible]	4	
					E-J13	240	161	7150	10	52	263	5	49200	20	34200	1	5000
PIII-2a	6.5	TF-115	19.05	0.975 *		950	1830	2480	59800	4570	480	20800	31050	5700	22100	314	0
						258	1664	-1518	59799	4501	100	20795	-14580	5680	-13878	311	0
2b	6.5	TF-127	25.46	1.175		1300	1070	2550	19600	4600	150	6110	52400		32800	38	
	13					466	870	-2268	19538	4517	-308	6104	-2550	-24	-10556	34	0
						724	2534	-3785	79378	9017	-208	26899	-17170	5657	-24435	344	0
2c	6.5	TF-142	21.41	1.175		1100	850	3200	20100	4000	150		59200		36800	370	
	19.5					266	650	-1616	20088	3917	-208	-6	4210	-24	-5558	366	0
						989	3185	-5402	99467	12934	-517	26893	-12960	5634	-30992	710	0
2d	6.5	TF-157	21.00	1.250 **		1100	840	4000	21600	2730	250	4200	58200	3400	36300	323	
	26					212	628	-1125	21588	2641	-238	4194	-300	3375	-9825	319	0
						1202	3812	-6528	121054	15575	-754	31087	-13260	9008	-40818	1029	0
2e	6.5	TF-188	16.42	1.175		1600	1030	3600	97300	2750	260	3800	67200	9500	47800	388	
	32.5					766	830	-1218	97788	2707	-198	3794	12210	9476	4442	364	0
						1968	4642	-7745	218842	18282	-752	34881	-1050	18465	-36375	1413	0
2f	6.5	TF-211	20.50	1.175		2000	980	5790	52700	2260	180	3300	59500	4900	47800	396	
	39					1166	780	-1118	52688	2177	-278	3294	4510	4876	4442	392	0
						3135	5423	-6862	271531	20456	-1231	36175	3460	23862	-31932	1804	0
2g	6.5	TF-228	21.67	1.175		2200	1230	4100	24100	2400	220	2000	63500	2600	52900	546	
	45.5					1366	1030	-718	24088	2317	-238	1994	8510	2576	9542	542	0
						4499	6453	-9560	295619	22775	-1469	40170	11970	25936	-22359	3345	0
2h	6.5	TF-242	20.01	1.175		2600	1300	3800	11600	2200	200	960	59800	1600	74200	540	
	52					1165	1100	-1018	11588	2117	-258	954	4810	1576	30642	536	0
						5665	7553	-10598	307207	24891	-1727	41124	16780	27514	8452	2882	0
2i	6.5	TF-259	24.04	1.175		2400	1370	3400	10600	1600	300	580	53400	1700	64400	728	
	58.5					1566	1170	-1418	10588	1517	-158	494	-1590	1676	21042	724	0
						7230	8724	-12015	317796	26408	-1886	41618	15170	29191	29495	3606	0
2j	6.5	TF-275	11.58	1.175		1200	1090	3000	11800	2100	280	560	53300	1860	118500	368	
	65					366	890	-1818	11788	2017	-178	554	-1690	1836	75142	364	0
						7596	9614	-13832	329584	28425	-2064	42172	13500	31028	104638	3976	0

Test #	Time Period	TF #	Solution Volume	H2O Added	Al	B	Ca	Fe	Li	Mg	Mn	Na	Ni	Si	U	K
2k	6.5	TF-293	9.87	1.175	1000	1825	3000	16100	2700	260	500	71300	3000	86600	615	
	71.5				166	1625	-1818	16088	2617	-196	494	16310	2976	43242	611	0
					7762	11239	-15650	345672	31041	-2262	42666	29810	34004	147880	4580	0
2l	6.5	TF-322	20.30	1.175	2000	930	2000	45700	1460	180	1600	13000	800	90900	254	
	78				1166	730	-2818	45688	1377	-278	1594	-41990	776	47542	250	0
					8928	11969	-16468	391360	32416	-2540	44260	-12180	34760	195422	4830	0
2m	13.0	TF-346	10.55	2.150	1100	1400	3300	14300	2250	260	870	65200	1300	84800	569	
	91				-426	1054	-5515	14276	2097	-578	859	-95120	1257	5465	561	0
					6501	13964	-23982	405639	34515	-3119	45119	-47500	36038	200288	5392	0
2n	13.0	TF-394	11.18	1.500 ***	1100	330	2300	28200	1950	190	1600	61300		58100	392	
	104				740	88	-8425	28185	1872	-204	1592	-12500	-30	6800	390	-7500
					9241	13092	-32408	433824	36367	-5323	46712	-60000	36006	207688	5782	-7500
2o	13.0	TF-425	11.56	1.150 ***	1200	600	2300	10300	1400	160	500	44400	2100	24800	193	
	117				924	415	-5922	10288	1340	-142	494	-12180	2077	-14530	192	-5750
					10165	13507	-38330	444112	37727	-3466	47206	-72180	38084	193158	5974	-13250
2p	13.0	TF-454	15.71	2.150	1600	2800	6300	13500	5500	230	400	176000	1700	87000	1175	21800
	130				1084	2454	-9072	13478	5388	-335	389	70220	1657	14330	1173	11050
					11249	15961	-47402	457591	43116	-3801	47595	-1960	39742	207488	7147	-2200
2q	14.0	TF-487	16.30	2.300	1600	1960	5200	3900	3400	80	180	95500	2000	68000	647	14800
	144				1048	1590	-11245	3877	3280	-525	165	-17660	1954	-10660	645	3300
					12297	17551	-58648	461466	46396	-4326	47764	-19620	41696	196828	7791	1100
2r	12.0	TF-539	20.17	1.350 ***	2200	1900	3600	9100	2400	340	340	68400	3800	44200	637	7900
	156				1662	1676	-6338	9086	2328	-26	333	12	3772	-3338	636	950
					13964	19227	-64986	470554	48724	-4352	48097	-19608	45468	193490	8427	2050
2s	13.0	TF-581	20.71	1.100 ***	100	110	270	240	170	10	24	5920	56	3630	38	630
	169				2071	2278	5592	4970	3521	207	497	119177	746	75177	787	13047
					1607	2101	-2273	4959	3464	-82	492	56057	724	37557	786	7547
					15771	21328	-67259	475513	52187	-4434	48528	36449	46171	231047	9213	9597

Test #	Time Period	TF #	Solution Volume	H2O Added	Al	B	Ca	Fe	Li	Mg	Mn	Na	Ni	Si	U	K	
2t	13.0 182	TF-688	18.78	1.310 ***	1990 1586 17356	1600 1389 22717	2200 -7166 -74426	5800 5757 481300	2600 2532 54719	190 -165 -4598	190 193 48772	68700 4248 40697	1000 974 41181	25200 -15602 215445	712 711 9924	9400 2850 12447	
2u	13.5 195.5	TF-689	22.11	1.620 ***	2200 1811 19167	2300 2039 24756	3300 -8283 -82709	18800 18784 500084	3300 3216 57935	310 -116 -4714	1300 1292 50064	75300 15596 56293	3300 3268 52493	42000 -18404 202841	800* 798 10722	10400 2200 14747	9.24
2v	12.5 208	TF-734	24.62	2.075	2500 2602 21169	1600 1266 26022	2500 -12336 -95045	9400 9379 509463	2300 2192 60127	240 -306 -5020	370 360 50423	62000 -40090 16203	1400 1358 51791	31300 -39665 162376	926 924 11646	5600 -1775 12973	8.72
2w	13 221	TF-772	21.01	2.15	2100 1564 22753	3400 3054 29076	4600 -10772 -105818	6100 6078 515542	5000 4885 65015	270 -295 -5316	480 469 50893	144600 38820 55023	2630 2587 54378	68700 -4830 157546	1414 1412 13858	22500 11750 24722	8.64
2x	13 234	TF-831	13.26	2.15	1460 944 23697	3710 3364 32440	5570 -9602 -115620	10740 10718 526260	3850 3738 68753	380 -185 -5501	650 639 51532	107300 1520 56543	2390 2347 56725	59300 -14230 143316	1591 1589 14647	15250 4500 29222	
2y	26 260	TF-869	17.4	4.1	1740 756 24453	4520 3860 36300	4080 -25315 -140935	5050 5009 531269	6095 5877 74630	209 -869 -6370	1660 1060 52591	135550 -66170 -7627	1220 1136 57863	73800 -66420 76896	2975 2971 17618	18600 -1900 27322	

Test #	Time Period	TF #	Solution Volume	H2O Added		Al	B	Ca	Fe	Li	Mg	Mn	Na	Ni	Si	U	K
					E-J13	710	170	4100	10	71	390	5	46800	20	36900	4	
					E-J13	140	161	7150	10	52	263	5	49200	20	34200	1	5000
PIV-1a	13	TF-154	21.00	1.475		7100	16600	4400	27900	22500	945	12800	136700		140100	4850	
						6053	16349	-1648	27385	22395	370	12793	67870	-30	85672	4845	0
	18	12.5	TF-199	17.19	1.4375	3400	13400	3400	32100	14800	530	2400	117400	5200	104900	5947	
		25.5				2379	13156	-2494	32086	14698	-31	2393	50125	5171	51856	5942	0
						8432	25505	-4141	59971	37093	339	15185	117995	5142	137529	10787	0
	1c	13.5	TF-239	18.90	1.5125	3800	12100	3400	10200	13800	360	500	116200	1500	95300	5300	
		39				2726	11843	-2801	10135	13693	-230	492	45415	1470	39489	5295	0
						11158	41348	-6942	70156	50786	109	15678	163410	6613	177016	16081	0
	1c	13	TF-270	21.97	1.475	4600	15800	5300	11000	16400	640	1000	135300	2300	117000	5954	
		52				3553	15547	-748	10985	16295	65	993	66279	2270	62572	5949	0
						14711	58697	-7690	81141	67081	174	16670	229680	8862	239590	22030	0
	1e	13	TF-314	18.49	1.475	3000	17800	3900	18700	18900	330	3200	125200	1800	117600	5140	
		65				1953	17549	-2148	18685	18795	-245	3193	56170	1770	63172	5135	0
						16664	74446	-9838	99826	85876	-71	19863	285850	10652	302762	27165	0
	1f	15.5	TF-347	10.39	1.6675	6300	34100	4300	14800	33400	350	800	199500	2800	244200	8832	
		80.5				5116	33817	-2537	14783	33282	-300	792	121461	2767	182669	8826	0
						21780	108263	-12374	114610	119158	-372	20655	407311	13419	485432	35991	0
	1g	10.5	TF-391	15.41	1.2875	1800	17000	7900	10500	10600	750	1200	105600	1500	76400	2927	
		91				886	16781	2621	10487	10509	246	1194	45345	1474	28891	2922	0
						22666	125044	-9753	125097	129667	-124	21848	452656	14893	514323	38913	0
	1h	13	TF-420	13.52	1.475	3200	17600	4300	9200	18800	270	300	136600	1500	119000	4813	
		104				2846	17363	-6246	9185	18723	-118	293	64030	1470	68555	4812	-7375
						25512	142406	-15999	134282	148390	-242	22141	516686	16364	582878	43725	-7375
	1	13.5	TF-449	14.54	1.5125	2900	18300	4500	3600	20500	260	190	143200	400	129800	6179	10600
		117.5				2537	18056	-6314	3585	20421	-138	182	68785	370	78072	6177	3038
						28049	160465	-22314	137867	168811	-377	22323	585471	16734	660950	49902	-4338
	1	14.5	TF-484	13.56	1.5875	20900	53800	7000	6000	65300	180	680	349700	720	467880	17927	16800
		132				20519	53544	-4351	7984	65217	-238	672	262595	748	413508	17925	8863
						48568	214007	-26664	145851	234029	-617	22995	843066	17482	1074458	67828	4515

Test #	Time Period	TF #	Solution Volume	H2O Added		Al	B	Ca	Fe	Li	Mg	Mn	Na	Ni	Si	U	K
					E-J13	710	170	4100	10	71	390	5	46800	20	36900	4	
					E-J13	240	161	7150	10	52	263	5	49200	20	34200	1	5000
1k	11	TF-523	19.74	1.325		11300	48700	11600	9700	38000	1900	1100	188200	1500	262600	10716	9200
	143					11432	48457	2126	9687	37931	1452	1093	123010	1474	217285	10715	2575
						60050	262494	-24538	155538	271960	835	24089	971076	18955	1291745	78542	7100
1l	13	TF-555	20.16	1.475		540	1760	250	470	1910	29	57	10100	81	14400	471	410
	156					10386	35482	5048	9475	38506	585	1149	203616	1633	290384	9495	8266
						10532	35244	-5506	9460	38429	197	1142	131046	1606	223359	9474	891
						70582	297738	-30044	164998	310389	1031	25231	1182122	20559	1531602	98036	7991
1m	13	TF-636	19.82	1.475													
	169					5200	23000	3400	4400	27700	300	700	168300	1000	200200	7313	10100
						4646	22763	-7146	4385	27623	-88	693	115730	970	149755	7312	2725
						75428	320501	-37190	169383	338012	943	25923	1217852	21529	1681357	95346	10716
1n	13	TF-670	19.37	1.475		2300	10700	5600	5000	14900	390	300	118000	1400	107700	4474	6600
	182					1946	10463	-4946	4985	14823	2	293	45430	1370	57255	4473	-775
						77374	330963	-42137	174369	352835	945	26216	1263282	22900	1738612	99820	9941
1o	13	TF-735	20.30	1.475		4500	15400	6300	9900	20900	570	1500	144100	2800	142900	5501	9300
	195					4146	15163	-4246	9865	20823	202	1493	71530	2770	92455	5500	1925
						81520	346126	-46383	184254	373659	1148	27708	1334812	25670	1831067	105320	11866
1p	13	TF-758	19.27	1.475		2300	8900	6000	8500	7200	540	1400	61100	1800	76200	2563	7300
	208					1946	8663	-4546	8685	7123	152	1393	8530	1770	27755	2562	-75
						83466	354788	-50929	195139	380762	1300	29101	1343342	27441	1658822	107881	11751
1q	13	TF-801	19.93	1.475		4200	2600	5300	8900	1800	300	600	46000	2000	55700	1022	12500
	221					3846	2363	-5246	8285	1723	-88	593	-26570	1970	5255	1021	5125
						87312	357151	-56176	202024	382505	1212	29694	1316772	29411	1664077	108902	16916
1r	26	TF-855	18.37	2.45		1800	2570	6250	5280	5150	490	510	91670	720	76050	1160	7900
	247					1212	2176	-11268	5856	5023	-244	495	-28570	671	-7740	1095	-4350
						88524	359326	-67443	207680	387528	967	30191	1287902	30062	1856367	109999	12566

Test #	Time Period	TF #	Solution Volume	H20 Added		Al	B	Ca	Fe	Li	Mg	Mn	Na	Ni	Si	U	K
					E-J13	710	170	4100	10	71	390	5	46800	20	36900	4	
					E-J13	240	161	7150	10	52	263	5	49200	20	34200	1	5000
2k	11	TF-524	19.57	1.325		2000	8600	9000	16200	10400	1600	550	103700	2200	102400	3287	5900
	143					1682	8387	-474	16187	10331	1252	545	38510	2174	57085	3286	-725
						16423	119735	-31368	251238	137180	422	27639	428910	20126	450728	40222	-5700
2l	13	TF-556	19.39	1.475		250	980	280	240	1380	16	21	9010	49	9280	345	540
	156					4846	19002	5429	4654	20741	310	407	174704	950	179939	6651	10471
						4494	18765	-5117	4639	20864	-78	400	102134	921	129494	6649	3096
						20917	138500	-36485	265877	158045	344	28039	531044	21046	580222	46672	-2804
2m	13	TF-641	18.87	1.475													
	169					3000	16400	5300	4700	18500	260	320	141200	1100	146800	5585	10900
						2646	16163	-5246	4685	18723	-126	313	68630	1070	96355	5584	3525
						23563	154662	-41731	270562	176768	216	26351	599674	22117	676577	52455	721
2n	13	TF-671	19.08	1.475		7600	22100	6500	6900	26700	590	880	187200	1700	213709	8528	14100
	182					7246	21863	-4046	6885	26623	112	793	114630	1670	163255	8527	6725
						30809	176525	-45777	277447	213391	326	29144	714304	23787	839832	60982	7446
2o	13	TF-736	20.01	1.475		2000	7600	6800	13800	9500	1000	320	107100	1300	72400	2801	8000
	195					1646	7363	-3746	13785	9723	612	313	34530	1270	21955	2800	625
						32455	183887	-49523	291232	213115	940	29457	748834	25058	861787	63781	8071
2p	13	TF-759	19.92	1.475		2000	4600	5800	7200	5900	440	760	66100	1300	74300	966	7600
	208					1646	4363	-4746	7185	5823	52	753	-6470	1270	23855	965	425
						34101	188250	-54270	298418	219932	992	30209	742364	26328	885642	64746	8496
2q	13	TF-802	14.18	1.475		4250	2130	5100	7500	1600	270	400	47600	1300	40400	666	12800
	221					3896	1893	-5446	7485	1523	-118	393	-24470	1270	-10045	665	5425
						37997	190142	-59716	305903	218461	874	30602	717594	27599	875597	65410	18921
2r	26	TF-858	16.62	2.45		1860	1170	5960	8750	3790	450	540	78940	1675	59400	596	7630
	247					1272	796	-11558	8726	2663	-194	526	-49600	1626	-24390	594	-4620
						29269	190936	-71273	314626	221124	680	31130	667794	29225	851207	66004	9301

Test #	Time Period	TF #	Solution Volume	H2O Added		Al	B	Ca	Fe	Li	Mg	Mn	Na	Ni	Si	U	K
					E-J13	710	170	4100	10	71	390	5	46800	20	36900	4	
					E-J13	240	161	7150	10	52	263	5	49200	20	34200	1	5000
Flow-Ba	13	TF-155	20.93	1.475		1670	3140	5650	35600	9420	980	15700	77700		43100	2030	
						623	2689	-395	35785	9515	825	15693	8670	-30	-11528	2025	0
2b	12.5	TF-200	17.88	1.4575		3200	15400	4100	22500	19500	540	3900	153000	5400	110600	5611	
	25.5					2579	15156	-1794	22486	19678	-21	3893	85725	5371	56956	5606	0
						3202	18045	-2191	55271	29013	304	19585	94395	5342	45629	7831	0
2c	13.5	TF-240	20.37	1.5125		2400	11600	3700	8400	13400	350	670	112200	1400	80500	3788	
	39					1326	11343	-2501	8385	13293	-240	662	41415	1370	24689	3782	0
						4528	29388	-4692	66656	42306	64	20248	155810	6712	70316	11613	0
2d	13	TF-271	24.16	1.475		2400	10000	3600	9400	8700	360	600	90600	1300	77100	3141	
	52					1353	9749	-2448	9385	8595	-215	593	21570	1270	22672	3136	0
						5881	39137	-7140	76041	50901	-151	20840	157380	7982	92590	14749	0
2e	13	TF-315	17.07	1.475		1700	7900	4100	24400	9900	320	1900	84000	2200	65700	2680	
	65					653	7649	-1945	24385	9795	-255	1893	14970	2170	11272	2675	0
						6534	46786	-9038	100426	60696	-405	22753	172350	10152	104262	17424	0
2f	15.5	TF-348	11.32	1.6625		1900	11100	3800	13600	10600	400	750	96000	3200	82500	2907	
	80.5					720	10817	-3016	13583	10482	-248	742	18195	3167	21154	2503	0
						7253	57604	-12104	114010	71178	-655	23475	190545	13519	125416	20327	0
2g	10.5	TF-392	15.52	1.2875		2000	13800	5100	98900	9700	730	2500	93700	1300	78700	2762	
	91					1086	13581	-179	98867	9609	228	2294	33645	1274	31191	2757	0
						8339	71185	-12282	212897	80737	-427	25768	224190	14594	156608	23084	0
2h	13	TF-419	14.02	1.475		1800	11500	4300	14300	12600	200	530	112900	1300	88900	3539	
	104					1446	11263	-6246	14285	12523	-188	523	40330	1270	38455	3538	-7375
						9785	82447	-18529	227182	93310	-615	26291	264520	15864	195062	26622	-7375
2i	13.5	TF-450	13.79	1.5125		2200	12300	5100	14200	14200	410	580	127700	550	140700	4440	8100
	117.5					1837	12056	-5714	14185	14121	12	572	53285	520	88972	4438	538
						11622	94504	-24243	241367	107432	-602	26863	317805	16384	284035	31060	-6838
2j	14.5	TF-485	14.77	1.5875		3500	17100	4700	3700	19500	190	240	150700	1600	163900	5878	9600
	132					3119	16844	-6651	3684	19417	-228	232	72595	1568	109608	5876	1662
						14741	111348	-30894	245051	126849	-830	27096	390400	17952	393642	36937	-5175

Test #	Time Period	TF #	Solution Volume	H2O Added		Al	B	Ca	Fe	Li	Mg	Mn	Na	Ni	Si	U
					E-J13	710	170	4100	10	71	390	5	46800	20	36900	4
PIV-3	26.5	TF-201	18.99	1.59		7600	19800	9700	46100	30200	1500	25100	205100	4900	163100	7748
						6471.1	19529.7	3181	46084.1	30087.11	879.9	25092.05	130688	4868.2	104429	7742.339
PIV-4	26.5	TF-202	15.3	1.51		9300	16800	8570	62900	39800	1700	20800	185100	6900	155800	7435
						8227.9	16543.3	2379	[illegible]	26892.79	1111.1	20792.45	114432	6869.8	100081	7429.624
PIV-5	52	TF-272	24.66	2.72		12600	42200	13300	89700	50160	1700	12100	372400	4300	350200	15190
						10868.8	41737.6	2148	89672.8	49906.88	639.2	12086.4	245104	4245.6	249832	15180.31
PIV-6	52	TF-273	23.36	2.85		9300	24400	14100	101000	40200	3400	46200	370200	10300	272900	7358
						7276.5	23915.5	2415	100971.5	39997.65	2288.5	46185.75	236820	10243	167735	7347.854

Test #	Time Period	TF #	Solution Volume	H2O Added		Al	B	Ca	Fe	Li	Mg	Mn	Na	Ni	Si	U	F
					E-J13	710	170	4100	10	71	398	5	46800	20	36900	4	
						240	161	7150	10	52	263	5	49200	20	34200	1	5000
PV-1a	15.5	TF-225	22.12	0.8000		2200	660	3540	94000	660	330	6000	15800	3300	79600	20	
						1632	524	260	93992	603	18	5996	-20640	3284	50080	17	0
1b	10.5	TF-253	20.60	0.5750		2000	1000	1700	26600	400	230	1100	10400	3300	123800	20	
	26					1592	902	-658	26594	359	6	1097	-16610	3288	102582	18	0
						3224	1426	-398	120586	962	24	7098	-37150	6572	152662	35	0
1c	13.5	TF-282	14.47	0.7250		1400	910	2700	43800	350	450	8000	15800	5900	34300	22	
	39.5					885	787	-272	43793	299	167	7996	-18130	5886	7548	19	0
						4109	2213	-670	164379	1261	191	15090	-55380	12458	160210	55	0
1d	12.5	TF-323	22.29	0.6500		2200	650	1400	7400	600	160	300	14300	850	20500	53	
	52					1738	540	-1265	7394	554	-94	297	-16120	837	-3485	51	0
						5848	2752	-1935	171772	1815	98	15386	-71500	13295	156725	105	0
1e	16.0	TF-355	13.07	0.8000		1300	400	2600	18000	2600	250	600	29300		22100	45	
	68					1108	271	-3120	17992	2558	40	596	-10060	-16	-5260	44	-4000
						6956	3024	-5055	189764	4373	137	15982	-81560	13279	151465	149	-4000
1f	12.0	TF-403	9.38	0.6500		900	280	1900	10100	820	250	450	14100		7500	54	
	80					744	175	-2748	10094	786	79	447	-17880	-13	-14730	53	-3250
						7700	3199	-7802	199858	5159	216	16429	-99440	13266	136735	203	-7250
1g	12.0	TF-426	12.69	0.6500		1200	380	2300	5700	1400	140	140	17900	380	11500	28	
	92					1044	275	-2348	5694	1366	-31	137	-14080	367	-10730	27	-3250
						8744	3474	-10150	205552	6526	185	16566	-113520	13633	126005	230	-10500
1h	18	TF-455	16.72	0.8750		1700	830	3800	4000	14700	170	150	140100	1100	69600	281	15200
	110					1490	689	-2456	3991	14654	-60	146	97050	1082	39675	280	10825
						10234	4164	-12606	209543	21180	125	16711	-16470	14716	165680	510	325
1i	7.5	TF-488	14.12	0.5000		1400	420	2800	3100	2000	230	230	19800	1400	11300	138	7100
	117.5					1280	340	-775	3095	1974	98	228	-4800	1390	-5800	138	4600
						11514	4503	-13381	212638	23154	224	16939	-21270	16106	159880	648	4925
1j	12.5	TF-532	19.28	0.6500		1900	580	2500	3900	190	210	190	11600	770	7700	19	5800
	130					1744	475	-2148	3894	156	39	187	-20380	757	-14530	18	2550
						13258	4978	-15529	216531	23310	253	17126	-41650	16862	145350	666	7475

Test #	Time Period	TF #	Solution Volume	H2O Added		Al	B	Ca	Fe	Li	Mg	Mn	Na	Ni	Si	U	K
					E-J13	710	170	4100	10	71	390	5	46800	20	36900	4	
						240	161	7150	10	52	263	5	49200	20	34200	1	5000
1k	13.0	TF-582	19.23	0.5875		100	30	150	250	22	12	9	720	53	270	2	300
	143					1923	577	2884	4808	423	231	173	13846	1019	5192	29	5769
						1758	456	-2031	4801	387	50	170	-19979	1005	-18320	28	2332
						15016	5445	-17560	221332	23698	313	17295	-61629	17868	127030	694	9806
1l	13.0	TF-642	18.06	0.6875													
	156					1800	600	2500	2200	4300	180	90	61900	360	25600	81	9400
						1635	489	-2416	2193	4264	-1	87	28075	346	2088	80	5962
						16650	5934	-19976	223525	27962	312	17382	-33554	18214	129117	775	15769
1m	13.0	TF-690	18.96	0.6875		190	570	1900	6400	1000	190	300	12700	600	7800	132	5700
	169					25	459	-3016	6393	964	9	297	-21125	586	-15712	131	2262
						16676	6393	-22991	229918	28926	321	17678	-54679	18800	113405	906	18032
1n	13.0	TF-737	21.01	0.6875		210	630	2300	4400	1400	210	190	23100	1100	15100	95	6300
	182					45	519	-2616	4393	1364	29	187	-10725	1086	-8412	94	2862
						16720	6913	-25607	234311	30290	350	17865	-65404	19887	104992	1000	20894
1o	14.0	TF-773	20.00	0.7250		200	1800	2900	5400	5800	200	260	90000	600	56400	570	13600
	196					26	1683	-2284	5393	5762	9	256	54339	586	31605	569	9975
						16746	8596	-27890	239704	36053	359	18121	-110[illegible]	20472	136597	1569	30869
1p	12	TF-832	9.31	0.6500		930	930	2800	3900	1400	230	290	25700	870	19200	257	3450
	208					774	825	-1848	3894	1366	59	277	-6280	857	-3030	256	200
						17520	9421	-29738	243598	37419	419	18398	-17654	21329	133567	1826	31059
1q	26	TF-870	15.48	1.1750		1550	2475	3715	6200	6850	200	294	86850	1080	62850	1145	12380
	234					1268	2286	-4686	6188	6589	-109	288	29040	1056	22665	1144	6505
						18788	11707	-34424	249786	44008	309	18686	11686	22386	156232	2970	37574

					Al	B	Ca	Fe	Li	Mg	Mn	Na	Ni	Si	U	Th
					710	170	4100	10	71	390	5	46800	20	36900	4	
					240	161	7150	10	52	263	5	49200	26	34200	1	5000
PV-2a	15.5	TF-226	22.15	0.8500	2200	660	4900	101700	660	330	6202	13500	4000	123400	28	
					1632	524	1620	101692	603	18	6198	-23940	3984	93880	17	0
					2300	1200	1600	11300	500	210	700	10800	2200	135600	24	
2b	10.5	TF-254	23.96	0.5750	1892	1102	-758	11294	459	-14	697	-16110	2138	114382	22	0
	26				3524	1626	862	112966	1062	4	6895	-40050	6172	208262	39	0
					1900	1700	3200	36300	12900	460	3500	85000	4300	40400	560	
2c	13.5	TF-283	16.36	0.6875	1412	1613	381	36293	12851	192	3497	52825	4256	15031	558	0
	39.5				4936	3239	1244	149279	13914	196	10892	12775	10459	223294	597	0
					2200	4460	8000	137900	14800	900	7400	80400	5100	285700	650	
PV-3	26	TF-255	22.32	0.9750	1508	4294	4002	137890	14731	520	7395	34770	5080	249722	647	0
					4800	10300	13700	119100	29100	1100	7700	169500	6500	613500	2906	
PV-4	52	TF-324	20.18	1.9500	3416	9968	5705	119080	28962	340	7690	78240	6461	541545	2899	0
					5600	7600	8200	101300	26200	1000	7600	151300	4800	447900	2532	
PV-5	52	TF-325	21.64	1.9500	4216	7468	205	101280	26062	240	7590	60040	4761	375945	2525	0
					1700	5400	5300	71600	23600	490	5600	215300	3700	787500	534	20300
PV-6	110	TF-456	17.50	4.0500	-1176	4712	-11305	71552	23312	-1090	5560	25760	3619	638055	520	50
					5025	8880	7540	70000	35850	840	5200	360000	3180	1293000	2462	45900
PV-7	254	TF-883	16.75*	4.5800	3925	8143	-25207	69954	35612	-365	5177	134664	3088	1136364	2457	23000

Test #	Time Period	TF #	Solution Volume	H2O2 Added		Al	B	Ca	Fe	Li	Mg	Mn	Na	Ni	Si	U	K
					E-313	710	170	4100	10	71	390	5	46800	20	36900	4	
					B-313	240	161	7150	10	52	263	5	49100	20	34200	1	5900
PVIII-1a	13	TF-318	21.93	2.150		2200	2800	4200	48900	9600	420	5300	76600	8300	44500	465	
						674	2434	-4615	48678	9447	-418	5289	-23820	8257	-39135	457	0
1b	13	TF-342	19.32	2.150		1900	1500	3700	43700	8500	270	3600	107200	8900	103900	253	
	26					374	1134	-5115	43676	8747	-563	3589	6560	8857	24565	244	0
						1047	3569	-9730	92557	18195	-967	8876	-17240	17114	-14570	702	0
1c	13	TF-388	12.16	2.150		1200	360	2200	60900	4300	260	2600	80700		42800	98	
	39					-326	-6	-6615	60878	4147	-576	2589	-13920	-43	-36535	89	0
						720	354	-16345	153436	12342	-1566	11468	-37160	17071	-51105	791	0
1d	13	TF-421	14.17	2.150		1400	720	3100	8100	3300	270	570	92100		53100	58	
	52					-126	354	-5715	8078	3147	-568	559	-8520	-43	-26235	49	0
						574	3918	-22060	161514	25489	-2134	12027	-45680	17028	-77340	841	0
1e	13	TF-451	13.72	2.150		1400	720	4400	9600	4700	410	480	141300	1000	77100	58	18500
	65					884	374	-10972	9578	4588	-155	467	35520	957	3570	56	7750
						1478	4292	-33032	171092	30079	-2269	12496	-101e0	17985	-73770	896	7750
1f	15	TF-489	17.86	2.450		1800	570	5400	9200	3200	210	770	111800	1500	68000	259	17500
	80					1212	176	-12118	5176	3073	-434	758	-6740	1451	-15790	257	5250
						2690	4467	-45150	176268	33150	-2724	13254	-16360	19436	-89560	1153	13900
1g	10.5	TF-525	18.61	1.780		1900	740	8000	9100	2000	860	780	86700	2000	59700	27	10400
	90.5					1473	453	-4727	9062	1907	392	771	-876	1964	-976	25	1500
						4163	4921	-49877	185350	35058	-2332	14025	-19776	21400	-90536	1178	14500
1h	13.5	TF-573	15.82	2.225		100	30	190	770	130	11	42	5110	100	3340	3	680
	104					1552	565	3576	14491	2447	207	790	96170	1882	62859	56	12795
						1348	206	-12333	14469	2331	-378	779	-13390	1838	-13236	54	1673
						5511	5127	-62210	199819	37389	-2710	14804	-33976	23158	-103772	1232	16173

Test #	Time Period	TF #	Solution Volume	H2O Added		Al	B	Ca	Fe	Li	Mg	Mn	Na	Ni	Si	U	K
					E-313	710	170	4100	10	71	390	5	46500	20	36900	4	
					E-313	240	161	7150	10	52	263	5	49200	20	34200	1	5000
1i	13.0	TF-634	20.64	2.150		2100	600	4300	42300	3700	270	10300	141800	39600	784[illegible]	29	19500
	117					1564	254	-11072	43278	3568	-295	10289	36620	39557	457	27	9050
						7095	5381	-73282	243098	40977	-3006	25094	2944	62795	-98[illegible]	1259	25223
1j	13.0	TF-686	18.74	2.150		2000	600	3400	9400	1800	200	300	82400	880	47200	20	10600
	130					1464	254	-11772	9378	1688	-365	289	-23380	837	-26330	18	-150
						8579	5635	-85265	252476	42665	-3371	25363	-20436	62632	-125[illegible]	1277	25073
1k	13.0	TF-731	18.81	2.150		1900	560	260	59610	1800	190	2300	77900	6200	46100	26	10900
	143					1384	214	-15112	59588	1688	-375	2289	-27880	6157	-27430	24	150
						9963	5849	-100367	312065	44353	-3746	27672	-45316	69759	-152[illegible]	1301	25224
1l	13.0	TF-767	22.71	2.15		2200	630	3100	20900	2700	220	800	110400	2300	57[illegible]	43	16100
	156					1684	334	-12272	20875	2588	-345	789	4620	2257	-15630	41	5350
						11647	6183	-112540	332743	46941	-4072	28461	-43696	72046	-166272	1342	30573
1m	14.0	TF-827	19.11	2.30		1900	575	3630	7260	2100	229	500	107780	2675	56480	59	16440
	170					1346	205	-12615	7237	1980	-376	488	-5360	2629	-20150	57	4940
						12995	6387	-125455	340180	48922	-4468	28950	-49076	74675	-186472	1399	35513
1n	25	TF-866	18.30	3.95		2375	850	5675	40080	3840	240	1100	119470	4400	122630	57	35020
	195					1427	214	-22568	40040	3635	-795	1080	-74670	4321	-12490	53	15570
						14422	6601	-138022	380221	52556	-5267	30030	-123146	78776	-209962	1452	51083

Test #	Time Period	TF #	Solution Volume	H20 Added		Al	B	Ca	Fe	Li	Mg	Mn	Na	Ni	Si	U	K
					E-J13	710	170	4100	10	71	390	5	46800	20	36900	4	
					E-J13	240	161	7150	10	52	263	5	49200	20	34200	1	5000
FVIII-2a	13	TF-319	20.34	2.15		2000	2700	3100	13600	7700	350	1500	73200	3500	52900	391	
						474	2334	-5715	13576	7547	-468	1489	-27420	3457	-26435	362	0
2b	13	TF-343	19.23	2.15		1500	2000	6900	79400	5700	1700	8500	94400	15400	87300	172	
	26					374	1634	-1915	79378	5547	862	8489	-6220	15357	7965	166	0
						847	3969	-7630	92957	13095	373	9978	-33640	18514	-18470	546	0
2c	13	TF-389	13.40	2.15		1300	400	1500	22400	270	150	1100	10500		7000	11	
	39					-226	34	-7315	22378	117	-688	1089	-90120	-43	-72335	2	0
						620	4004	-14945	115336	13212	-316	11068	-123760	18771	-90805	548	0
2d	13	TF-422	13.60	2.15		1400	775	3100	9500	3300	270	980	108000		59200	52	
	52					-126	410	-5715	9478	3147	-568	969	7380	-43	-19525	43	0
						494	4413	-20660	124814	16359	-864	12057	-116380	18729	-110340	552	0
2e	13	TF-452	14.37	2.15		5600	720	4500	6600	5200	430	370	188200	900	95600	67	24600
	65					5084	374	-10872	6578	5088	-135	359	82420	857	22070	65	13850
						5578	4787	-31532	131392	21448	-1019	12396	-33960	19585	-88270	656	13850
2f	15	TF-490	17.51	2.45		1800	890	5300	8800	2600	260	840	112900	2600	69000	27	15600
	80					1212	496	-12218	8776	2473	-384	828	-7640	2551	-14790	25	3350
						6790	5282	-43750	140168	23920	-1404	13224	-41600	22136	-103060	661	17200
2g	10.5	TF-526	20.04	1.76		2000	600	5600	7600	1700	280	600	96200	2000	65300	20	12600
	90.5					1573	313	-7127	7582	1607	-188	591	8624	1964	4424	18	3700
						8363	5576	-50877	147750	25528	-1592	13615	-32976	24100	-96636	699	20900
2h	13.5	TF-574	18.28	2.225		100	30	160	790	49	10	33	2540	56	1720	2	310
	104					1828	548	2925	14441	896	183	603	53743	1024	31442	33	5667
						1294	199	-12984	14419	760	-402	592	-55727	979	-44653	31	-5458
						9657	5796	-63861	162169	26308	-1794	14407	-58705	25080	-143289	730	15442

Test #	Time Period	TF #	Solution Volume	H20 Added		Al	B	Ca	Fe	Li	Mg	Mn	Na	Ni	Si	U	K
					E-313	710	170	4100	10	71	39	5	46800	20	36900	4	
					E-313	240	161	7150	10	52	262	5	49200	20	34200	1	5000
	2i	13.0	TF-635	18.86	2.150												
		117				1900	640	3000	9600	2300	200	300	118900	1800	e3700	774	17000
						1384	294	-12372	9578	2188	-365	289	13120	1757	.5170	772	6250
						11041	6080	-76233	171746	28496	-2360	14696	-75583	26837	-128119	1502	21692
	2j	13.0	TF-667	23.19	2.150												
		130				2300	700	2800	25000	1000	230	1200	66600	3200	34800	20	8600
						1784	354	-12572	24978	888	-335	1189	-39180	3157	-38730	18	-2150
						12825	6434	-88806	196726	29384	-2655	15886	-114763	29994	-166849	1520	19542
	2k	13.0	TF-732	22.28	2.150												
		143				2200	670	2900	52800	1600	220	1200	101600	6000	75000	403	14000
						1684	324	-12472	52778	1688	-345	1189	-4180	5957	4470	401	3250
						14509	6758	-101278	249505	31072	-3041	17075	-118943	35951	-162379	1920	22792
	2l	13	TF-770	21.85	2.15												
		156				2200	660	2900	18400	1800	220	1600	134600	5700	53300	26	17000
						1684	314	-12472	18378	1688	-345	1589	28820	5657	-20230	24	6250
						16193	7071	-113751	267883	32760	-3386	18664	-90123	41608	-182609	1944	29042
	2a	14	TF-828	19.58	2.30												
		170				4100	2550	19200	18600	5680	740	1760	280000	2940	144500	1155	40530
						3545	2180	2755	18577	5560	135	1748	166840	2874	65840	1153	29030
						19741	9251	-110996	286460	38321	-3251	20413	76717	44502	-116769	3097	58072

Test #	Time Period	TF #	Solution Volume	H20 Added		Al	B	Ca	Fe	Li	Mg	Mn	Na	Ni	Si	U	K
					E-J13	710	170	4100	10	71	399	5	46800	20	36900	4	
					E-J13	240	161	7150	10	52	263	5	49200	20	34200	1	5000
PVIII-3	13	TF-320	21.42	2.15		2100	2700	4300	9900	11800	450	1300	118900	2800	72000	1101	
						574	2334	-4515	9878	11647	-388	1289	18280	2757	-7335	1093	0
PVIII-4	26	TF-344	18.83	4.10		2600	6700	7700	117700	25200	800	4700	29000	13200	220300	1105	
						-311	6003	-9110	117659	24909	-799	4650	-162880	13118	69019	1090	0
PVIII-5	39	TF-370	14.05	6.05		3000	7400	15500	8600	23900	770	6400	323200		156000	984	
						-1296	6372	-9305	8540	23470	-1590	6370	40060	-121	-67245	962	0
PVIII-6	52	TF-423	13.63	8.00		6700	34800	12900	39700	54800	845	5700	520700		396600	13766	
						1020	33440	-15900	39620	54232	-2275	5660	146300	-160	101400	13738	0
PVIII-7	104	TF-572	25.90	15.60		4500	46600	32600	5200	70000	500	1000	888400	1300	751100	17120	85000
						-2510	44018	-55150	5044	69041	-4593	922	139600	988	196520	17084	6000*
PVIII-8	104	TF-576	25.91	15.60		17900	77200	8600	24400	128500	1500	4100	1110000	2200	966100	18200	75400
						10490	74618	-79150	24244	127541	-3593	4022	361200	1888	411520	18164	-2600*
	8b	66	TF-829	14.38	9.90	13370	75200	10070	23580	94330	546	5160	750640	2010	651410	17256	40840
		170				10994	73606	-60715	23481	93815	-2058	5110	263560	1812	312830	17246	-8660
						21484	148224	-139865	47725	221356	-5651	9132	624760	3700	724350	35411	-11260
	8c	25	TF_867	18.70	3.95	1870	8230	4300	26370	14590	300	1600	211310	5800	131460	2525	19075
		195				922	7594	-23942	26330	14385	-739	1580	16770	5721	-3630	2521	-675
						22406	155818	-163808	74056	235740	-6390	10713	641730	9421	720720	37932	-11935

Distribution for ANL-91/36

Internal:

A. Anderson
J. K. Bates (25)
J. E. Battles
J. C. Cunnane
T. J. Gerding
J. E. Harmon
J. E. Helt
M. J. Steindler
ANL Patent Dept.
ANL Contract File
TIS Files (3)

External:

DOE-OSTI (2)
ANL Library
Manager, Chicago Operations Office, DOE
A. Bindokas, DOE-CH
J. Haugen, DOE-CH
Chemical Technology Division Review Committee Members:
S. Baron, Brookhaven National Laboratory, Upton, NY
N. Jarrett, Noel Jarrett Associates, Lower Burrell, PA
L. Newman, Brookhaven National Laboratory, Upton, NY
J. Stringer, Electric Power Research Institute, Palo Alto, CA
J. B. Wagner, Arizona State University, Tempe, AZ
R. G. Wymer, Oak Ridge National Laboratory, Oak Ridge, TN
E. B. Yeager, Case Western Reserve University, Cleveland, OH
C. R. Allen, Nuclear Waste Technical Review Board, Pasadena, CA
J. Allison, USDOE, Environmental Restoration & Waste Management, Germantown, MD
E. Anderson, Mountain West Research-Southwest, Inc., Phoenix, AZ
D. H. Appel, U.S. Geological Survey, Denver, CO
Associate Director, USDOE, Storage and Transportation, OCRWM, Washington, DC
Associate Director, USDOE, Contract Business Management, OCRWM, Washington, DC
Aa. Barkatt, Catholic University of America, Vitreous State Laboratory, Washington, DC
J. W. Bartlett, USDOE, Civilian Radioactive Waste Manage., Washington, DC
S. Bates, Idaho Falls, ID
D. A. Beck, U.S. Geological Survey, Las Vegas, NV
C. G. Bell, Jr., University of Nevada, Las Vegas, NV
A. Berusch, USDOE, Civilian Radioactive Waste Manage., Washington, DC
N. E. Bibler, Westinghouse Savannah River Co., Aiken, SC
E. P. Binnall, Lawrence Berkeley Laboratory, Berkeley, CA
M. Blanchard, DOE Field Office, Nevada, Las Vegas, NV
T. E. Blejwas, Sandia National Laboratory, Albuquerque, NM (5)
J. Blink, Lawrence Livermore National Laboratory, Las Vegas, NV
W. Bourcier, Lawrence Livermore National Laboratory, Livermore, CA
J. C. Bresee, USDOE, Civilian Radioactive Waste Manage., Washington, DC
S. J. Brocoum, USDOE, Civilian Radioactive Waste Manage., Washington, DC
R. L. Bullock, Raytheon Services Nevada, Las Vegas, NV
M. H. Campbell, Westinghouse Hanford Co., Richland, WA
D. Campbell, U.S. Bureau of Reclamation, Denver, CO

J. E. Cantlon, Nuclear Waste Technical Review Board, East Lansing, MI
M. W. Carter, Nuclear Waste Technical Review Board, Atlanta, GA
K. W. Causseaux, U. S. Geological Survey, Denver, CO
Center for Nuclear Waste Regulatory Analyses, San Antonio, TX
K. A. Chacey, USDOE, Waste Management, Germantown, MD
Chief, DOE Field Office, Nevada, U.S. Geological Survey, Las Vegas, NV
P. Childress, Lynchburg, VA
P. Cloke, Science Applications International Corp., Las Vegas, NV
M. O. Cloninger, Yucca Mountain Project Office, Las Vegas, NV
B. W. Colston, Raytheon Services Nevada, Las Vegas, NV
Community Planning and Development, North Las Vegas, NV
C. F. Costa, U. S. Environmental Protection Agency, Las Vegas, NV
D. U. Deere, Nuclear Waste Technical Review Board, Arlington, VA
Department of Comprehensive Planning, Clark County, Las Vegas, NV
Director of Community Planning, Boulder City, NV
J. F. Divine, U. S. Geological Survey, Reston, VA
M. J. Dorsey, Reynolds Electric & Engineering Co., Inc., Las Vegas, NV (2)
R. S. Dyer, Yucca Mountain Project Office, Las Vegas, NV
Economic Development Department, Las Vegas, NV
D. R. Elle, USDOE, DOE Field Office, Nevada, Las Vegas, NV
R. C. Ewing, University of New Mexico, Albuquerque, NM
E. Ezra, EG&G Energy Measurements, Inc., Las Vegas, NV
R. Fish, TRW Environmental Safety Systems, Las Vegas, NV
P. K. Fitzsimmons, USDOE, DOE Field Office, Nevada, Las Vegas, NV
A. L. Flint, U.S. Geological Survey, Mercury, NV
J. Fordham, Water Resources Center, Desert Research Institute, Reno, NV
J. Foremaster, City of Caliente, Caliente, NV (5)
D. Foust, TRW Environmental Safety Systems, Las Vegas, NV
D. L. Fraser, Reynolds Electrical & Engineering Co., Inc., Las Vegas, NV
C. P. Gertz, USDOE, Civilian Radioactive Waste Manage., Washington, DC
C. P. Gertz, USDOE, DOE Field Office, Nevada, Las Vegas, NV (5)
P. A. Glancy, U.S. Geological Survey, Carson City, NV
V. M. Glanzman, U. S. Geological Survey, Denver, CO
S. E. Gomberg, USDOE, Civilian Radioactive Waste Manage., Washington, DC
J. Hale, USDOE, Civilian Radioactive Waste Manage., Washington, DC
D. Harrison-Giesler, Yucca Mountain Project Office, Las Vegas, NV
C. K. Hastings, Pacific Northwest Laboratories, Richland, WA
T. Hay, Office of the Governor, State of Nevada, Carson City, NV
L. R. Hayes, U. S. Geological Survey, Denver, CO (6)
D. Hedges, Roy F. Weston, Inc., Las Vegas, NV
E. J. Helley, U.S. Geological Survey, Menlo Park, CA
R. J. Herbst, Los Alamos National Laboratory, Los Alamos, NM (4)
C. Interrante, U. S. Nuclear Regulatory Commission, Washington, DC
T. H. Isaacs, USDOE, Civilian Radioactive Waste Manage., Washington, DC
R. E. Jackson, Roy F. Weston, Inc., Washington, DC
C. Jantzen, Westinghouse Savannah River Co., Aiken, SC
L. J. Jardine, Lawrence Livermore National Laboratory, Livermore, CA
C. H. Johnson, Nuclear Waste Project Office, State of Nevada, Carson City, NV
H. N. Kalia, Los Alamos National Laboratory, Las Vegas, NV
W. S. Ketola, USDOE, West Valley Project Office, West Valley, NY

B. G. Kitchen, E. I. DuPont, Savannah River Laboratory, Aiken, SC
D. A. Knecht, Westinghouse Idaho Nuclear Co., Idaho Falls, ID
W. L. Kuhn, Battelle Pacific Northwest Laboratory, Richland, WA
D. Langmuir, Nuclear Waste Technical Review Board, Golden, CO
W. Lee, University of California, Berkeley, CA
H. Leider, Lawrence Livermore National Laboratory, Livermore, CA
Lincoln County Commission, Pioche, NV
R. R. Loux, Jr., Nuclear Waste Project Office, State of Nevada, Carson City, NV (3)
R. E. Lowder, MAC Technical Services, Las Vegas, NV
R. W. Lynch, Sandia National Laboratories, Albuquerque, NM
H. Manaktala, Southwest Research Institute, San Antonio, TX
S. Marschman, Pacific Northwest Laboratory, Richland, WA
J. Matuszek, State of New York, Department of Health, Albany, NY
G. B. Mellinger, Battelle Pacific Northwest Laboratory, Richland, WA
M. Mifflin, Water Resources Center, Desert Research Institute, Las Vegas, NV
R. Morissette, Science Applications International Corp., Las Vegas, NV
P. K. Nair, Center for Nuclear Waste Reg. Analyses, Southwest Research Institute, San Antonio, TX
J. L. Nelson, Westinghouse Hanford Co., Richland, WA
J. H. Nelson, Science Applications International Corp., Las Vegas, NV
D. Warner North, Nuclear Waste Technical Review Board, Decision Focus, Inc., Los Altos, CA
NRC Document Control Desk, U. S. Nuclear Regulatory Commission, Washington, DC
W. O'Connell, Lawrence Livermore National Laboratory, Livermore, CA
ONWI Library, Battelle Columbus Laboratory, Columbus, OH
R. Palmer, West Valley Nuclear Services, West Valley, NY
G. J. Parker, USDOE, Civilian Radioactive Waste Manage., Washington, DC
W. D. Pearson, Savannah River Laboratory, Aiken, SC
I. Pegg, Catholic University of America, Vitreous State Laboratory, Washington, DC
F. G. Peters, USDOE, Civilian Radioactive Waste Manage., Washington, DC
T. H. Pigford, University of California, Berkeley, CA
Planning Department, Nye County, Tonopah, NV
M. J. Plodinec, E. I. DuPont, Savannah River Laboratory, Aiken, SC
P. T. Prestholt, NRC Site Representative, Las Vegas, NV
D. L. Price, Nuclear Waste Technical Review Board, Blacksburg, VA
R. F. Pritchett, Reynolds Electrical & Engineering Co., Inc., Las Vegas, NV
Project Directorate, U. S. Nuclear Regulatory Commission, Washington, DC
R. B. Raup, Jr., U.S. Geological Survey, Denver, CO
J. Roberts, USDOE, Civilian Radioactive Waste Manage., Washington, DC
S. Rousso, USDOE, Civilian Radioactive Waste Manage., Washington, DC
C. G. Russomanno, USDOE, Civilian Radioactive Waste Manage., Washington, DC
SAIC-T&MSS Library, Science Applications International Corp., Las Vegas, NV (2)
J. D. Saltzman, USDOE, Civilian Radioactive Waste Manage., Washington, DC
J. H. Sass, U.S. Geological Survey, Flagstaff, AZ
P. S. Schaus, Westinghouse Hanford Co., Richland, WA
V. R. Schneider, U.S. Geological Survey, Reston, VA
Senior Project Manager for Yucca Mountain, U.S. Nuclear Regulatory Commission, Washington, DC
D. E. Shelor, USDOE, Civilian Radioactive Waste Manage., Washington, DC
D. Stahl, B&W Fuel Co., Las Vegas, NV
R. Stout, Lawrence Livermore National Laboratory, Livermore, CA
D. Strachan, Battelle Pacific Northwest Laboratories, Richland, WA
A. T. Tamura, USDOE, Office of Scientific & Technical Information, Oak Ridge, TN

Technical Information Center, Roy F. Weston, Inc., Washington, DC
Technical Information Officer, USDOE, DOE Field Office, Nevada, Las Vegas, NV (10)
M. ten-Brink Buchholtz, Lawrence Livermore National Laboratory, Livermore, CA
M. Tomozawa, Rensselaer Polytechnic Institute, Troy, NY
R. Van Konynenburg, Lawrence Livermore National Laboratory, Livermore, CA
E. D. Verink, Nuclear Waste Technical Review Board, Gainesville, FL
R. V. Watkins, U.S. Geological Survey, Denver, CO
C. L. West, USDOE, DOE Field Office, Nevada, Las Vegas, NV
S. S. C. Wu, U.S. Geological Survey, Flagstaff, AZ
D. Zesiger, U.S. Geological Survey, Las Vegas, NV
Commission of the European Communities, Brussels, BELGIUM
C. Davison, Atomic Energy Canada Ltd., Manitoba, CANADA
K. Dormuth, Atomic Energy Canada Ltd., Manitoba, CANADA
L. Johnson, Atomic Energy Canada Ltd., Manitoba, CANADA
R. Odoj, Institut for Chemische Technologie, Julich, WEST GERMANY
F. P. Sergent, Atomic Energy of Canada, Ltd., Manitoba, CANADA
G. Simmons, Atomic Energy Canada Ltd., Manitoba, CANADA
E. Vernaz, Centre d'Etudes Nucleares de la Valle du Rhone, FRANCE
L. Werme, Svensk Karnbranslehantering AB, Stockholm, SWEDEN

The following number is for Office of Civilian Radioactive Waste Management Records Management purposes only and should not be used when ordering this document:

Accession Number: NNA.911206.0022

END

DATE FILMED

4/29/92